FUNDAMENTAL STUDIES OF COMPETITIVE EQUILIBRIA AT SILICA SURFACES

Ву

Barrack Perez Stubbs

A DISSERTATION

Submitted to
Michigan State University
in partial fulfilment of the requirement
for the degree of

Chemistry – Doctor of Philosophy

2019

ABSTRACT

FUNDAMENTAL STUDIES OF COMPETITIVE EQUILIBRIA AT SILICA SURFACES

By

Barrack Perez Stubbs

The fundamental interactions such as physisorption at solid-liquid interfaces are not fully characterized. The physical properties and chemical reactivity at the silica surface is one that is subject to much investigation. A variety of analytical techniques, including solid state nuclear magnetic resonance (SS-NMR) and high-performance liquid chromatography (HPLC) were utilized to help characterize the surface of silica. These techniques were combined in order to understand the fundamental mechanisms of surface interactions such as adsorption mechanisms and chemical reactivity. The pH, ionic strength, and mobile phase compositions were varied throughout the experiments as a basis for assessing reactivity.

The SS-NMR data shows a correlation between pH and labile surface hydrogens. At higher pH values, the transfer of excitation from labile surface hydrogens to surface silicon atoms is diminished. A change in peak ratios that correspond to labile primary silanols and surface bridging siloxanes was observed. The relative concentration of bridging siloxanes is constant whereas the signal from primary silanols is greatly diminished.

Aqueous, normal-phase HPLC shows the various interactions of phenol with the silica surface. Multiple peaks were generated from a single analyte when the water/methanol concentration was at least 20%/80%. At 90% and 100% methanol, a single peak is shown for phenol. The ratio and number of peaks depends on conditions such as solvent composition, pH, ionic strength, flow rate, and temperature. We argue that the distribution of surface silanol sites is responsible for the generation of multiple peaks that are seen in the extreme aqueous conditions.

These sites, as well as the water in the mobile phase, modify the mass transport term in the Van Deemter equation. The conditions and results obtained in these experiments are explained below with an emphasis on mass transport.

Additionally, other analytical techniques such as scanning electron microscopy, thermogravimetric analysis, and inductively coupled plasma were used to help characterize the silica surface. Through these techniques, values for surface silanol concentration ranging from $1.6\mu\text{mol/m}^2$ to $7.0\mu\text{mol/m}^2$ were obtained. The physical morphology of the silica surface was also characterized before and after exposure to basic environments.

ACKNOWLEDGEMENTS

A special thank you is given to my research advisor, Dr. Gary Blanchard under who's instruction and tutelage I was able to develop into the independent researcher that I am today and to Sheryl Blanchard who helped keep me fed during my time at MSU. I would also like to thank my research group for supporting me in my endeavours and helping me prepare for my presentation and for keeping me grounded along the way. I would also like to thank Dr. Kathryn Severin and Dr. Daniel Holmes for help in training me on and for the use of the instruments I needed to help complete this project.

Lastly, I would like to thank my family, especially my grandmother who raised me as her own and supported me through all of my scholarly pursuits.

TABLE OF CONTENTS

LIST OF TABLES	vi
LIST OF FIGURES	vii
Chapter 1 Introduction	1
LITERATURE CITED	7
Chapter 2	10
Introduction	10
LITERATURE CITED	17
Chapter 3	20
Abstract	20
Introduction	21
Experimental	27
Results and Discussion	29
Conclusion	46
LITERATURE CITED	48
Chapter 4	52
Abstract	52
Introduction	52
Experimental	58
Results and Discussion	59
Conclusion	77
LITERATURE CITED	79
Chapter 5	83
Conclusions	83
Future Directions	86
APPENDIX	88
LITERATURE CITED	106

LIST OF TABLES

Table 2.1 Surface tension values for the interfaces in the contact angle experiment.	15
Table 3.1 Quantification of Na ⁺ liberated in ICP experiments.	44

LIST OF FIGURES

Figure 2.1 Model of the effect of K_{Na} on the transition pH of the contact angle at a fixed Na concentration.
Figure 2.2 Model of the effect of ionic strength on the transition pH of the contact angle at a constant K_{Na} .
Figure 3.1 Relative abundance of SiO ⁻ functionality as a function of pH and pNa. 25
Figure 3.2 Relative abundace of SiO ⁻ Na ⁺ functionality as a function of pH and pNa. 26
Figure 3.3 Relative abundace of SiOH functionality as a function of pH and pNa. 26
Figure 3.4 SEM image of native silica gel at 500x magnification. General size and shape of the silica gel can be seen. Particle size is roughly 50µm.
Figure 3.5 Image of the native silica surface (untreated). Image shows the native features of the silica gel. Magnification is at 5000x.
Figure 3.6 Image of the silica surface after treatment with KOH (left) and NaOH (right) Magnification is at 5000x.
Figure 3.7 Image of silica gel after treatment with NaOH followed by regeneration with 2% nitricacid. Image magnification is at 5000x.
Figure 3.8 Solid state ²⁹ Si NMR spectrum of native silica gel suspended in a pH 2 aqueous solution Peak assignments are as indicated in the text. 34
Figure 3.9 Solid state ²⁹ Si NMR spectrum of native silica gel suspended in a pH 6.5 aqueou solution. Peak assignments are as indicated in the text. 35
Figure 3.10 ²⁹ Si NMR spectra of the silica surface upon exposure to Na ⁺ . The pH of the system i approximately 2.
Figure 3.11 Effect of Na ⁺ on the silica gel ²⁹ Si NMR. The pH of the system is approximately 6.5
Figure 3.12 ²³ Na solid state NMR showing a single environment for interactions with the silica surface.
Figure 3.13 A proposed structure of the silica surface after Na ⁺ adsorption. Sodium coverage i not 100%
Figure 3.14 Zeta potential measurements of silica gel suspended in solutions of either NaCl o HCl. Small amounts of NaOH were used in pH >7 measurements.

Figure 3.16 Example TGA data showing the dehydration of the silica surface. This surtreated with NaOH before TGA analysis.	face was 45
Figure 4.1 van Deemter plot showing the dependence of H(u) on flow rate. A, B, and C are Deemter factors that govern H(u) and u is the flow rate of the system.	e the van 56
Figure 4.2 Chromatogram showing the splitting of peaks at 20% eater/80% methanol.	60
Figure 4.3 Overlay of phenol chromatograms showing peak dependence as the concent methanol decreases.	ration of 61
Figure 4.4 Mobile phase dependent retention time data. Each color corresponds to a peathe chromatographic data.	k seen in 62
Figure 4.5 Effect of temperature on the peak shape of the chromatograms.	65
Figure 4.6 Dependence of the number of peaks and peak width on the flow rate.	67
Figure 4.7 Statistical model of the three dominant surface groups that affect the chrom The C_s values are for each type of surface group.	atogram. 70
Figure 4.8 An enhanced view of Figure 4.7 showing the differences in retention time a values.	t low C_m
Figure 4.9 A statistical model showing the overlap of peaks with similar C_s values for the chemical groups on the surface. Values are at a specific flow rate and C_m .	different 71
Figure 4.10 pH dependence of the shape of the chromatograms.	72
Figure 4.11 Distribution of surface silanol groups. Each terminal -OH functionality is caundergoing proton dissociation equilibria.	apable of 73
Figure 4.12 Effect of Na ⁺ on the chromatogram at pH 2.	76
Figure 4.13 Effect of Na ⁺ on the chromatogram at pH 6.5.	76
Figure A.1 Chromatogram of phenol at 100% methanol. A single peak is shown correspondent analyte.	onding to 89
Figure A.2 Chromatogram of phenol at 90% methanol/10% water. A single peak is corresponding to the analyte.	s shown 90
Figure A.3 Chromatogram of phenol at 80% methanol/20% water. Multiple peaks are sleephenol analyte.	hown for 91
Figure A.4 Chromatogram of phenol at 70% methanol/30% water. Multiple peaks are sl	hown for

43

92

Figure 3.15 Calibration graph of Na⁺ ICP data.

the phenol analyte.

Figure A.5 Chromatogram of phenol at 60% methanol/40% water. When compared to Figure Peak ratios have changed noticeably.	gure A.4 93
Figure A.6 Chromatogram of phenol at 50% methanol/50% water.	94
Figure A.7 Chromatogram of phenol at 40% methanol/60% water.	95
Figure A.8 Chromatogram of phenol at 30% methanol/70% water.	96
Figure A.9 Chromatogram of phenol at 20% methanol/80% water.	97
Figure A.10 Chromatogram of phenol at 10% methanol/90% water.	98
Figure A.11 Chromatogram of phenol at 100% water. The chromatogram is drastically than that shown in Figure A.1.	different 99
Figure A.12 Flow rate dependence of the shape of the chromatogram.	100
Figure A.13 29 Si solid state NMR spectra of silica gel at approximately pH 2. Ionic streng 0M.	gth is 101
Figure A.14 ²⁹ Si solid state NMR spectra of silica gel at approximately pH 2. Ionic streng 0.1M. Figure A.15 Effect of Na ⁺ on the silica gel ²⁹ Si NMR. The pH of the system is approximately pH 2.	102
Figure A.16 ²⁹ Si solid state NMR spectra of silica gel at approximately pH 6. Ionic streng 0.1M.	gth is 104
Figure A.17 ²³ Na solid state NMR of the silica gel after exposure to NaOH.	105

Chapter 1

Introduction

The chemistry that occurs at interfaces dominates a number of scientific areas, ranging from chemical separations and sensing to energy conversion and heterogeneous catalysis. ¹⁻³ Because of the variety of phenomena and processes that proceed at interfaces, there is great range of surface structures, morphologies and chemical functionalities that have been utilized. Interfaces can range from being highly-ordered single crystals to amorphous and highly irregular, with the details of the interface depending on the conditions under which it was formed and processed. ⁴ Especially for structurally complex oxide surfaces, characterization and gaining a detailed understanding of interface properties remains a challenge. In addition to morphological features (pores, voids, cracks, etc.) there can be multiple reactive chemical functionalities present on such surfaces. These qualities invite further experimental and theoretical investigation in order to achieve a detailed understanding of these complex interfaces for a given application. The work presented in this dissertation focuses on several experimental methodologies in an attempt to gain a more thorough understanding of silica, especially with respect to the competitive equilibria that are operative and play a key role in the interfacial properties of this ubiquitous material.

Oxide surfaces where a metal or metalloid has been oxidized to some extent have found great use for everything from semiconductor physics to chemical separations and sensing. It is the combination of chemically reactive functionality (-OH) and the ability to form an insulating layer that has facilitated the wide use of oxides, and at the same time has limited the ability to interrogate the surface functionality present on these surfaces. Examples of this type of surface include silica, titania, and iron oxide surfaces.² These materials provide a useful physical support for chemical reactions and processes. When hydroxyl functionalities are available at the surface, they can be

used as anchoring sights for a host of chemical functionalities which can be tailored for target applications.⁵ Another key feature, depending on how the oxide was prepared, is a characteristically high surface area to volume ratio.⁶⁻⁷ This physical property is useful for certain applications such as surface-mediated chemical reactions or chemical separations, for example. It is important to note, however, that a high surface area-to-volume ratio can limit access to some fraction of surface functionalities, resulting an intrinsically heterogeneous interface.

Due to the wide variety of available oxide surfaces, there are a great range of possible applications. Conductive oxides such as indium-doped tin oxide or fluorine-doped tin oxide find use as electrodes for either analytical or synthetic applications. The ability to be able to control surface potential and surface charge density of such transparent electrode, they find use in spectro-electrochemical applications or for applications where charge gradients can be controlled (*i.e.* ionic liquids).⁸ Titania, another oxide, is utilized in dye-sensitized solar cells as electron acceptors.⁹

Perhaps the most widely used oxide is silicon dioxide (silica). What makes silica so useful are its combined properties of wide availability and a surface that is amenable to chemical functionalization, ¹⁰ accounting for its use as liquid chromatographic stationary phases and in capillary electrophoresis. ¹¹⁻¹² For the latter technique, it is the ability of the surface silanol functionalities to release their protons and assume a negative formal charge. Capillary electrophoresis is a separation technique that involves the migration of analytes through a capillary across which a high voltage electric field is applied. The mechanism of separation depends on the size and charge of the analyte species as well as the existence of spatially fixed charged sites on the silica capillary surface. Depending on the pH of the fluid (mobile phase), the silica surface can be charged. The surface of silica has a pKa of *ca*. 4.5. For pH values above 5, the silica capillary surface charge is neutralized by cations in solution through the formation of an electric double

layer. When an electric field is applied across the length of the capillary, the cations are drawn toward the negative electrode (cathode). As the cations move toward the cathode, they entrain water molecules resulting in solvent flow through the capillary the cathode in what is termed electroosmotic flow. This flow is the reason why all analytes, regardless of charge, move toward the cathode. The rate of electroosmotic flow depends on the charge density of the surface, as gauged by its ζ potential. The relationship between the ζ potential and the electroosmotic mobility, μ_{eo} , is given by Eq. 1.1, $^{11, 13-14}$

$$\mu_{eo} = \frac{\varepsilon \zeta}{6\pi \eta} \tag{1.1}$$

where ε is the dielectric constant and η is the viscosity of the solvent system. The dependence of the ζ potential on both solution properties and on the morphological and structural heterogeneities that characterize the silica surface is a useful means of surface characterization. The ζ potential relies heavily on the concentration of surface hydroxyl groups per unit area.

In addition to using the silica surface as a means of achieving bulk flow (electrophoresis), pressure can also be used to achieve bulk flow, and in this application the silica surface is also essential. High performance liquid chromatography, HPLC, uses pressure to achieve flow of the mobile phase and silica is used as the stationary phase (normal phase) or as the support surface on which chemical modifications are made (reverse phase). base surface for separations. Depending on the mode of chromatography, the surface is either polar or non-polar. Polar surfaces used are either bare silanol or amine-terminated surfaces, which are useful for separating polar analytes due to comparatively strong interactions with the stationary phase. Non-polar surfaces are typically covalently bound C_8 or C_{18} aliphatic chains, although other organic functionalities are readily available. With a non-polar stationary phase, analytes undergo partitioning between adsorption

onto or into the stationary phase and dissolution into the mobile phase to achieve separation. When the surface of this silica is modified in some fashion, this is called a bonded phase column, and owing to the morphological complexity of the silica support surface, quantitative reaction of the silanol sites is, in general, very difficult to achieve. Under such circumstances, residual unreacted surface silanol functionalities can participate in the separation process, leading to band asymmetries and loss of resolution. In an effort to mitigate such effect, organic-modified silica surfaces are often reacted with a chloromethylsilane (*e.g.* Me₃SiCl, Me₂SiCl₂) to "cap" any remaining silanol functionalities.^{2, 12}

The silica surface is one that is complex in nature and has a large distribution of morphologies and reactivities. The different silanol groups on the surface and their accessibility are responsible for the variation in observed reactivities. The several silanol functionalities on a silica surface are typically designated Q⁰, Q¹, Q² and Q³, with the superscripted number indicating the number of hydroxyl groups bound to the silicon atom. Bridging siloxanes (Si-O-Si) are designated Q⁰, primary silanols (SiOH) are Q¹, geminal silanols (Si(OH)₂) are Q², and tertiary silanols (Si(OH)₃) are Q³. Within the Q¹ silanols there are isolated silanols which have no nearby neighbors, and vicinal silanols which are hydrogen bonded to their nearest neighbor. The silanol groups are acidic in nature and as such they are characterized by pKa values ranging from 4.5 to 8.5. The distribution of these groups depends on the methods used in surface synthesis and processing. The understanding of the chemical and morphological factors that collectively determine the pKa values of a given silanol group remain to be understood at more than a qualitative level. Understanding the silica surface and the associative equilibria that characterize the distribution of surface silanol functionalities is the focus of much of the work presented here.

It is possible to gain insight into the silica surface through measurement techniques where the silica is used as a component. Changes in experimental conditions, surface exposure, and surface modification can allow for the study of the silica surface in ways that have not yet been explored. For example, if one was to take advantage of capillary electrophoresis, conditions such as ionic strength, voltage, and pH can be utilized to elucidate features and characteristics that derive from the atomic- and microscopic scale properties of silica. Previous work sought to understand the pKa and surface energies of silanol(s) by using a non-polar liquid to probe the surface energy through contact angle measurements.¹⁷ In that work, a silica surface in contact with an aqueous overlayer was evaluated by measuring the contact angle of carbon tetrachloride with the silica surface as a function of pH and ionic strength of the aqueous overlayer. By measuring the water-CCl₄ contact angle, it was shown there is a competing equilibrium for deprotonated silanol sites on the silica surface. These equilibria depend on the relative concentrations of protons and metal ions, in this case sodium, in the aqueous overlayer. A Na⁺ equilibrium constant was reported to be 7 x 10⁻³ for a silica surface (the analogous equilibrium constant for H⁺ is 3x10⁻⁵).

The work presented in this dissertation is divided into two major parts. The first involves the use of several analytical techniques to characterize the silica surface. By use of thermogravimetric analysis, the surface silanol groups can be quantified via dehydration studies. The formation of siloxane bridges releases water and results in a net loss of mass that can be analyzed quantitatively. Bare and functionalized silica can be used to adsorb metal ions from solution. ¹⁸⁻²¹ Inductively coupled plasma was used to quantify reactive silanol species by taking advantage of cation exchange at the silica surface. Combing this information with solid state ²³Na NMR measurements provides further characterization of the silica surface and the interactions present when silica functions as a cation exchanger. Variable pH solid state ²⁹Si NMR was used

to probe the distribution of silanols groups on the surface. Scanning electron microscopy was used to image the surface before and after exposure to highly alkaline environments. These experiments contributed to the understanding of the physical morphology of the surface.

The second major part of this dissertation involves the use of aqueous normal phase chromatography as a method of further characterizing interactions at the solid-liquid interface. By utilizing an unbonded silica column, conditions such as pH, ionic strength, temperature, flow rate, and mobile phase composition were varied. Phenol was used as a simple molecular marker to probe the interactions. It should be noted that what was performed here was not a separation, nor was it intended to be one. A conventional chromatographic system was used to investigate the silica surface under conditions that are atypical for chromatographic separations. Data showed that in a regime limited by mass transport, it is possible to sample the heterogeneity of the surface of the stationary phase.²²⁻²³ That is, it is possible for a single analyte to experience a range of interactions with the stationary phase, giving rise to multiple retention times. These features are generated by the differences in adsorption energy for each type of site on the surface. While a single analyte should, statistically, sample each type of site equally, the extreme conditions of these experiments have revealed the underlying interactions with the surface that are important in such separation schemes.

LITERATURE CITED

LITERATURE CITED

- 1. Grossman, P. D.; Colburn, J. C., Capillary Electrophoresis Theory & Practice. 1992.
- 2. Pesek, J. J.; Tang, V. H., The modification of alumina, zirconia, thoria and titania for potential use as HPLC stationary phases through a silanization/hydrosilation reaction scheme. *Chromatographia* **1994**, *39* (11-12), 649-654.
- 3. van de Loosdrecht, J.;van der Kraan, A. M.;van Dillen, A. J.;Geus, J. W., Metal-Supported Interaction: Titania-Supported and Silica-Supported Nickel Catalysts. *Journal of Catalysis* **1997**, *170* (2), 217-226.
- 4. Rahman, I. A.; Padavettan, V., Synthesis of Silica Nanoparticles by Sol-Gel: Size-Dependent Properties, Surface Modification, and Applications in Silica-Polymer Nanocomposites—A Review. *Journal of Nanomaterials* **2012**, *2012*.
- 5. Boehm, H. P., Acidic and Basic Properties of Hydroxylated Metal Oxide Surfaces. *Discuss. Faraday Soc.* **1971,** 52, 264-275.
- 6. Brinker, C. J.;Brow, R. K.;Tallant, D. R.;Kirkpatrick, R. J., Surface Structure and Chemistry of High Surface Area Silica Gels. *Journal of Non-Crystalline Solids* **1990**, *120* (1-3), 26-33.
- 7. Su, C.;Lin, K.;Lin, Y.;You, B., Preparation and Characterization of High-Surface-Area Titanium Dioxide by Sol-Gel Process. *Journal of Porous Materials* **2006**, *13* (3-4), 251-258.
- 8. Ma, K.; Jarosova, R.; Swain, G. M.; Blanchard, G. J., Charge-Induced Long-Range Order in a Room-Temperature Ionic Liquid. *Langmuir* **2016**, *32* (37), 9507-9512.
- 9. O'Regan, B.;Grätzel, M., A low-cost, high-efficiency solar cell based on dye-sensitized TiO2 films. *Nature* **1991**, *353*, 737-740.
- 10. Liberman, A.; Mendez, N.; Trogler, W. C.; Kummel, A. C., Synthesis and Surface Functionalization of Silica Nanoparticles for Nanomedicine. *Surface Science Reports* **2014**, *69* (2-3), 132-158.
- 11. Schwer, C.; Kenndler, E., Electrophoresis in Fused-Silica Capillaries: The Influence of Organic Solvents on the Electroosmotic Velocity and the Zeta Potential. *Analytical Chemistry* **1991**, *63*, 1801-1807.
- 12. Krupczyńska, K.;Buszewski, B.;Jandera, P. Characterizing HPLC Stationary Phases 2004, p. 227 234.
- 13. Sze, A.; Erickson, D.; Ren, L.; Li, D., Zeta-Potential Measurement Using the Smoluchowski Equation and the Slope of the Current-Time Relationship in Electroosmotic Flow. *Journal of Colloid and Interface Science* **2003**, *261* (2), 402-410.

- 14. Fu, L. M.; Yin, J. Y.; Yang, R. J., Analysis of Electroosmotic Flow with Step Change in Zeta Potential. *Journal of Colloid and Interface Science* **2003**, 258 (2), 266-275.
- 15. Zhuravlev, L. T., The Surface Chemistry of Amorphous Silica. Zhuravlev model. *Colloids and Surfaces* **2000**, (173), 1-38.
- 16. Pfeiffer-Laplaud, M.; Gaigeot, M.; Sulpizi, M., pKa at Quartz/Electrolyte Interfaces. *Journal of Physical Chemistry Letters* **2016**, *7* (16), 3229.
- 17. Stubbs, B.;Blanchard, G. J., Measuring Competing Equilibria at a Silica Surface through the Contact Angle of a Nonpolar Liquid. *Langmuir* **2017**, *33* (38), 9632-9636.
- 18. Karnib, M.; Kabbani, A.; Holail, H.; Olama, Z., Heavy Metal Removal Using Activated Carbon, Silica and Silica Activated Carbon Composite. *Energy procedia* **2014**, *50*, 113-120.
- 19. Repo, E.; Warchoł, J.; Bhatnagar, A.; Sillanpää, M., Heavy metals adsorption by novel EDTA-modified chitosan-silica hybrid materials. *Journal of Colloid and Interface Science* **2011**, *358* (1), 261-267.
- 20. Kosmulski, M., Adsorption of Cadmium on alumina and silica: analysis of the values of stability constants of surface complexes calculated for different parameters of triple layer model. *Colloids and Surfaces* **1996**, *117*, 201-214.
- 21. Bois, L.;Bonhommé, A.;Ribes, A.;Pais, B.;Raffin, G.;Tessier, F., Functionalized Silica for Heavy Metal Ions Adsorption. *Colloids and Surfaces A: Physicochemical and Engineering Aspects* **2003**, *221* (1-3), 221-230.
- 22. Gritti, F.; Guiochon, G., Effect of the Surface Heterogeneity of the Stationary Phase on the Range of Concentrations for Linear Chromatography. *Anal. Chem.* **2005**, 77 (4), 1020-1030.
- 23. Gritti, F.;Guiochon, G., Heterogeneity of the Adsorption echanism of Low Molecular Weight Compounds in Reversed-Phase Liquid Chromatography. *Anal. Chem.* **2006**, 78 (16), 5823-5834.

Chapter 2

Introduction

Hydrous metal oxides can exhibit hydroxyl group dissociation and surface ionization to produce functionalities that can participate in metal ion complexation.¹ Silica can function as a cation exchanger, interacting with metal ions in solution and a number of different species can exist simultaneously at the silica surface.²⁻³ The relative amounts of each species depends sensitively on solution pH and metal ion concentration.⁴ It is possible to conduct experiments that take advantage of the change in the nature of the surface after exposure to metal ions. These experiments can be used to generate models that can help predict experimental outcomes based on acquired data. Contact angle experiments were used in conjunction with mathematical modelling to investigate the nature of the competitive equilibria on the silanol surface.⁵ Accurate models allow for predictive control of a system. These models can be compared to experimental data as a method of extracting parameters such as equilibrium constants.

Previous work sought to elucidate the nature of competitive equilibria at the solid/liquid interface of silica using carbon tetrachloride as a probe liquid.⁵ Solution phase metal ions compete with protons for sites on the silica surface. This competition is dependent on solution ionic strength and pH.⁶⁻⁷ The surface complexation model accounts for the competitive interaction that occurs at the solid-solution interface.⁸ In the system studied, the competitive equilibria are between proton and sodium ion interaction with surface siloxide functionalities. The first relevant equilibrium is the protonation / deprotonation of the silanol groups as a function of pH (Eq. 2.1), and the second equilibrium is the association of metal ions (Na⁺) with the siloxide groups (Eq. 2.3).⁹ The equation for the first reaction is given by

$$SiOH \rightleftharpoons SiO^{-} + H^{+} \tag{2.1}$$

The equilibrium expression for this reaction as follows

$$K_{a} = \frac{[SiO^{-}][H^{+}]}{[SiOH]}$$
 (2.2)

Where K_a is the acid dissociation constant for the silanol groups and [SiO $^-$], [H $^+$], and [SiOH] are the equilibrium concentrations of each of the species. For pH values higher than the pKa, the system the forward reaction dominates. The second equilibrium is

$$SiO^{-} + Na^{+} \rightleftharpoons SiO^{-}Na^{+} \tag{2.3}$$

This equation can be used to show the formation of the sodium adduct with the deprotonated surface. The equilibrium expression for this reaction is

$$K_{Na} = \frac{[SiO^{-}][Na^{+}]}{[SiONa]}$$
(2.4)

Where K_{Na} reflects the free energy of interaction between SiO^- and Na^+ . The dissociation reactions 2.1 and 2.3 are linked through the surface concentration of SiO^- . Under the assumption that $[SiO^-]$ is a small and nearly constant over the relevant pH and pNa range,

$$\frac{K_{Na}}{K_a} = \frac{[SiOH][Na^+]}{[H^+][SiONa]} \tag{2.5}$$

We make this assumption for the sake of simplicity and address its validity in Chapter 3, where the surface concentration of SiO is accounted for explicitly. By varying the concentrations of H⁺

or Na⁺, the equilibria shift to generate the silanol surface (increased protons), sodium siloxide surface (increased Na⁺), or the deprotonated silanol surface (low ionic strength, high pH).

The surface is characterized by its intrinsic surface energy. At the interface, there are three phases in direct contact; the solid surface, the liquid drop (CCl₄ here), and the aqueous medium that covers both. When these three phases meet at a boundary, their energies balance and result in the liquid drop making a specific contact angle, θ , with the surface. This angle is given by Young's Equation.¹⁰

$$\cos \theta = \frac{\gamma_{SV} - \gamma_{SL}}{\gamma_{IV}} \tag{2.6}$$

The quantities γ are the surface energies at each of the interfaces. There is the solid-liquid interface, γ_{SL} , the solid-vapor interface, γ_{SV} , and the liquid-vapor interface, γ_{LV} . Changes in surface association are accompanied by changes in surface energies γ_{SL} and γ_{SV} . This gives rise to new contact angles of the drop with the surface. These equations were used in conjunction with experimental contact angle data to evaluate changes in the equilibria that determine the relevant surface reactivity. This change in surface reactivity can be seen as a change in the contact angle that the CCl₄ droplet makes with the silica surface.

The experimental setup utilized carbon tetrachloride to probe the silica surface covered by an aqueous solution. Measurements were taken using an aqueous overlayer to control the pH of the surface. Contact angle readings were measured using a VCA 2000 Video Contact Angle System and accompanying software. The experimental data gathered were used in conjunction with models to show how competing ions change the silica surface energy. The modelling illustrates the effects of pH and pNa, metal ion concentration, on the energies of the system.

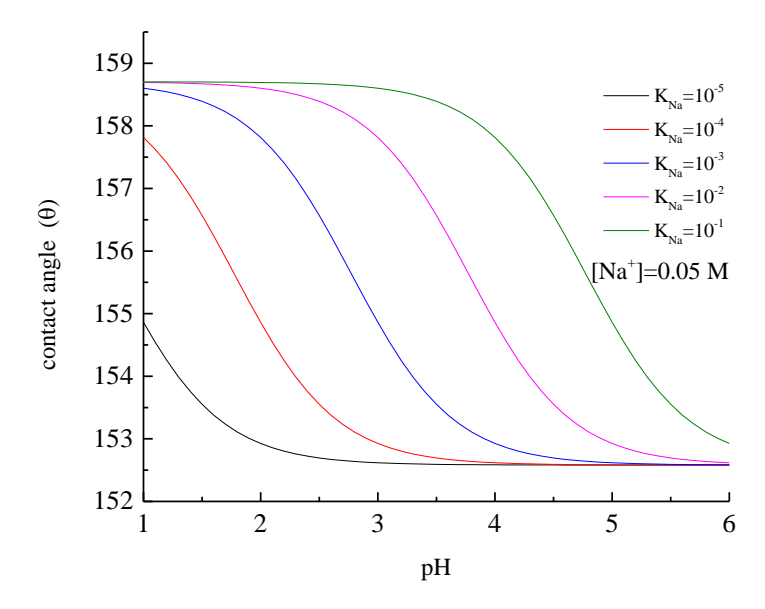


Figure 2.1 Model of the effect of K_{Na} on the transition pH of the contact angle at a fixed Na^+ concentration.⁵

Figure 2.1 shows the effect of the equilibrium constant K_{Na} on the transition pH of the contact angle. The larger the equilibrium constant, the higher the apparent pKa of the surface. At fixed sodium concentration, changing the concentration of the protons favors either the protonated form, low pH, or the sodium adduct, high pH. Since charge neutrality must be maintained, these are the two dominant forms when there are sodium ions in solution.

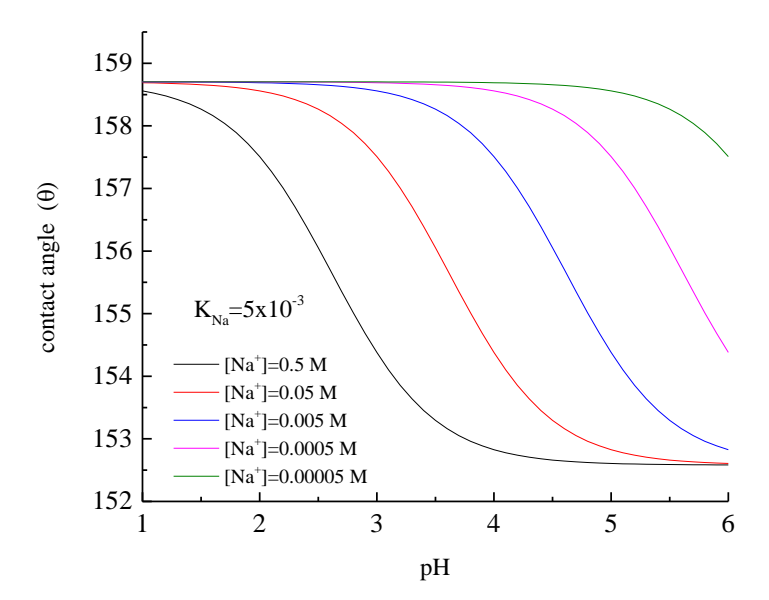


Figure 2.2 Model of the effect of ionic strength on the transition pH of the contact angle at a constant $K_{\rm Na}$.⁵

Figure 2.2 shows the effect of changing Na^+ concentration on the apparent surface pKa at fixed K_{Na} . Since the surface must be kept neutral by a counterion, the effect of pH depends on the concentration of the counterion, Na^+ . The higher the ionic strength, the more favored the sodium adduct. This has the effect of lowering the apparent pKa due to the Na^+ ions displacing H^+ from the surface silanol groups. At a fixed K_{Na} , we see that higher ionic strength lowers the pH at which the change of contact angle occurs. This can be explained as the higher Na^+ concentration shifting the equilibrium to favor the formation of SiO^-Na^+ . As the pH increases, the SiO^-Na^+ form is more likely than the SiOH form. As such, we see higher transition pH values as the concentration of the Na^+ decreases. This is due to the main factor being the deprotonation of the silanol surface.

Using these data, interfacial energy values can be calculated. The interfaces are defined as follows, γ_{SL} is the silica-carbon tetrachloride boundary, γ_{SV} is the silica-water boundary, and γ_{LV} is the carbon tetrachloride-water boundary. While it is not possible to calculate absolute values

using just the contact angle data, it is possible to calculate the change in surface energies. To begin, we make the assumption that the SiOX-CCl₄ interfacial energy is nominally constant due to the extreme differences in polarity at this interface. It is then possible to calculate the CCl₄-Water by the Wilhelmy plate method. It is also assumed that this value does not vary with pH. The exact values for SiOH-H₂O and SiO Na⁺-H₂O are then calculated via the contact angle on those surfaces. This data is summarized in Table 2.1. As is shown, the difference between the SiOH-H₂O interface and the SiO Na⁺-H₂O interface is approximately 2 mN/m. The change in surface energy is related to the change in surface polarity. With a covalent interaction changing to an ionic interaction. While the effect is shown here with a change from H⁺ to Na⁺ it is also possible to show this effect by changing the identity of the metal ion in solution as the surface energy depends on the charge density of the metal ion. SioX-CCl⁴ With this difference in contact angle and surface energies, it is possible to calculate the exact value of $\gamma_{\text{SioX-CCl}^4}$. This difference in surface tension is what gives rise to the change in contact angle as a function of pH. The small change in surface energies is reflected by small but measurable changes in the contact angle.

γsioh-h2O	48 mN/m
γsioNa-H2O	50 mN/m
γsiox-ccl4	90 mN/m
γCCl4-H2O	45 mN/m

Table 2.1 Surface tension values for the interfaces in the contact angle experiment.⁵

Through a combination of modelling and experiments, we are able to calculate surface energy values for the silica surface. These changes in surface energy help point toward the competitive equilibria that proceeds at the surface. The competition of protons with metal ions such as sodium change the chemical nature of the silica surface depending on their relative concentrations. The nature of the surface is of great importance in many applications and the implications of this study were fundamental to the experiments performed here within.

LITERATURE CITED

LITERATURE CITED

- 1. Davis, J. A.;Leckie, J. O., Surface Ionization and Complexation at the Oxide/Water Interface II. Surface Properties of Amorphous Iron Oxyhydroxide and adsorption of Metal Ions. *Journal of Colloid and Interface Science* **1978**, *67* (1), 90-107.
- 2. Jeon, C.;Höll, W. H., Application of the Surface Complexation Model to Heavy Metal Sorption Equilibria Onto Aminated Chitosan. *Hydrometallurgy* **2004**, *71* (3-4), 421-428.
- 3. Sjöberg, S., Silica in Aqueous Environments. *Journal of Non-Crystalline Solids* **1996,** *196*, 51-57.
- 4. Štamberg, K.; Venkatesan, K. A.; Rao, P. R. V., Surface Complexation Modeling of Uranyl Ion Sorption on Mesoporous Silica. *Colloids and Surfaces A: Physicochemical and Engineering Aspects* **2003**, *221* (1-3), 149-162.
- 5. Stubbs, B.;Blanchard, G. J., Measuring Competing Equilibria at a Silica Surface through the Contact Angle of a Nonpolar Liquid. *Langmuir* **2017**, *33* (38), 9632-9636.
- 6. James, R. O.; MacNaughton, M. G., The Adsorption of Aqueous Heavy Metals on Inorganic Minerals. *Geochimica et Cosmochimica Acta* **1977**, *41* (11), 1549-1555.
- 7. Elzinga, E. J.; Sparks, D. L., X-ray Absorption Spectroscopy Study of the Effects of pH and Ionic Strength on Pb(II) Sorption to Amorphous Silica. *Environ. Sci. Technol.* **2002**, *36* (20), 4352-4357.
- 8. Marmier, N.;Delisée, A.;Fromage, F., Surface Complexation Modeling of Yb(III) and Cs(I) Sorption on Silica. *Journal of Colloid and Interface Science* **1999**, *212* (2), 228-233.
- 9. Schindler, P. W.; Fürst, B.; Dick, R.; Wolf, P. U., Ligand Properties of Surface Silanol Groups. I. Surface Complex Formation with Fe3+, Cu2+, Cd2+, and Pb2+. *Journal of Colloid and Interface Science* **1976**, *55* (2), 469-475.
- 10. Young, T., An Essay on the Cohesion of Fluid. *Physical Transactions of the Royal Society of London* **1805**, (95), 65-87.
- 11. Padday, J. F.; Russell, D. R., The Measurement of the Surface Tension of Pure Liquids and Solutions. *Journal of Colloid Science* **1960**, *15* (6), 503-511.
- 12. Hauner, I. M.; Deblais, A.; Beattie, J. K.; Kellay, H.; Bonn, D., The Dynamic Surface Tension of Water. *J. Phys. Chem. Lett.* **2017**, *8* (7), 1599-1603.
- 13. Sakuma, H.; Andersson, M. P.; Bechgaard, K.; Stipp, S. L. S., Surface Tension Alteration on Calcite, Induced by Ion Substitution. *J. Phys. Chem. C* **2014**, *118* (6), 3078-3087.

- 14. Potapova, E.; Yang, X.; Grahn, M.; Holmgren, A.; Forsmo, S. P. E.; Fredriksson, A.; Hedlund, J., The Effect of Calcium Ions, Sodium Silicate and Surfactant on Charge and Wettability of Magnetite. *Colloids and Surfaces A: Physicochemical and Engineering Aspects* **2011**, *386* (1-3), 79-86.
- 15. Kakati, A.; Sangwai, J. S., Wettability Alteration of Mineral Surface during Low-Salinity Water Flooding: Role of Salt Type, Pure Alkanes, and Model Oils Containing Polar Components. *Energy Fuels* **2018**, *32* (3), 3127-3137.
- 16. Roshan, H.; Al-Yaseri, A. Z.; Sarmadivaleh, M.; Iglauer, S., On Wettability of Shale Rocks. *Journal of Colloid and Interface Science* **2016**, *475*, 104-111.

Chapter 3

Abstract

The focus of this chapter is on characterizing surface chemical functionality and morphological properties of silica. The quantities of interest include the silanol group density and the propensity of the surface silanol groups to undergo exchange between the hydroxyl protons and solution phase Na⁺ cations, the surface area and the extent of charge exhibited by the silica surface. Adsorption isotherm and thermogravimetric analyses were used to address the surface area and silanol group density. Inductively coupled plasma emission spectrometry was used to characterize the equilibrium between H⁺ and Na⁺ for interaction with surface silanol sites as a function of experimental conditions. The data from these measurements provided information on surface silanol group density (1.6 µmol/m² to 7.0 µmol/m² depending on the method and conditions used). BET isotherm data provided surface areas for the silica gel used in these experiments of 400 m²/g, which decreased to 290 m²/g following treatment with sodium hydroxide. Surface morphology was investigated using scanning electron microscopy. Treatment of the silica gel with sodium increased the conductivity of the surface as seen in the SEM imaging experiments. Changes in surface morphology following treatment of silica gel with NaOH were observed.

Solid state ²⁹Si and ²³Na NMR data provide insight into the structural distribution of silanol sites and the effect of sodium ions interacting with the silica surface. ²⁹Si NMR was performed using cross polarization, with the magnitude of the cross-polarization signal being mediated by the sodium interacting with the surface. When the Na⁺ displaces H⁺ from the surface, cross polarization is effectively turned off. This relationship was used to evaluate the reactivity of the

different types of siloxide functionalities on the silica surface. The ²³Na NMR was performed by direct polarization of the sodium atoms and shows a single type of sodium on the surface, implying all siloxides binding the sodium ions in an equivalent manner.

Zeta potential measurements as a function of pH and ionic strength reveal the effective charge on the silica surface. As solution phase pH increases, the silica surface potential becomes more negative due to deprotonation. The addition of Na⁺ to the solution neutralizes the charge on the surface due to complexation with surface siloxide functionality.

Introduction

Silica is a material that finds wide uses not only because of its range of bulk morphological properties, which range from large solid sheet glass through sand and finely divided silica gel, but also because of the chemical properties of its surface. The surface of silica is outwardly simple, given the existence of only Si-O-Si and Si-OH functionality. Such outward simplicity is deceiving, however, because the chemically labile Si-OH functionality can be present in either associated or dissociated form and because of the amorphous nature of the material, steric shielding and areal density of surface silanol functionalities can vary widely. It is these properties that determine collectively the utility of the bulk material for a particular application. For example, in order to make a highly stable structural material, it is desirable to have a silica surface predominantly composed of siloxane (Si-O-Si) bridge groups, and for chromatographic separations it is preferable to use silica that has a comparatively high density of surface silanol functionalities. It is the larger purpose of this work to characterize the silica surface with emphasis on the competing equilibria that the siloxide (SiO) group can compete in, and the consequences of that competition on

materials properties that influence processes of practical significance, such as chromatographic and/or electrophoretic separation.

The surface silanols that are central to the materials properties of silica are categorized as primary silanols have one hydroxyl group attached to a silicon atom, secondary silanols have two hydroxyl groups and tertiary silanols have three hydroxyls.³ These three distinct moieties are designated Q¹, Q² and Q³, respectively. Bridging siloxanes, which possess no terminal hydroxyl functionality, are designated Q⁰. In general, all functionalities, Q0 through Q3, are seen on a silica surface, but their distribution and spatial variations in areal density are not well understood. For example, the actual surface silanol density of silica lies in the range of 4 to 8 µmol/m², with the value at any given point on the surface depending on how the silica was prepared and morphological features contained in the region of interest.³ Silica is considered to be an amorphous material but that characterization does not imply that the distribution of silanol groups is necessarily random. Rather there is known to be spatial variation in the distribution of silanol groups, with "islands" of relatively high density that are ca. 15 nm in diameter, separated by narrower regions of low density. Taken collectively, even with these morphological features, a detailed nanometer-scale description of morphology and group distribution has not been achieved to date.

Silicon oxide(s) have been used widely for their adsorptive properties. Silica gels are known for their ability to function as a weakly acidic ion exchanger.⁴ This property has led to its use in a variety of separation techniques, including ion exchange chromatography. As discussed above, it is the silanol moiety or a derivative of that group that is the chemically active component of the silica surface. The Si-OH functional group exhibits an equilibrium between protonated and deprotonated forms, and the deprotonated form is capable of interactions with cations other than

H⁺. The consequences of these competitive interactions can have a substantial effect on the properties of the resulting silica surface. The adsorption of metal ions from aqueous solution is governed by the equilibrium process where

$$Si-OH + M^{n+} \rightleftharpoons Si-OM^{(n-1)+} + H^{+}$$
 (3.1)

This net reaction is dependent on two experimental factors that control the competing equilibria. These are the proton concentration and the metal ion concentration. The majority of concern in this area is the competitive interactions between H⁺ and Na⁺ for interactions with siloxide.⁵ The reasons for this are two-fold; first that the majority of aqueous buffer solutions used in chromatographic (electrophoretic) applications contain Na⁺ and second, that the competition between H⁺ and Na⁺ is expected to be highly dependent on experimental conditions because of the similarity of the equilibrium constants for the two association reactions. It is thought that this similarity is the result of the fact that Na⁺ is somewhat similar to H⁺ in terms of size. The exchange reaction of interest is

$$Si-OH + Na^+ \rightleftharpoons Si-ONa + H^+$$
 (3.2)

Which can be separated into two dissociation equations

$$Si-OH \rightleftharpoons Si-O^- + H^+$$
 (3.3)

$$Si-ONa \rightleftharpoons Si-O^- + Na^+$$
 (3.4)

The corresponding equilibrium expressions are

$$K_a = \frac{[SiO^-][H^+]}{[SiOH]} \tag{3.5}$$

$$K_{Na} = \frac{[SiO^-][Na^+]}{[SiONa]} \tag{3.6}$$

Although we do not know explicitly what the total concentration of silanol and related species is for a given interface, we do know that the total number of silanol groups is divided between three species, Si-OH, Si-ONa and Si-O⁻. Normalizing the total concentration to one surface layer of silanol and expressing concentrations as a fraction of the whole,

$$[SiOH] + [SiONa] + [SiO^{-}] = 1 \tag{3.7}$$

The central issue is to understand and characterize the relative amounts of each form of silanol functionality that are present for a given set of experimental conditions. Expressions for each species can be derived that contain only the relevant equilibrium constants and the concentrations of each solution phase species under our experimental control.

$$[SiO^{-}] = \frac{K_a K_{Na}}{K_{Na}[H^{+}] + K_a [Na^{+}] + K_a K_{Na}}$$
(3.8)

$$[SiONa] = \frac{K_a[Na^+]}{K_{Na}[H^+] + K_a[Na^+] + K_aK_{Na}}$$
(3.9)

$$[SiOH] = \frac{K_{Na}[H^+]}{K_{Na}[H^+] + K_a[Na^+] + K_aK_{Na}}$$
(3.10)

With these equations the fractional concentration of each surface species can be calculated as a function of $[H^+]$ and $[Na^+]$. For silica, there are known to be two pKas (*vide infra*), in the vicinity of pKa₁ = 4.5 (19% of all sites) and pKa₂ = 8.5 (81% of all sites).⁶ In calculations of the fractional contributions of each species, we treat the net surface as a linear superposition of the two subpopulations of silanols. These calculations are presented in Figs. 3.1, 3.2 and 3.3, where the

concentrations of H⁺ and Na⁺ are presented as pH and pNa. The predictions made by these plots are important in their own right, especially for applications that depend sensitively on the surface charge density of silica (e.g. electrophoresis), but also because they provide useful insight into the interpretation of data that give insight into the chemical environment experienced by these silanol species. We consider next the techniques used in surface characterization and the information available from each.

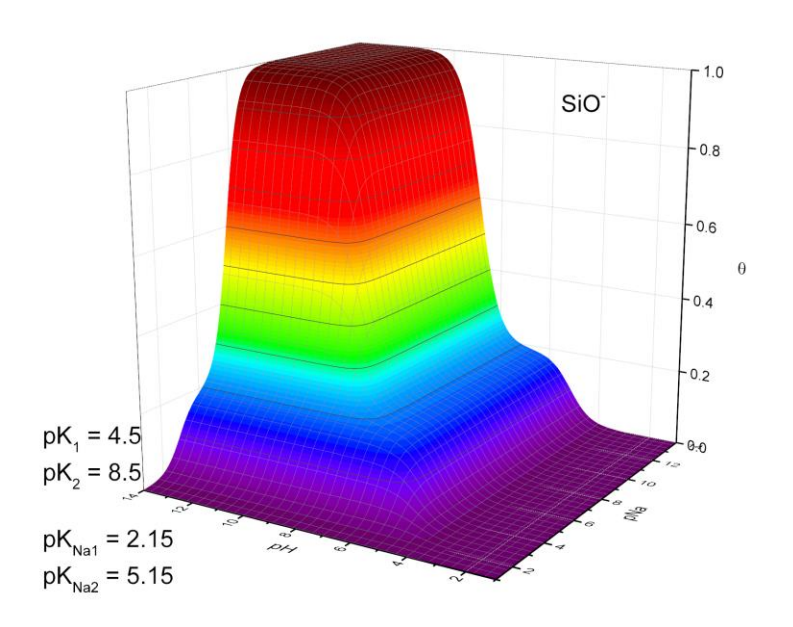


Figure 3.1 Relative abundace of SiO⁻ functionality as a function of pH and pNa.

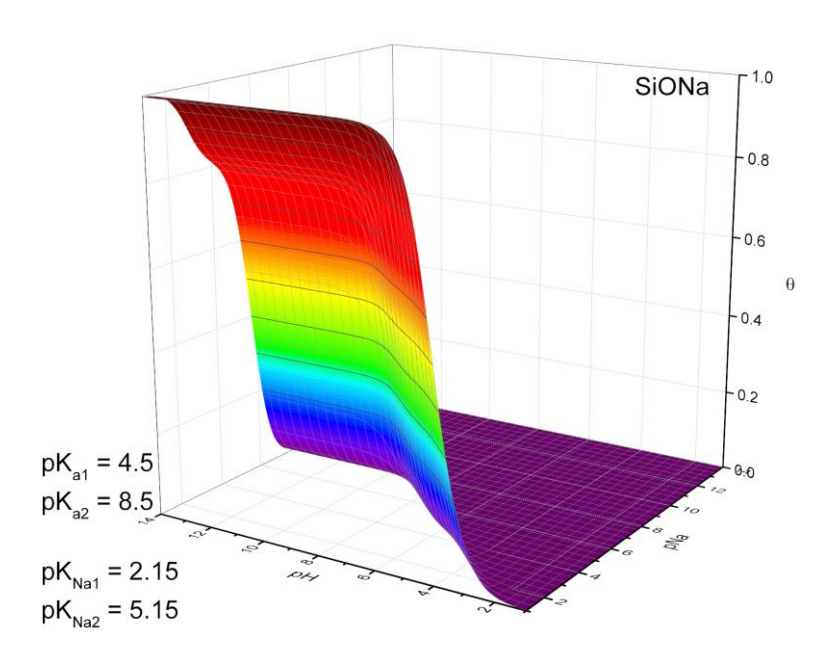


Figure 3.2 Relative abundace of SiO-Na+ functionality as a function of pH and pNa.

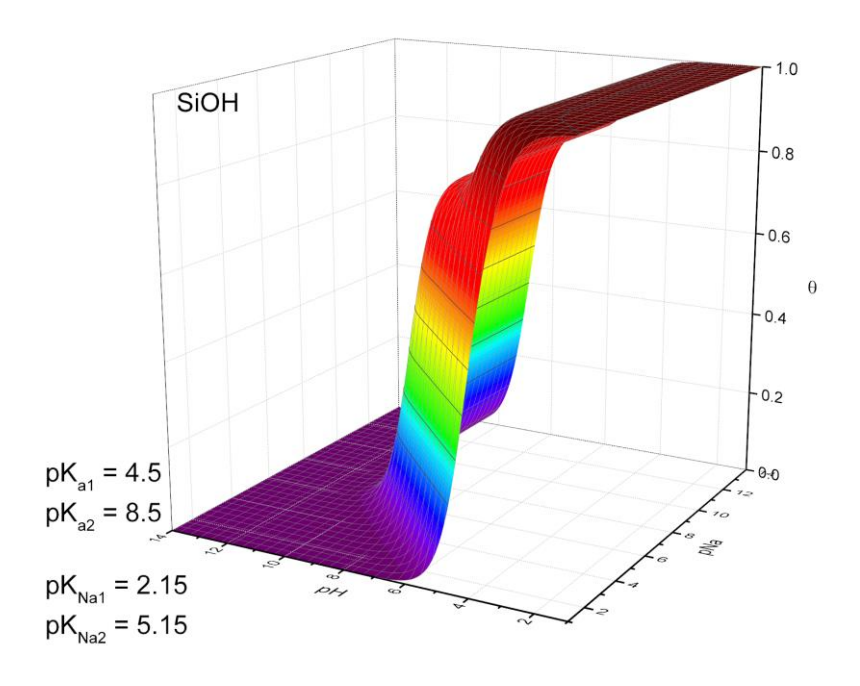


Figure 3.3 Relative abundace of SiOH functionality as a function of pH and pNa.

Experimental

Zeta Potential

Zeta potential solutions were made by suspending 100mg of silica gel (*Aldrich*, *grade 40*, 6-12 *mesh*). Solutions were made at a serious of pH values ranging from pH 1 to pH 11. The pH was adjusted with either hydrochloric acid (*CCI*) or sodium hydroxide (*Mallinckrodt*). The amount of sodium hydroxide used provided negligible ionic strength. A second serious of solutions were made in approximated the same pH range but utilized sodium chloride (*Mallinckrodt*) to provide an ionic strength of 0.1M. Analysis was carried out on a Malvern Instruments ZetaSizer.

Inductively Coupled Plasma

Approximately 10 grams of silica gel (*Aldrich*, *grade 40*, *6-12 mesh*) was weighed out into a beaker. This silica gel was incubated with 0.1M sodium hydroxide (*Mallinckrodt*) for about 5 minutes. This process deprotonates the surfaces and pushes the equilibrium in favor of the formation of the sodium siloxide surface. The silica gel was then rinsed with 0.1M ammonia solution (*Mallinckrodt*) to remove excess sodium hydroxide. This was done to keep the pH sufficiently high so as not to regenerate the silanol groups on the surface and to keep the sodium adsorbed. The sample was then decanted and allowed to dry in an oven overnight at 100°C. After drying, the silica gel was divided into smaller samples of accurately known weights. These samples were then rinsed with 20mL of 2% nitric acid (*Aldrich*) to release the sodium into solution. ICP solutions were then made by diluting the aqueous solutions by a factor of 500 into volumetric glassware. The solutions were made up with 2% nitric acid. ICP standards were made at

concentrations of 0ppm, 5ppm, 10ppm, and 20ppm sodium chloride (*J.T. Baker*). ICP analysis was done on a Varian 710-ES Axial ICP-OES.

Nuclear Magnetic Resonance

Silica gel (*Aldrich, grade 40, 6-12 mesh*) was placed into solution at pH values from approximately 3 to 6. Two sets of solutions were made. One set with only hydrochloric acid solution and the other set with 0.1M sodium chloride (*J.T. Baker*). The saturated silica gel was then placed into a 5mm zirconia rotor and placed into a 5mm chemagnetics CP-MAS probe. The NMR spectrometer was a 9.4T Varian Infinity-Plus spectrometer. For silicon cross polarization experiments, 3200 scans were acquired with a 12ms contact time. ²⁹Si frequency was 79.41MHz. For silicon one-pulse experiments, ¹H decoupling was utilized with a pulse delay of 200s and 64 scan acquisition. For ²³Na one-pulse experiments, spectral frequency was 105.74MHz, pulse delay was 0.1s, and 3200 scans were acquired.

For all ²³Na experiments samples were rinsed with ammonia solution or methanol and then dried overnight before acquisition. All experiments were run at ambient temperature. Silicon reference compound was 4,4-dimethyl-4-silapentane-1-sulfonic acid. Sodium reference compound was sodium chloride. All samples were subject to magic angle spinning at 4kHz.

BET Analysis

Particles were subject to BET analysis on a Micromeritics ASAP 2020 instrument.

Thermogravimetric Analysis

Particles were subject to TGA using a Perkin Elmer Thermogravimetric Analysis TGA 7. Analysis was run in air. Temperature program was as follows; isothermal at 50°C for 1 minute, temperature scan at 40°C/min to 150°C, isothermal at 150°C for 15 minutes, temperature scan at 40°C/min to 700°C, and finally isothermal at 700°C for 15 minutes. For sodium samples and additional hold step was carried out at 350°C for 15 minutes before the ramp to 700°C.

Scanning Electron Microscopy

SEM images were taken using a Carl Zeiss Auriga CrossBeam EVO LS25 scanning electron microscope. This was done to ascertain particles size distribution. Images were acquired at 10⁻⁵ Torr. Accelerating voltage was 2 kV.

Results and Discussion

There are two parts to the work presented in this Chapter. The first lies in characterizing the chemical identity of the different surface species that are present on silica and the second deals with the experimental distribution of these types of sites as a function of experimental conditions. We consider these separately, with the recognition that information from all of the results presented here forms, collectively, a description of the interface. We start with an examination of the mesoscopic morphology of the silica surface, then consider the chemical functionality that is present, and close with a discussion of how different surface species participate as a function of experimental conditions.

Scanning Electron Microscopy

The spatial resolution achievable using SEM is substantially lower than that required to understand the chemical processes that operate on the surface of the silica materials we use. That said, it is instructive to examine SEM images of silica to understand the particle size, shape and distribution. Another interesting issue to examine is the morphological changes that occur on silica surfaces as a function of the chemical conditions the sample is exposed to. One complication of obtaining SEM images of silica is the insulating nature of the material. Typically, SEM requires that the sample, or a thin coating on the sample surface, needs to be conductive in order to obtain images without charging-related distortion. Advances in the technology of SEM, however, have made possible the imaging of insulating materials.

SEM images were taken at several magnifications to assess the morphology of the silica surface over some range of length scales. These images were used to evaluate the effect of treating the surface with Na^+ .

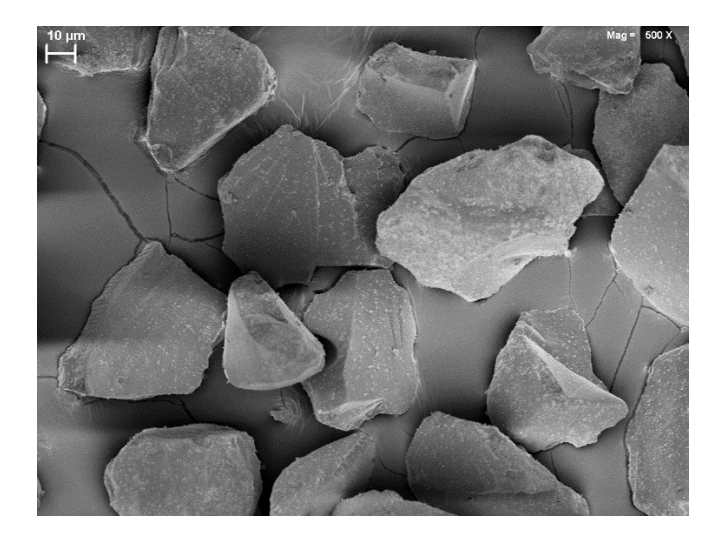


Figure 3.4 SEM image of native silica gel at 500x magnification. General size and shape of the silica gel can be seen. Particle size is roughly 50µm.



Figure 3.5 Image of the native silica surface (untreated). Image shows the native features of the silica gel. Magnification is at 5000x.

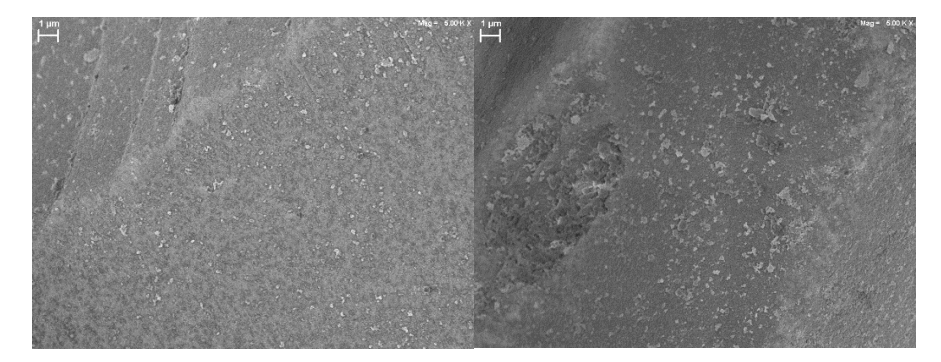


Figure 3.6 Image of the silica surface after treatment with KOH (left) and NaOH (right). Magnification is at 5000x.



Figure 3.7 Image of silica gel after treatment with NaOH followed by regeneration with 2% nitric acid. Image magnification is at 5000x

At 500x magnification the macroscopic size and shape of the silica particles is clear, but there is little or no information on the surface of these silica particles. The particle sizes are roughly 50 µm side-to-side. The apparent brightness of the particles is related to the extent to which the electrons from the electron beam can be conducted to ground. We can also see variations in gray scale color of that are associated with the particles due to their density and conductivity, properties that will depend to at least some extent on the relative amount of Na⁺ bound to the silica surface. In figure 3.4, since the surface is insulating, it is brighter than the surface upon treatment with Na⁺. Upon treatment with sodium or potassium, the surface appears smoother. Silica is soluble to some extent in highly basic media, which could account for the changes in the SEM images. This is likely responsible for the decrease in surface area seen with the BET analysis (*vide infra*). By reducing the roughness of the surface, we reduce the overall available surface area.⁹ The second change is that the certain of the features are darker upon exposure to NaOH and KOH. This is likely due to the presence of Na⁺ or K⁺ on/in the surface layer.

Solid State Nuclear Magnetic Resonance

Solid state NMR spectroscopy was used to characterize the silica surface according to the type and relative amount of chemical functionalities present under a series of controlled conditions. For such measurements the functionality of interest is the surface silanol present is any of several possible forms. To gain surface specific, a cross-polarization method is used where polarization is introduced in the solution phase and transferred to the surface of silica suspended in the solution. The means of generating spatially localized signal is by excitation transfer from the solution phase (¹H nuclei) to ²⁹Si nuclei that can come into direct contact with the excited polarized nuclei. Such an excitation transfer process is termed cross polarization. Cross polarization relies on excitation

transfer from abundant nuclei, in this case hydrogen, to low abundant nuclei, in this experiment silicon. 10-11 The protons on the silica surface are excited by the external magnetic field. The energy is then transferred to the low abundant nuclei, in this case silicon, by low energy pulses across both channels. The length of time over which this transfer is allowed to occur is termed the contact time, which can be varied to optimize the efficiency of the process. After the transfer of energy, the protons and the silicon are decoupled. The free induction decay of the silicon polarization is then monitored. During the cross polarization, the Hartmann-Hahn matching condition must be met. The Hartmann-Hahn condition is that the Larmor frequencies of both nuclei involved in the cross polarization are matched. The length of time for which this condition is met depends on the material and is typically between 5 ms and 20 ms for silica gel experiments. During this time, the protons and silicon atoms are in resonance, facilitating the exchange of polarization. 12

The NMR active nuclei of silicon, ²⁹Si, has a natural abundance of 4.7% and a spin multiplicity of 1/2. ¹³ The NMR active ¹H accounts for 99.98% of hydrogen and has a nuclear spin multiplicity of 1/2. The proximity of the hydrogens to the silicon atoms means that the cross polarization is efficient and can be used to enhance the signal from the silicon nuclei. Since the experiment relies on an excitation transfer from hydrogen to silicon, the technique is selective for silicon nuclei on the silica surface. ¹¹

 23 Na solid state NMR was also used as a method of determining the types of bonding to the silica surface. $^{14-15}$ 23 Na has a natural abundance of 100% and has a spin multiplicity of 3/2. 16 As such, it is an easy target for direct polarization NMR experiments. 23 Na is characterized by short T_1 times, facilitating rapid data collection. 23 Na NMR experiments can provide information on the types of environments occupied by Na⁺ at the silica surface.

 29 Si NMR assignments for silica are well documented in the literature. The distribution of silanols can be seen in Figure 3.8 and are assigned, in order of increasingly negative chemical shift, Q^2 , Q^1 , and Q^0 silica groups on the surface. The peak at -123 ppm corresponds to the bridging siloxanes, the peak at -113 ppm corresponds to Q^1 silanols, and the peak at -104 ppm corresponds to geminal or Q^2 silanols.

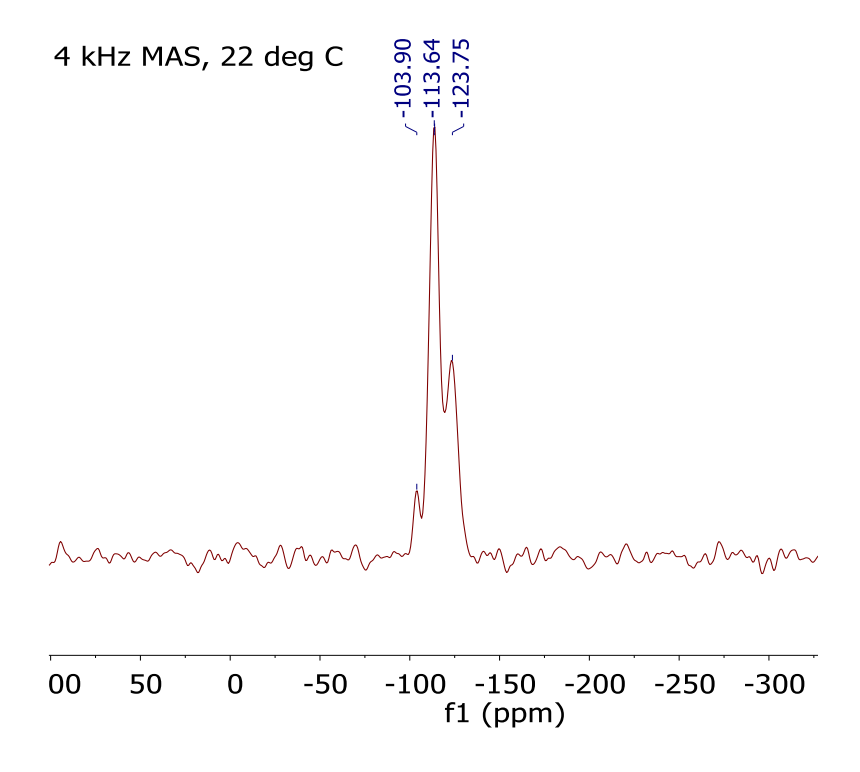


Figure 3.8 Solid state ²⁹Si NMR spectrum of native silica gel suspended in a pH 2 aqueous solution. Peak assignments are as indicated in the text.

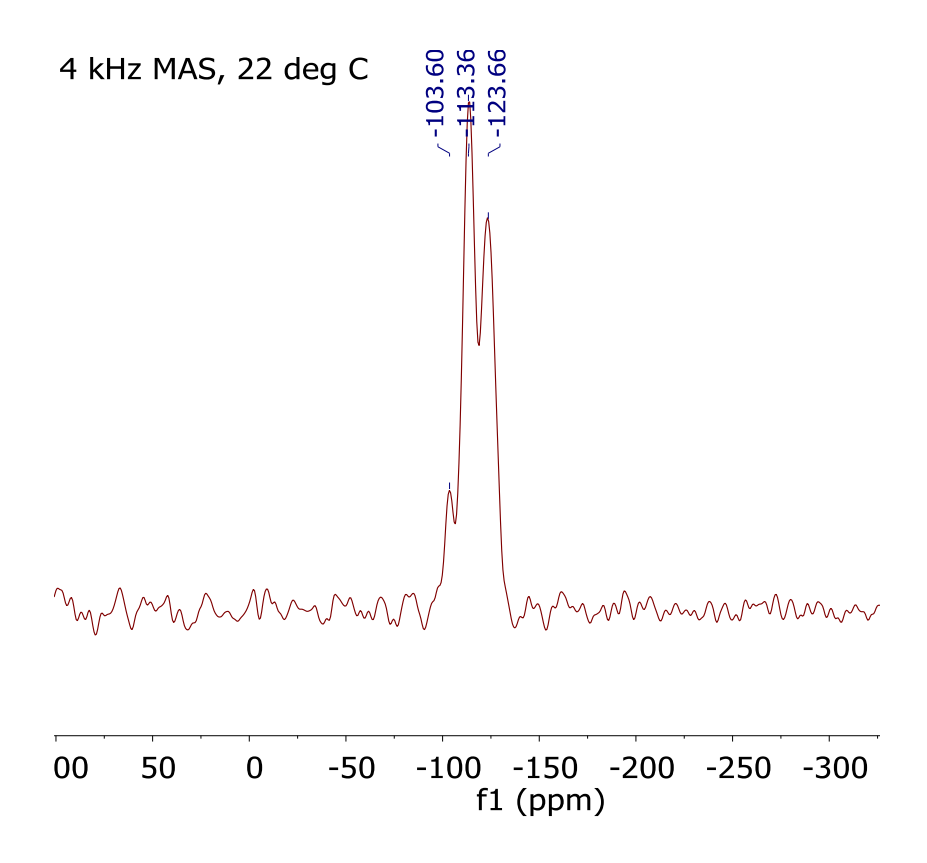


Figure 3.9 Solid state ²⁹Si NMR spectrum of native silica gel suspended in a pH 6.5 aqueous solution. Peak assignments are as indicated in the text.

From the data set where the silica gel is not exposed to Na⁺, we can see a slight change in the spectra between pH 2 and pH 6.5 (Figs. 3.8 and 3.9). The transfer of excitation is efficient below the pKa, 4.5 because the silanol groups are protonated. When the surface is deprotonated, the dissociated protons likely remain in proximity to the siloxide moiety by virtue of electrostatic interactions. Such close proximity does not, however, afford efficient coupling and excitation transfer is less efficient, resulting in a change in the ratio of the Q⁰ and Q¹ peaks. The efficiency of cross polarization of the Q⁰ silicon atoms is invariant with respect to pH. Transfer of excitation is entirely through space. The change in the strength of the Q¹ signal represents a move from through bond cross polarization to entirely through space. The residence time of the hydrogen

to the deprotonated siloxide is small compared to the measurement time. As such what we observe is an average of associated and dissociated species giving rise to the Q^1 signal.

Excitation transfer facilitated by cross polarization is a through-space interaction and there is still some weak association of the protons to the surface even at pH 6.5. With the addition of Na⁺, the NMR spectra for pH below the pKa of silanol (4.5) is similar to that of samples that do not contain added Na⁺ (Fig. 3.10). This is because of the higher concentration of hydrogen ions dominating the competitive equilibria (Eqs. 12 and 13). For conditions where $[Na^+] \ge [H^+]$, the peak ratios in the NMR spectra are seen to change (Fig. 3.11).

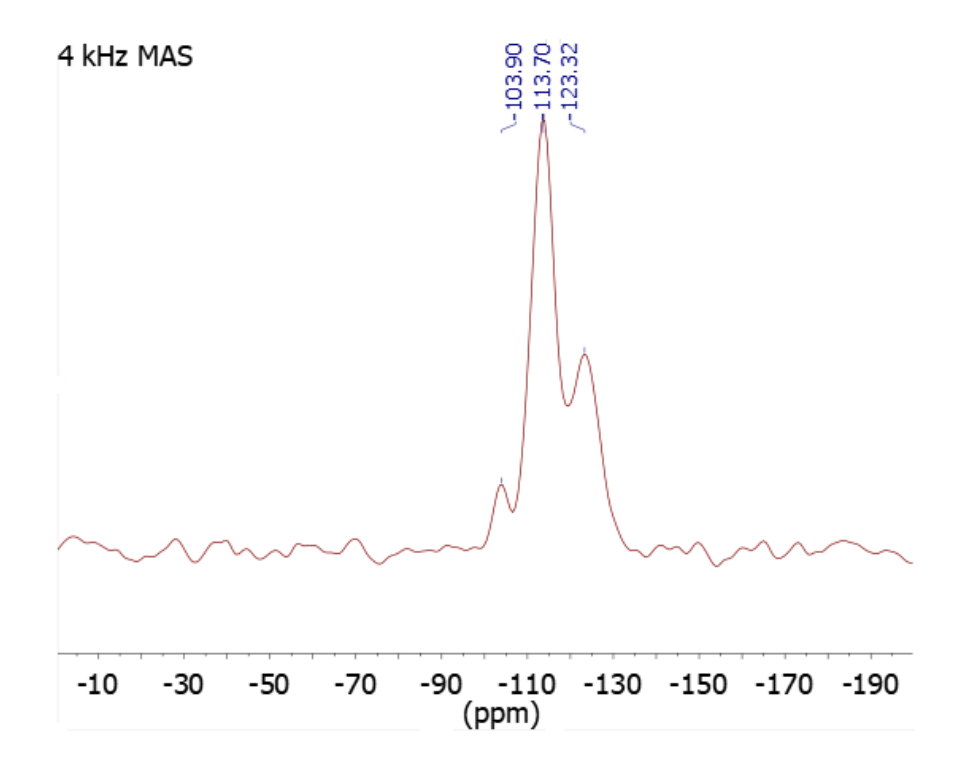


Figure 3.10 29 Si NMR Spectra of the silica surface upon exposure to Na $^+$. The pH of the system is approximately 2.

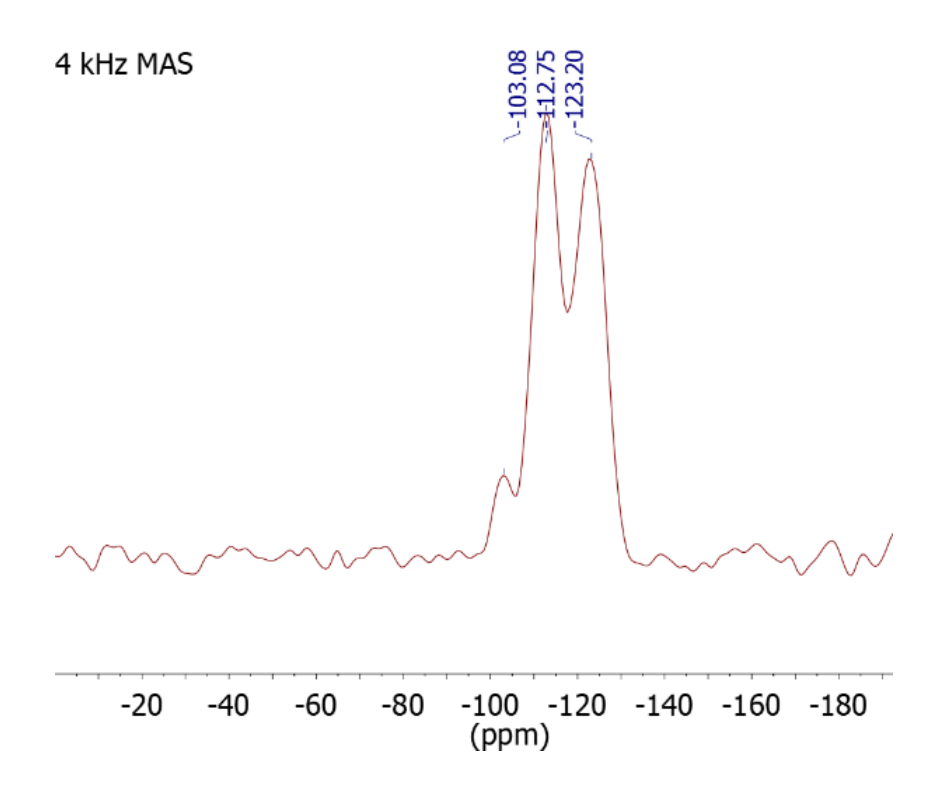


Figure 3.11 Effect of Na⁺ on the silica gel ²⁹Si NMR. The pH of the system is approximately 6.5.

Cross polarization relies on excitation transfer from abundant nuclei, in this case hydrogen, to low abundance nuclei, silicon. When Na^+ is present near the surface, it competes with H^+ for association with anionic siloxide groups. This competition was evaluated previously using contact angle measurements to probe silica surface energy as a function of $[H^+]$ and $[Na^+]$. When the pH is above the pKa of silica, $[Na^+]$ exceeds $[H^+]$, displacing H^+ from the siloxide sites. Excitation transfer from 1H to ^{29}Si is effectively eliminated through the cross-polarization mechanism. In the system with high $[Na^+]$ the ratio of Q^1 to Q^0 is lower than in the absence of Na^+ .

For the 29Si NMR data there appears to be no significant change in chemical shifts of the several species, and this is not a surprising result. We do see however, that the relative ratios of the peaks indicate that there is not overall conservation of signal. Specifically, as the pH of the systems varies, the intensities of the Q^1 and Q^2 peaks (associated with protonated silanols changes

relative to that for Q^0 (bridging siloxane). This finding is consistent with the overall change in extent of protonation with pH. In order to evaluate the properties of the siloxides that have gone silent in cross-coupling experiments, we use 23 Na NMR measurements.

²³Na NMR was performed to evaluate the nature of interactions between Na⁺ and the silica surface. The ²³Na NMR data show that there is only one environment experienced by Na⁺, with the resonance being at a chemical shift of -7.37ppm. This chemical shift is referenced to sodium chloride (0 ppm shift). Literature sources establish a range of chemical shift values for sodium silicates.¹⁵ The type of binding we see is near the chemical shift for one sodium in Na₂SiO₂(OH)₂*5H₂O. The first sodium has a shift of -1.5ppm and the second has a shift of -7.2ppm.

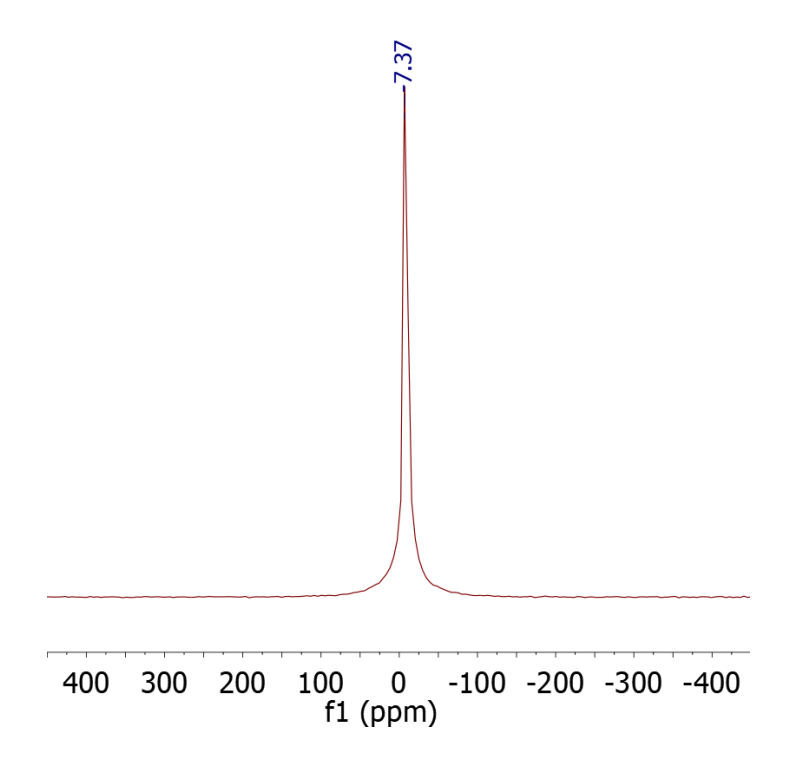


Figure 3.12 ²³Na solid state NMR showing a single environment for interactions with the silica surface.

The data suggests that there is no discernible difference in shielding whether the sodium is bonded to primary silanols or geminal silanols. There are two possible interpretations of this finding. The first is that the resonance is sufficiently broad, and the chemical shifts associated with the primary vs. geminal silanol environments are similar enough that there is a difference but it is not resolvable. The second is that the environments for the primary and geminal species really are the same. In either event, the difference between the two environments is very small, as we have schematized in Fig. 3.13. Comparing ²⁹Si NMR data with ²³Na NMR data allows for several observations. The first is that not all hydrogens are displaced from the surface even in cases where pH > pKa. Despite the equilibrium being shifted to favor the dissociated siloxide form, the implication here is that there can still be protonated (-OH) functionality present on the silica surface, but the fraction of time that it is protonated is much less than the time it is dissociated. Under this condition of dynamic equilibrium, there is opportunity for transfer through crosscoupling even at high pH. The second observation is that competitive equilibria do indeed explain the Na⁺ and H⁺ concentration dependencies described in Eq. 11. Indeed, the similarity of the possible primary and geminal Na⁺ interactions with siloxide suggests a highly dynamic equilibrium for complexation with Na⁺ as well. The fast association and dissociation kinetics of both H⁺ and Na⁺ are consistent with the functional forms of the NMR data as well as the concentration dependencies we have reported.

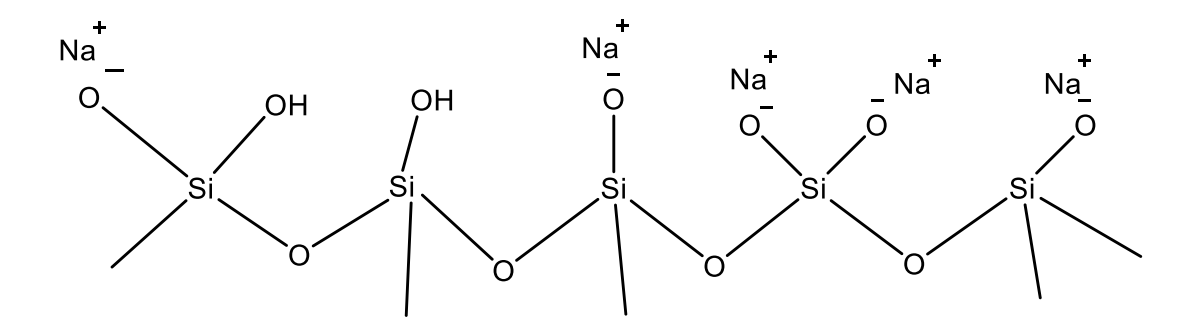


Figure 3.13 A proposed structure of the silica surface after Na⁺ adsorption. Sodium coverage is not 100%

Zeta Potential

The issue of available surface charge for a silica surface is central to the utility of this class of materials. We considered above the expected amount of dissociation of silanol functionalities as a function of pH and pNa, and the ²⁹Si and ²³Na NMR data demonstrate changes in the distribution of the chemical state of these labile functionalities with variation in experimental conditions. All of this information is useful but determining experimentally the amount of charge present on a silica surface can be challenging. The zeta potential is a quantity that, while not tied from first principles to the surface charge density, is a measure of the effective surface potential. The zeta potential is related to the electric double layer that forms at a charged interface, and it is therefore expected to vary not only with surface charge density but also with the ionic strength and chemical identity of solution constituents. ¹⁹ Zeta potential is measured readily and because of the factors that contribute this quantity, it is a useful means of characterizing the relative extent of dissociation present at a surface. Zeta potential is a quantity that has been used to assess the stability of colloidal suspensions, ²⁰ and silica gel suspensions are readily prepared under the range of conditions we are concerned with here.

As noted above, the pH of the solution in which the silica resides determines the extent to which the surface is protonated. This property is central to the use of silica in applications such as capillary electrophoresis, where electroosmotic flow is related directly to the fraction of SiO surface constituents and thus the zeta potential of the surface.²¹⁻²²

Figure 3.14 details the zeta potential measurements acquired. At pH values below 4.5, the silica surface is neutral and is characterized by a zeta potential near zero. Above 4.5, the silica surface is deprotonated and has negative zeta potential values. The data below shows a trend of zeta potential as a function of pH with and without the presence of Na⁺. As the pH increases, the zeta potential moves from approximately 0mV to about -15mV due to the deprotonation of the silanol groups. The deprotonation in the vicinity of the first pKa (ca. 4.5) is only for the most labile of hydrogens which account for about 20% of the surface. The remaining silanols are characterized by a pKa of ca. 8.5. As the pH increases to about 7, the zeta potential drops to about -30mV.

Upon addition of Na⁺ we observe changes in zeta potential as a function of pH that differ from what was seen in the absence of Na⁺. When the pH is below the pKa, the surface is still effectively neutral. However, when the pH becomes greater than the pKa, the silanols are deprotonated and attract Na⁺ ions. The association of SiO⁻ and Na⁺ serves to neutralize some of the surface charge, making the zeta potential less negative.²³ Experimentally, the zeta potential upon addition of 0.1M Na⁺ is only about -5mV as opposed to -15mV without Na⁺. At high pH, the zeta potential becomes more negative, ca. -30mV, consistent with calculated predictions as the surface is deprotonated more fully.

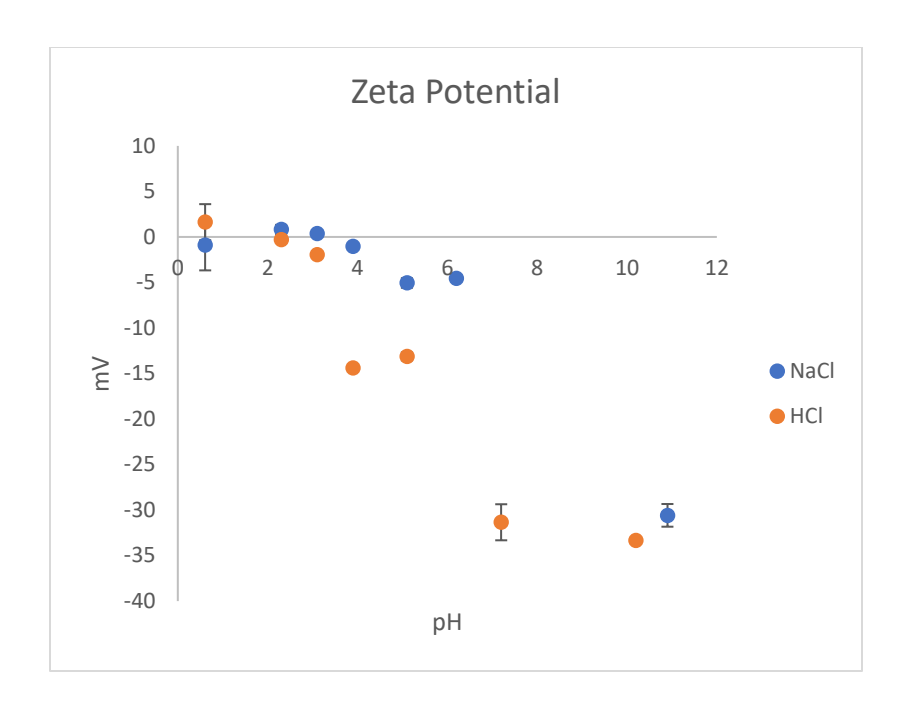


Figure 3.14 Zeta potential measurements of silica gel suspended in solutions of either NaCl or HCl. Small amounts of NaOH were used in pH >7 measurements.

Inductively Coupled Plasma

Inductively coupled plasma was used as a technique to quantify the amount of active silanol groups on the surface. Since silica gel is an ion exchanger, it can absorb metal ions, in this case sodium, from aqueous solution. 4, 24-25 Depending on the pH and the ionic strength of the solution, the sodium atoms adsorb to the surface forming sodium siloxide bonds. Excess sodium hydroxide must be removed to avoid carry over of sodium that is not bound to the surface. By rinsing the silica gel with methanol unbound sodium and excess sodium hydroxide are removed from the solid. The surface is then regenerated with a solution of nitric acid. Since the pH of the solution is dropped below the pKa of the surface, the surface silanols are regenerated and the sodium ions are released into solution. This aqueous overlayer is then analyzed by ICP to quantify the amount of sodium that was adsorbed onto the surface.

A key question when dealing with silica is that of the areal density of surface silanol groups. This is a question that can be addressed in several ways, one of which is by measuring surface loading of Na⁺. Under the appropriate initial conditions (high pH, exposure to Na⁺) Assuming Na⁺ is monodentate, and that Na⁺ dissociated from the surface siloxide can be measured directly allows quantification of the surface silanols that took part in an adsorption reaction. We measure the amount of Na+ dissociated from silica using inductively coupled plasma (ICP) atomic emission spectroscopy.²⁶

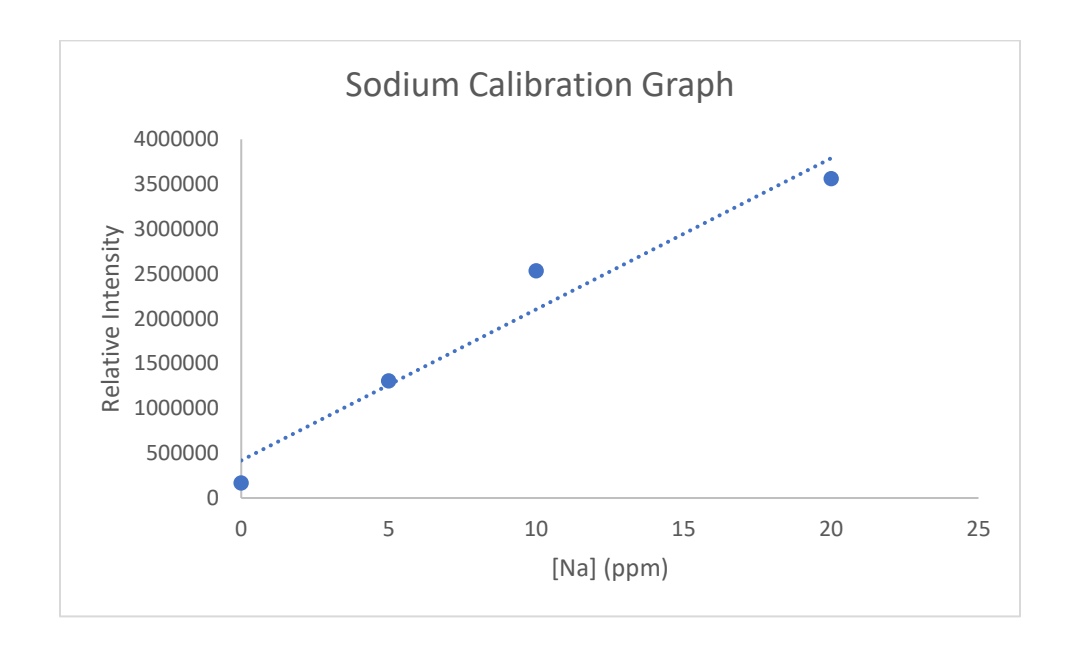


Figure 3.15 Calibration graph of Na⁺ ICP data.

Trial	[Na] ppm	mass of Na ⁺ in soln. (mg)	mass of Na ⁺ liberated (mg)	mass of Na ⁺ liberated per gram of SiO ₂ (mg/g)
1	2.45	0.245	24.5	15.7
2	2.96	0.296	29.6	18.0
3	2.28	0.228	22.8	14.7
4	2.21	0.221	22.1	14.8
5	1.84	0.184	18.4	11.9
6	2.17	0.217	21.7	13.0
Average	2.32	0.232	23.2	14.7

Table 3.1 Quantification of Na⁺ liberated in ICP experiments.

ICP, used in conjunction with BET isotherm data and NMR data can be used to calculate the areal density of surface functional groups (Fig. 3.15, Table 3.1). From the BET data we have two experimentally determined surface areas, one without sodium on the surface and one with. From the ²³Na NMR data we observe only one binding site to within the resolution of the measurement. The ICP data show that 14.7 mg of Na⁺ is adsorbed from solution per gram of silica gel. Assuming a uniform distribution of adsorption sites when averaged over a sufficiently large (µm) length scale, the concentration of surface functional groups that undergo sodium siloxide formation is in the range of 1.6 µmol/m² to 2.2 µmol/m². Literature values for surface silanol concentration are typically in the range of 5 μ mol/m² to 8 μ mol/m². In our determination, there are assumptions that may account for the apparent discrepancy. Our experiments sense the chemically accessible and active silanol groups that are capable of undergoing Na⁺ exchange. The ICP experiment was carried out using 0.1M NaOH to exhaustively deprotonate the silica functionalities and provide Na⁺. The ²⁹Si NMR data show that not every silanol group undergoes Na⁺ exchange. There is still signal from primary silanols. In addition, we have assumed that Na⁺ does not interact with the bridging siloxanes. If there were Na⁺-siloxane interactions, it would give rise to more Na⁺ binding (and release) than for the formation of SiO-Na⁺, and we observe a negative deviation from the expected areal density. Thus, this latter possibility is unlikely.

Thermogravimetric Analysis

Another means of estimating the silanol group density is by dehydration of the silica. Dehydration can be quantitated through thermogravimetric analysis (TGA). There are two steps in the dehydration process. The first is removal of adsorbed water at or slightly above the boiling point of water. Once adsorbed water is removed, surface condensation of silanol groups to form siloxane bridges is achieved by heating to temperatures above 600°C. The hydroxyl groups lose molecular water when forming bridging siloxanes and this loss of water can be quantified.²⁷⁻²⁸ Another way of expressing this is that we quantitate the conversion of Q² and Q¹ sites to Q⁰ sites.

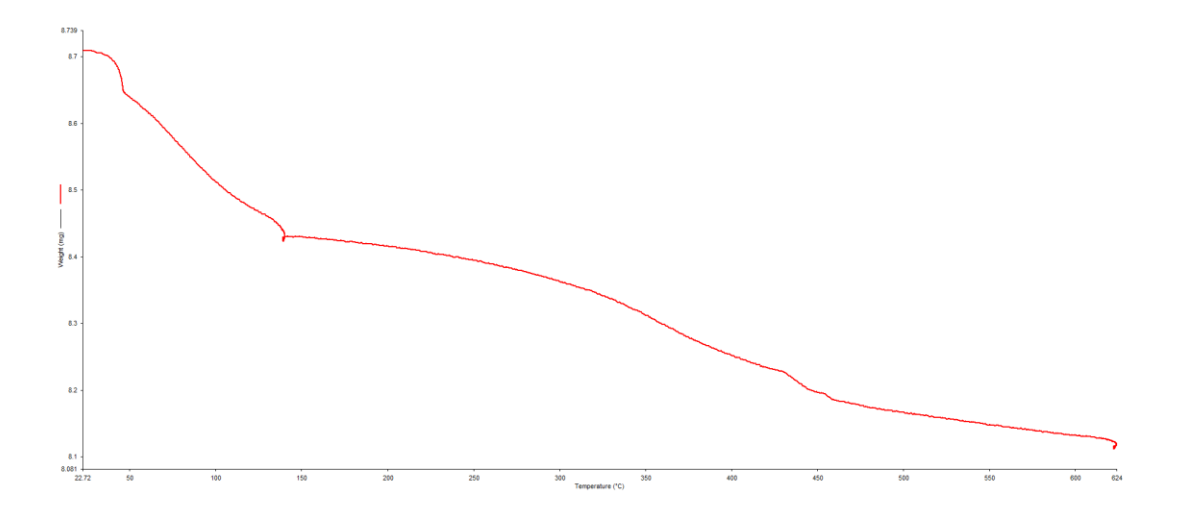


Figure 3.16 Example TGA data showing the dehydration of the silica surface. This surface was treated with NaOH before TGA analysis.

We use TGA to quantitate loss of silanol groups (Fig. 3.16).³ Using a dry silica mass of 8.442 mg and a surface area of $402.9 \text{ m}^2/\text{g}$, obtained by BET analysis, the initial surface OH density was calculated to be $3.56 \,\mu\text{mol/m}^2$. When treated with NaOH, using a dry mass of 8.427 mg and a surface area of $293.7 \, \text{m}^2/\text{g}$ (BET analysis), a value of $7.02 \,\mu\text{mol/m}^2$ was calculated from TGA data. While these numbers are near those expected from the literature, the increased silanol density

of the NaOH-treated surface requires that the base etched the silica to produce higher surface area to be accounted for. It may also be possible that remaining trace NaOH deliquesced upon exposure to atmosphere and introduced additional water to the system.²⁹ The amount of water present can was determined by a more detailed TGA analysis. By holding the temperature constant at 350°C it was calculated that there are 3.56 µmol/m² of water being held by NaOH, or ca. two water molecules per Na⁺. In this way we account for approximately half of the surface silanols.

The concentration of surface silanols in the second Na⁺ dehydration is *ca*. 3.11 µmol/m². We posit that, to within the uncertainty of the measurement, this is the same as the silanol density determined by ICP analysis, and these numbers are consistent or very slightly lower than the typical literature range of silanol groups.

Conclusion

Using these various techniques, the silica surface was further characterized and its reactivity to various chemical conditions was investigated. The nature of the silica surface depends greatly on its production methods and its chemical exposure prior to use. Exposure to metal ions displaces protons from the surface. This is especially true at high pH values that facilitate deprotonation of the surface. These deprotonated sites can be effectively quantified by grafting with group one cations such as sodium or potassium. By treating the system with an appropriate base such as sodium hydroxide, rinsing with ammonium hydroxide, oven drying, and then resuspending in an appropriate acid such as nitric acid, the concentration of metal ions bound to the surface can be measured.

The physical morphologies of the silica surface can be analyzed with scanning electron microscopy to show the changes in the nature of the surface after chemical treatment. Grafting of metal ions to the surface was confirmed by watching the nature of the surface change from insulating to conductive. The association of metal ions with the surface was also confirmed by zeta potential measurements. We see a reduction in zeta potential with an increase in ionic strength.

Additionally, these sites can be investigated by other methods such as NMR due to the electrostatic attraction of the metal ion to the surface. This gives insight into the type of binding metal ions have with the surface. Coverage of the surface is maximized by use of strong base to deprotonate the entire surface. By showing a single peak in the sodium NMR we confirm a single type of binding of monovalent sodium to the silica surface.

LITERATURE CITED

LITERATURE CITED

- 1. Zhuravlev, L. T., The Surface Chemistry of Amorphous Silica. Zhuravlev model. *Colloids and Surfaces* **2000**, (173), 1-38.
- 2. Lochmüller, C. H.; Kersey, M. T., Effect of Thermal Pretreatment on the Surface Reactivity of Amorphous Silica. *Langmuir* **1988**, *4* (3), 572-578.
- 3. Zhuravlev, L. T., Concentration of Hydroxyl Groups on the Surface of Amorphous Silicas. *Langmuir* **1987**, *3*, 316-318.
- 4. Ahrland, S.; Grenthe, I.; Noren, B., The Ion Exchange Properties of Silica Gel. *Acta Chemica Scandinavica* **1960**, *14*, 1059-1076.
- 5. Stubbs, B.;Blanchard, G. J., Measuring Competing Equilibria at a Silica Surface through the Contact Angle of a Nonpolar Liquid. *Langmuir* **2017**, *33* (38), 9632-9636.
- 6. Schrader, A. M.; Monroe, J. I.; Sheil, R.; Dobbs, H. A.; Keller, T. J.; Li, Y.; Jain, S.; Shell, M. S.; Israelachvili, J. N.; Han, S., Surface Chemical Heterogeneity Modulates Silica Surface Hydration. *Proceedings of the National Acadey of Sciences* **2018**, *115* (12), 2890-2895.
- 7. Endo, A.; Yamada, M.; Kataoka, S.; Sano, T.; Inagi, Y.; AMiyaki, A., Direct Observation of Surface Structure of Mesoporous Silica With Low Acceleration Voltage FE-SEM. *Colloids and Surfaces A: Physicochemical and Engineering Aspects* **2010**, *357* (1-3), 11-16.
- 8. Donald, A. M., The Use of Environmental Scanning Electron Microscopy for Imaging Wet and Insulating Materials. *Nature Materials* **2003**, *2*, 511-516.
- 9. Crundwell, F. K., On the Mechanism of the Dissolution of Quartz and Silica in Aqueous Solutions. *ACS Omega* **2017**, *2* (3), 1116-1127.
- 10. Sindorf, D. W.;Maciel, G. E., 29-Si NMR Study of Dehydrated/Rehydrated Silica Gel Using Cross Polarization and Magic Angle Spinning. *J. Am. Chem. Soc.* **1983**, *105*, 1487-1497.
- 11. Maciel, G. E.; Sindorf, D. W., Silicon-29 Nuclear Magnetic Resonance Study of the Surface of SIlica Gel by Cross Polarization and Magic-Angle Spinning. *J. Am. Chem. Soc.* **1980**, *102*, 7606-7607.
- 12. Kolodziejski, W.;Klinowski, J., Kinetics of Cross-Polarization in Solid State NMR: A Guide for Chemists. *Chem. Rev.* **2002**, *102* (3), 613-628.
- 13. NMR Periodic Table: Silicon NMR. http://triton.iqfr.csic.es/guide/eNMR/chem/Si.html (accessed 30 August 2019).

- 14. Wong, A.; Wu, G., Solid- State Nuclear Magnetic Resonance of Sodium Complexes with Crown Ethers, Cryptands, and Naturally Occurring Antibiotic Ionophores: A direct Probe to the Sodium-Binding Sites. *J. Phys. Chem. A* **2000**, *104* (51), 11844-11852.
- 15. Koller, H.; Engelhardt, G.; Kentgens, A. P. M.; Sauer, J., 23Na NMR Spectroscopy of Solids: Interpretation of Quadrupole Interaction Parameters and Chemical Shifts. *J. Phys. Chem.* **1994**, 98, 1544-1551.
- 16. Mackenzie, K. J. D.;Smith, M. E., *Multinuclear Solid-State NMR of Inorganic Materials*. Pergamon: Kidlington, Oxford, 2002; Vol. 6.
- 17. Vega, A. J.; Scherer, G. W., Study of Structural Evolution of Silica Gel Using 1-H and 29-Si NMR. *Journal of Non-Crystalline Solids* **1989**, *111*, 153-166.
- 18. Brus, J.; Jegoroc, A., Through-Bonds and Through-Space Solid-State NMR Correlations at Natural Isotopic Abundance: Signal Assignment and Structural Study of Simvastatin. *J. Phys. Chem. A* **2004**, *108* (18), 3955-3964.
- 19. Wang, M.;Revil, A., Electrochemical Charge of Silica Surfaces at High Ionic Strength in Narrow Channels. *Journal of Colloid and Interface Science* **2010**, *343* (1), 381-386.
- 20. Juniop, J. A. A.; Baldo, J. B., The Behavior of Zeta Potential of Silica Suspensions. *New Journal of Glass and Ceramics* **2014**, (4), 29-37.
- 21. Sze, A.; Erickson, D.; Ren, L.; Li, D., Zeta-Potential Measurement Using the Smoluchowski Equation and the Slope of the Current-Time Relationship in Electroosmotic Flow. *Journal of Colloid and Interface Science* **2003**, *261* (2), 402-410.
- 22. Schwer, C.; Kenndler, E., Electrophoresis in Fused-Silica Capillaries: The Influence of Organic Solvents on the Electroosmotic Velocity and the Zeta Potential. *Analytical Chemistry* **1991**, *63*, 1801-1807.
- 23. Qin, W.; Wu, J.; Jiao, F., Mechanism of Different Particle Sizes of Quartz Activated by Metallic Ion in Butyl Xanthate Solution. *Journal of Central South University* **2017**, *24* (1), 56-61.
- 24. Repo, E.; Warchoł, J.; Bhatnagar, A.; Sillanpää, M., Heavy metals adsorption by novel EDTA-modified chitosan-silica hybrid materials. *Journal of Colloid and Interface Science* **2011**, *358* (1), 261-267.
- 25. Karnib, M.; Kabbani, A.; Holail, H.; Olama, Z., Heavy Metal Removal Using Activated Carbon, Silica and Silica Activated Carbon Composite. *Energy procedia* **2014**, *50*, 113-120.
- 26. Wang, Z.;Schwartz, A. J.;Ray, S. J.;Hieftje, G. M., Determination of Trace Sodium, Lithium, Magnesium, and Potassium Impurities in Colloidal Silica by Slurry Introduction Into An Atmospheric-Pressure Solution-Cathode Glow Discharge and Atomic Emission Spectrometry. *J. Anal. At. Spectrom.* **2013**, *28*, 234-240.

- 27. Mueller, R.; Kammler, H. K.; Wegner, K.; Pratsinis, S. E., OH Surface Density of SiO2 and TiO2 by Thermogravimetric Analysis. *Langmuir* **2003**, *19* (1), 160-165.
- 28. Peng, L.; Qisui, W.; Xi, L.; Chaocan, Z., Investigation of the States of Water and OH Groups on the Surface of Silica. *Colloid and Surfaces A: Physicochemical and Engineering Aspects* **2009**, *334* (1-3), 112-115.
- 29. Rowley, C. N.;Roux, B., The Solvation Structure of Na+ and K+ in Liquid Water Determined from High Level ab Initio Molecular Dynamics Simulations. *J. Chem. Theory Comput.* **2012**, *8* (10), 3526-3535.

Chapter 4

Abstract

Aqueous normal phase high performance liquid chromatography (HPLC) was utilized to characterize the distribution of species present on a silica surface. The effects of mobile phase composition on the elution time of phenol were investigated using a normal phase column. The mobile phase was varied between 100% methanol and 100% water. A single peak eluted for 100% methanol mobile phase. At the other extreme, multiple peaks eluted for phenol in water. We posit that the multiple peaks are seen due to the effects of the distribution of silanol groups on the silica surface. The energies of interaction between the several types of silanol functionality and phenol differ and under the appropriate experimental conditions these different interactions can be resolved. The mass transport between the stationary phase and mobile phase was the dominant effect seen in these experiments. The surface mass transport term of the van Deemter equation is a combination at least three mass transport terms for the different types of silanols that are on the surface.

Introduction

The overarching goal of this work is to understand the role of the Si-OX functionality in determining the properties of silica surfaces. While this may appear to be a simplistic goal on its face owing to the fact that Si-O is the dominant chemical bond in silica, the morphology of this material and the different forms that the Si-O bond may take have served to make this material sufficiently complex that the determination of something as simple as the surface Si-OH density

is known to only within a factor of two.¹⁻² Understanding the surface chemistry and morphology of silica has significant commercial and practical implications, however. Silica is used widely in chemical separations, as a structural material for chemical and other containers, and as a building material. For the latter two applications, exposure of silica to extreme environmental and chemical conditions can alter the properties of the material. In addition, sand, which is primarily particulate silica, is one of the most common materials on the planet.³

In our earlier work we focused on the relationship between the surface silanol functionality and the species in immediate contact with it. Specifically, we found that the surface energy difference between a silanol (Si-OH) and a sodium siloxide (Si-ONa) surface was modest but could be controlled through the action of competitive equilibria. This work addressed the question of the role of solution phase pH and ionic strength in determining the relative abundance of Si-O-functionality on the surface of silica. That information is of immediate importance in chemical separations such as capillary electrophoresis, where the amount of surface charge carried by the silica capillary inner surface determines the fluid flow behavior of the system. In this Chapter, we consider the broader question of the role of different surface Si-O functionality on the properties of the silica surface.

Chromatographic separations have made extensive use of silica, in part because it can be prepared in a variety of morphologies, ranging from narrow-bore capillaries to finely divided particulate.⁶ Silica has found use in the latter form primarily because of the achievable surfacearea to volume ratio.⁷ In addition, the silica surface, while understood to a limited extent, is sufficiently chemically reactive that a variety of modifications have been performed to control surface polarity, hydrophobicity and other macroscopic properties.⁸ Modified silica is the material upon which reverse phase HPLC relies, for example.⁹

Because the technology of chromatography is well developed, the study of the surface properties of silica can be performed using this instrumentation. A normal phase HPLC packed column is a physical structure that provides a comparatively high accessible silica surface area and allows for controlled flow of specific solution phase compounds over the stationary phase. The difficulty in using such an experimental configuration is that when used in a manner that is typical for efficient chemical separations, all information regarding the heterogeneity of the silica (stationary phase) surface is averaged over a very large number of molecule-surface interactions. For this reason, any detailed information on the distribution of surface-sites with which analyte molecules interact is obscured. In the work reported here, however, the goal was not to achieve efficient separation of multiple analytes. The goal of this work was to evaluate the different types of silica surface sites using a single analyte molecule. While this may be antithetical to the traditional application of chromatographic separations, it is useful to describe the system in the parlance of chemical separations to make connection to the separations literature.

One of the issues with chemical separations is the ability to compare results from one system to another, and as a consequence of the various configurations a standardized methodology of expressing separation efficiency has been devised. The most widely used independent variables in chemical separations are temperature of the system and the rate at which the mobile phase is passed through the stationary phase, typically described as a flowrate or a mobile phase velocity (u).¹⁰ The dependent variables are the time required for analyte(s) to elute from the column (t_R) and the shape of the distribution of analyte(s) exiting the stationary phase (σ). The quantity t_R is measured relative to the time it takes for a non-interacting species to pass over the chromatographic stationary phase, referred to as the dead time.¹¹ The ability to achieve a chemical separation is determined by the resolution of the system, which is a measure of the system to distinguish

between two analyte peaks, which depends on the width of the peaks (σ) and difference in retention time (t_R) for the two species.¹²

Ultimately, chromatographic separation is an inefficient process, comparing slight differences in the way in which two or more (similar) compounds interact with the stationary phase surface. For most stationary phases, there is not a high degree of chemical specificity for the adsorption of analytes. In other words, the energy of interaction between the analyte and the stationary phase surface (expressed as K_{eq} or ΔG) differs very little for structurally similar analytes, and it is only by virtue of the large number of equilibration cycles of adsorption and desorption of the analyte(s) from the stationary phase surface that a separation can be observed. There are several experimental quantities that serve to broaden chromatographic peaks and thus serve to limit resolution, and these factors have been described by van Deemter. ¹³ To evaluate the separation efficiency, an artificial construct termed a "theoretical plate" has been developed to describe the physical thickness of a zone required for the equilibration of an analyte with the stationary phase (H). The term H is "height equivalent theoretical plate", and it is expected to depend on the morphological properties of the stationary phase, Brownian diffusion of the analyte(s) in the mobile phase, and the kinetics of the equilibration process for adsorption and solvation. The van Deemter equation¹⁴ is given by

$$H = A + \frac{B}{u} + \left(C_s + C_m\right)u\tag{4.1}$$

Where H is defined above, u is the flow velocity of the mobile phase, A is a term that describes that distribution of pathways through the stationary phase, B is a term that accounts for Brownian diffusion of analyte in the mobile phase, and the terms C_s and C_m are referred to as the mass transfer terms for the stationary phase (s) and mobile phase (m), respectively. It is important

to note that this equation is purely empirical and is not derived from first principles. None the less, it is still useful in describing the relationship between H and u, and the experimental properties of the system. The functional form of H(u) is shown in Fig. 4.1, with the contribution of each of the terms being shown also.

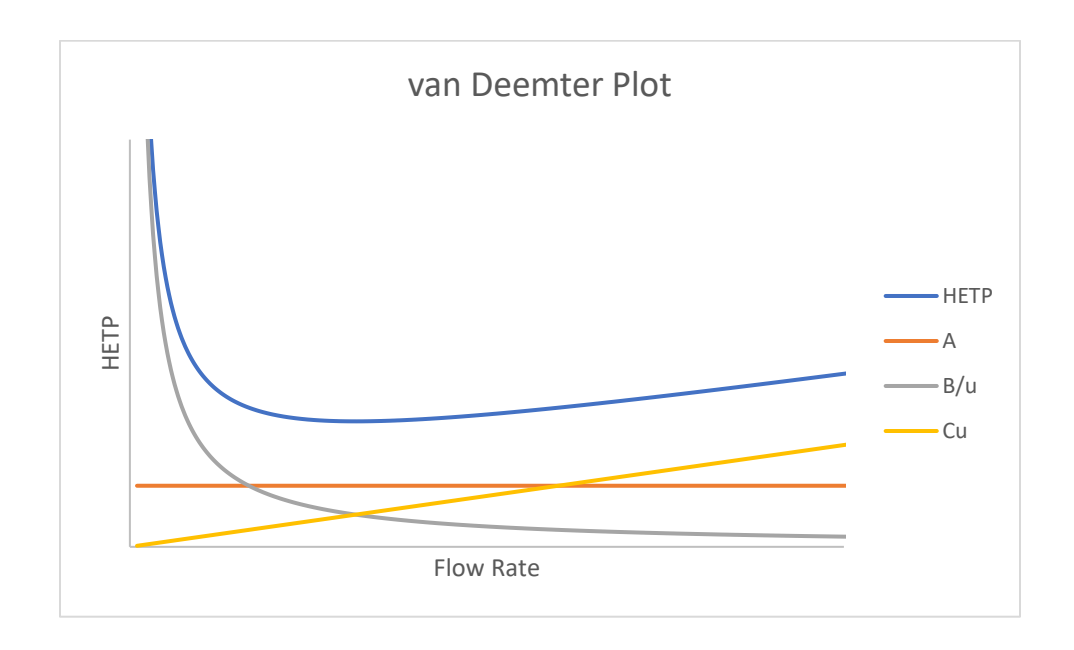


Figure 4.1 van Deemter plot showing the dependence of H(u) on flow rate. A, B, and C are the van Deemter factors that govern H(u) and u is the flow rate of the system.

For typical applications in separations, the goal is to determine the experimental that provide the smallest value of H (dH/du = 0), which physically corresponds to the shortest length of stationary phase required to achieve an equilibrium condition between the analyte in the solution (mobile) phase and adsorbed to the surface of the stationary phase. Such a condition typically obtains for values of N on the order of tens of thousands to hundreds of thousands for reverse phase HPLC or normal phase HPLC. $^{15-16}A$ is the term that describes diffusion through the material in the column. Since the column does not have ideal packing, the analyte has various paths that it can take through the packing material as it traverses the column. B describes longitudinal diffusion

through the column. As the separation progresses, the analyte band broadens as it travels through the column. 17 C is the mass transfer coefficient. It deals with the partitioning of the analyte between the mobile and stationary phases. The flow rate, u, affects the B and C terms of the equation as both terms involve mass transport with the stationary phase. 18 The higher the flow rate, the less time the analyte has to interact with the column, C term. This typically lowers the separation efficiency. Additionally, the lower the flow rate the poorer the separation efficiency. This is due to the diffusional term having a greater effect on the separation. The slower the flow rate, the more the effects of longitudinal diffusion exert themselves. Due to these two effects, there exists an optimal flow rate at which the mass transport term is maximized, and the longitudinal diffusion term is minimized. The combination of these leads to a flow rate at which separation efficiency is maximized.

The mechanism for separation involves partitioning of the analyte between the mobile phase and the stationary phase. 19-20 As the analytes enter the column, they are typically dissolved in a carrier solvent. As they enter the column, the analytes dissolve into the mobile phase. From here, they partition onto the stationary phase where they are held back based on the strength of their interactions. The strength of the interaction determines how long the analytes stick to the stationary phase before they redissolve into the mobile phase. This process continues for the length of the column. As different analytes have different affinities for the stationary phase, the separation increases as the sample plug travels down the column. As the analytes exit the column, they are observed by the detector. The length of time from injection into the column to detector is known as the retention time. The more discernible the difference in affinity for the stationary phase, the larger the difference in retention time for the analytes. The length of the column helps determine the resolution between the peaks.

The chromatogram shows the analytes as they elute from the column. In an ideal separation scheme, each analyte is shown as an individual peak that is separate from other peaks. The time difference between these peaks is known as the resolution. The peaks show Gaussian distribution since there is a slight delay between when the analyte is first picked up by the detector to when all of the analyte has cleared the detector. The broadness of the peak is determined by many factors, most importantly the longitudinal diffusion. The longer the analytes are allowed to diffuse throughout the column, the broader the peaks once the analytes reach the detector.

As noted above, the larger purpose of this work is to characterize the properties of the silica surface, with the knowledge that there are multiple different chemical and physical environments present under any given set of conditions for temperatures below the melting point of silica. In order to characterize these surface sites, we use NMR measurements to determine the structural identity of the various sites (Chapter 3) and a variant of normal phase HPLC measurements to evaluate the differences in chemical interactions between a molecular probe (phenol) and the different surface silica species. With this frame of reference, we describe below a series of experiments designed to interrogate the molecular interactions of different Si-O species on the silica surface.

Experimental

HPLC grade water (Sigma) and HPLC grade methanol (Sigma) were utilized as mobile phase constituents in this work. Sodium chloride (Sigma, 99.8%) was to adjust ionic strength where appropriate, 0 M and 0.1 M. The pH of the system using 100% water was adjusted using hydrochloric acid. The pH was adjusted from pH 2 to pH 6. Analysis was done on a Shimadzu

HPLC instrument. An Ascentis Si silica column, dimensions $15 \text{ cm} \times 4.6 \text{ mm}$, $5 \mu \text{m}$ was purchased from Supelco. For experiments designed to gauge the effect of mobile phase composition, water and methanol were varied from 0% to 100% (v/v). Phenol (Sigma, $\geq 99\%$) was used as the molecular probe and was dissolved in ethanol (Koptec, 100%) at a concentration of 1 mg/mL. Column temperature was thermoregulated to 30°C for all measurements. Detection was by UV absorbance at 254 nm (deuterium lamp) with a spectral bandwidth of 4 nm on a PDA Multiarray detector.

Results and Discussion

The data reported in this chapter appear to represent anomalous behavior relative to that seen for a traditional chromatographic separation, and it is important to first address the reasons for the functional form of the data. As noted above, a typical chromatographic separation involves a sample containing multiple components and the chromatographic process produces a single peak for each detected analyte. The data we report here are for a single analyte and under certain experimental conditions, up to four peaks can result from the single constituent. This unusual result requires verification through control experiments and an explanation.

The first order of business is to verify that the analyte is pure. This has been established by comparison of reported ¹H and ¹³C NMR spectra of phenol to that we acquired for the phenol used in this work. The spectra matched with no additional peaks. UV-visible absorbance spectra and fluorescence spectra also revealed no bands other than those expected for phenol. Thin layer chromatography using silica plates and a variety of solvent systems revealed no additional constituents in the phenol used in this work.

Under the assumption that the phenol is sufficiently pure to produce one peak under typical chromatographic operating conditions, the key issue is the presence of several chromatographic peaks under conditions where the mobile phase contains 20% (v/v) or more of water (Fig 4.2).

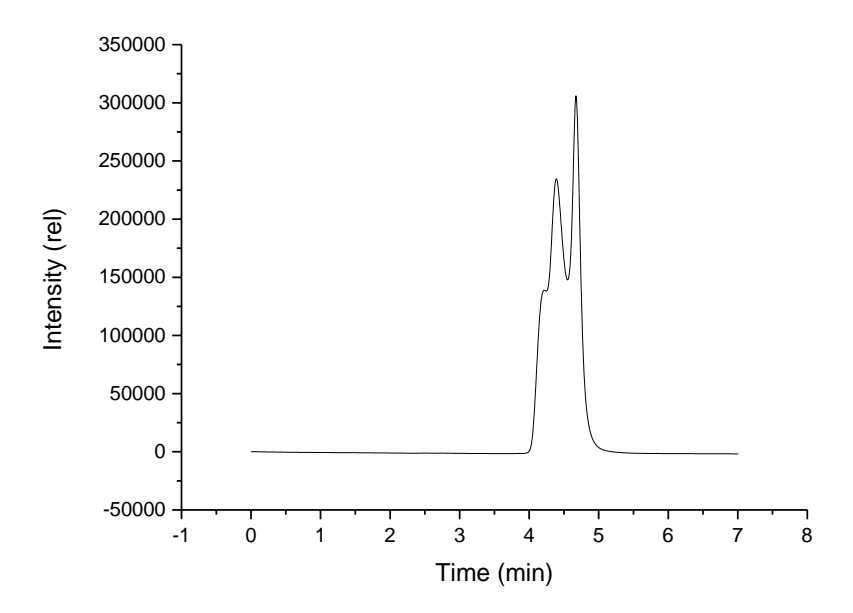


Figure 4.2 Chromatogram showing the splitting of peaks at 20% water/80% methanol.

Such a finding runs counter to what is expected for chromatographic separations, where one peak corresponds to one analyte. The implication is that the interactions between the analyte and column can be separated into discrete categories that are not equivalent. If there is only one type of analyte present, the implication of these data is that there are multiple inequivalent adsorption sites on the silica stationary phase. Under typical chromatographic conditions, there a given analyte molecule experiences interactions with the stationary phase a large number of times, the assumption is either that all of the different types of stationary phase are sampled by an analyte during the separation, or that the stationary phase is characterized by a single type of adsorption

sites. Our data demonstrate that, under the appropriate conditions, it is possible to distinguish between types of surface sites, and that the interactions between analyte and surface sites is sufficiently limited in numbering that site-averaging by the analyte cannot proceed. Another way to phrase this is that we are operating under conditions of very low chromatographic resolution.

The specific system under evaluation is phenol in water and water/methanol binary solvents eluted over a silica column. Shown in Fig. 4.3 is the data series showing how the chromatogram of the single phenol analyte changes with the composition of the mobile phase. For 100% methanol mobile phase, phenol is sufficiently soluble that partitioning between the stationary phase and the mobile phase produces a single chromatographic peak. Tailing of this peak can be seen with the addition of 10% water to the mobile phase, and for 20% water three distinct but not fully resolved bands are seen. For higher water content, the three bands exhibit band-specific changes in retention time (Fig. 4.5)

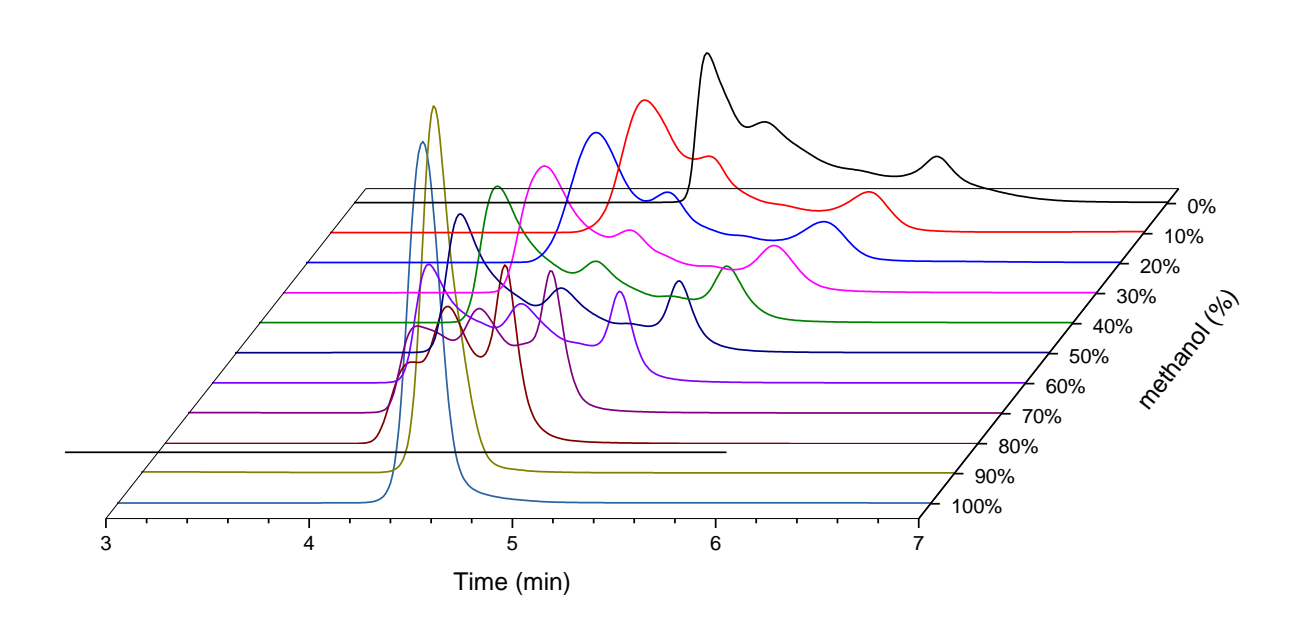


Figure 4.3 Overlay of phenol chromatograms showing peak dependence as the concentration of methanol decreases.

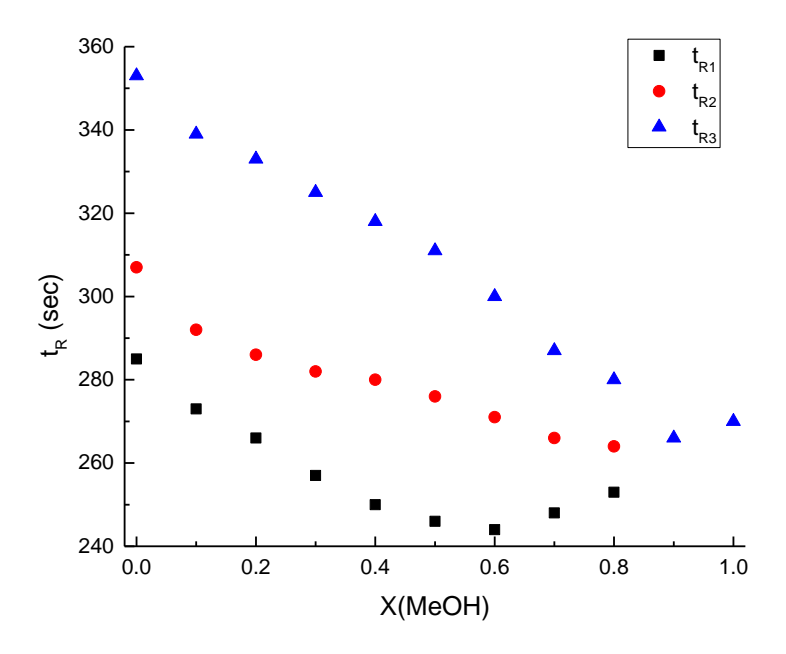


Figure 4.4 Mobile phase dependent retention time data. Each color corresponds to a peak seen in the chromatographic data.

In the van Deemter equation, the C term deals with mass transport between the mobile and stationary phases. The term is the sum of both components, C_s and C_m which are the mass transport terms for the stationary phase and the mobile phase, respectively. At high methanol concentrations, $C_m > C_s$. Mass transport into the mobile phase dominates the C-term in Eq. 4.1 and gives rise to a single peak in the chromatogram. As the concentration of water in the mobile phase increases, the relative importance of the interaction of phenol with the stationary phase increases. This is due, in part, to the decreased solubility of phenol in the more polar mobile phase. The term C_m decreases, increasing the importance of the nominally constant C_s term. The effects of phenol-silica interactions, as expressed through the C_s term, come to dominate as the effect of C_m decreases. Chromatograms recorded with mobile phases of 80% or less methanol exhibit multiple peaks for phenol elution. This effect must be accounted for by the van Deemter equation.

We posit that, as the C_m term decreases relative to the Cs term, the contribution from several different types of silanol functionalities on the surface each contribute to the observed chromatograms.^{14, 21}

The experimental conditions here closely resemble that of hydrophilic interaction liquid chromatography, HILIC. In HILIC experiments binary aqueous/organic mobile phases are used to enhance separation. Though the exact mechanism of a HILIC separation is not fully understood, the literature suggests the importance of the aqueous modifier. In HILIC, the stationary phase is polar. The stationary phase, being hydrophilic, interacts strongly with water in solution. It is commonly thought that the polar stationary phase strongly adsorbs a few layers of water. ²²⁻²³ As such, the mobile phase solution near the surface is water rich when compared to the bulk solution. This makes the HILIC mechanism two-fold. In order for the analyte to interact with the column it must partition into this water layer. Partitioning is dependent on the polarity of the analyte, which must displace water molecules and adsorb onto the stationary phase. ²⁴ These interactions are mediated by the amount of water in the system. By controlling the water concentration, and by extension the kinetics of adsorption and desorption, the speed at with the analyte traverse the column can be modulated. ²⁵

There is a statistical argument that must be countered if one is to accept this interpretation of the data. If we consider a single phenol molecule, it should sample, statistically, each type of silanol that exists on the surface as it adsorbs and desorbs during its passage through the column. If this is true one would expect a single peak for the phenol with the width reflecting the distribution of interaction energies of phenol with each type of silanol site. The experimental data show at least three peaks when the water concentration in the mobile phase is 20% or higher. The presence of three peaks implies that sampling of the different types of silanol sites by phenol is not

sufficiently extensive to provide a single distribution. Another way of expressing this is that the number of theoretical plates is sufficiently small, because of mass transport issues, that we are observing multiple populations of phenol based on their (initial) interactions with different types of silanol sites on the stationary phase. While the C_m term is constant for a given mobile phase composition, and small, for phenol bound to the multiple silanol sites, the terms C_{si} for each type of silanol site are sufficiently different to cause a change in elution time. Since the C_{si} terms have different values this leads to different retention times shown on the chromatogram.

Because of the comparatively limited solubility of phenol in water, it is possible, at least in principle, that the phenol exists as monomers, dimers, and multimers in aqueous solution. One way to evaluate whether such clustering influences our data is to acquire chromatograms at a series of column temperatures. If multimers do contribute to the reported multiple peaks, their lifetimes would have to be on the order of minutes in order to be resolved by the column. While this is highly unlikely on energetic grounds, phenol can π -stack. The energy of interaction for π -stacking is modest, on the order of 2 to 4 kcal/mol. 26-27 Despite the fact that phenol has a saturation concentration in water of 0.88 M, the phenol aromatic rings may interact in an aqueous environment. We note that the presence of the hydroxyl functionality in phenol provides it the opportunity to participate in hydrogen bonding with water (hence its solubility in water).²⁸ Typical hydrogen bond energy can range from 2 to 10 kcal/mol,²⁹ depending on the system, making this process more favorable energetically than π -stacking, suggesting that the dominant interaction between phenol and water is hydrogen bonding. Despite this plausibility argument against aggregation phenomena, we acquired experimental data to test for such intermolecular interactions. For the temperature-dependent measurements, the flow rate was kept constant and the mobile phase was 100% water. The column temperatures at which data were recorded were

60°C and 80°C. The aqueous mobile phase constrained the range of accessible temperatures to be between 0°C and 100°C. The melting point of phenol is 40.5°C but this should not affect the measurements once the phenol is dissolved in the aqueous mobile phase.

When comparing the data acquired at elevated temperatures to that acquired at 30°C, there are significant differences in the shapes of the chromatograms (and slight retention time shift) but the overarching point is that there remain multiple peaks in the chromatograms at all temperatures (Fig 4.5). Temperature-dependent changes are expected because of the range of interaction energies between phenol and the silica stationary phase. The larger point, however, is that without substantial changes in the number of chromatographic peaks, there is not support for there being a contribution to these data from aggregated or multimeric species. The clear implication of these data is that the separation seen is not a separation of different analyte constituents but is based on different environments presented by the stationary phase to a single analyte.

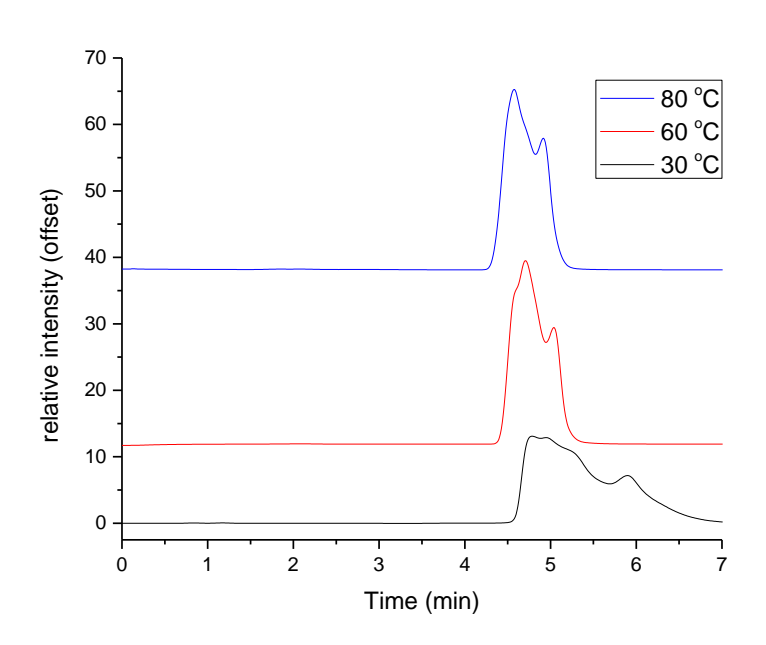


Figure 4.5 Effect of temperature on the peak shape of the chromatograms.

Effect of Flow Rate

We consider next how to interpret these data as those arising from a single analyte in the mobile phase. Any discussion of chromatographic separation invites interpretation in the context of the terms contained in the van Deemter equation. An immediate implication of the data shown in Fig. 4.3 is that the number of theoretical plates in this separation scheme is very small. A large value of H can obtain for two reasons. Based on Eq. 4.1, H is seen to decrease with increasing mobile phase flow velocity, reach a minimum and then increase with increasing flow velocity. The term A is flow velocity-independent, the B term, which corresponds to the contribution from Brownian motion of the analyte in the mobile phase, scales inversely with flow velocity, and the C term, which is related to mass transport (kinetics of adsorption and dissolution) is related linearly to flow velocity.³⁰ It is not possible for an individual measurement to determine where a given separation lies on this curve. Performing a series of measurements at different flow velocities, however, can assist in resolving this issue. We show the chromatograms for phenol in water with the silica stationary phase in Fig. 4.6. These data show that the number of resolved peaks in the chromatogram decreases with increasing flowrate.¹⁰

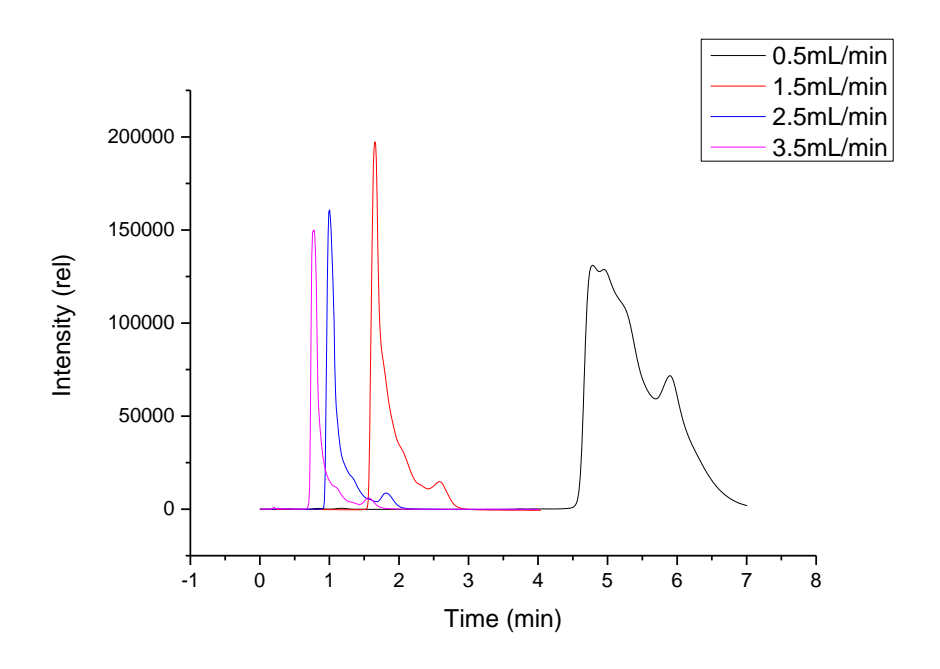


Figure 4.6 Dependence of the number of peaks and peak width on the flow rate.

Under the conditions of this experiment, the number of peaks is proportional to the theoretical plate height. Few theoretical plates correspond to a large H and poor averaging of phenol interactions with stationary phase adsorption sites. A single peak represents more extensive averaging over the different stationary phase sites, implying smaller H. Thus, the data in Fig. 4.6 show that the faster the flowrate, the fewer the peaks, implying that it is the B term, related to the diffusion of phenol in the mobile phase, plays a dominant role in determining H.¹⁸

The comparatively low solubility of phenol in water relative to that in methanol suggests that mass transfer effects also play a role in the observed anomalous behavior. The van Deemter equation can be expressed to provide more insight into the constituents of the A, B and C terms. When expressed in this manner (Eq. 4.2), the role of mass transfer phenomena can be described somewhat more clearly.

$$H = 2\lambda d_{p} + \frac{2\gamma D_{M}}{u} + \frac{K_{S}d_{f}^{2}}{D_{S}}u + \frac{K_{M}d_{p}^{2}}{D_{M}}u$$
(4.2)

Where the D terms are the diffusion constants for phenol on the stationary phase (subscript S) and in the mobile phase (subscript M), γ , K_S and K_M are constants, d_f is the effective "thickness" of the stationary phase and d_p is the silica stationary phase particle diameter. For our systems, d_f is related to the areal density of surface silanol groups. Of particular importance to the system under investigation is that for water as the solvent, D_S is very small, leading to a large mass transfer term. As the amount of methanol in the mobile phase is increased, D_S becomes less important because less time is spent by the phenol analyte on the stationary phase, and for small values of u the second term in Eq. 4.2 which is reciprocally related to the flow velocity. Based on the chromatographic results, we estimate H for 100% water mobile phase. For a system to resolve three peaks, the implication is that the adsorption time is long, *i.e.* on the order of the total retention time for each peak. The loss of resolution in such a system, giving rise to the peak overlap we observe, can be assumed to be dominated by diffusion, D_M . Using this limit and the dimensions of the column, we estimate the number of theoretical plates to be 24. This is indeed a vanishingly small number of theoretical plates. The value of operating a chromatographic separation under such conditions is that it allows for the evaluation of site-heterogeneity in the stationary phase.

Ultimately, even in the diffusion-limited regime, the factor that is controlling the different retention times of a single analyte on the silica column is the difference in mass transport terms for the individual sites on the column. In the van Deemter equation, the C term carries a dependence on the stationary phase, C_S , and a dependence on the mobile phase, C_M . Both of these terms are inversely related to the diffusion rate constant for the system.

$$\frac{dn_A}{dt} = k_C A \Delta C_A$$

$$C_S \propto k_C^{-1}$$
(4.3)

Where for a given analyte A, k_C is the diffusion rate constant for adsorption, A is the area of the phase involved in the adsorption/desorption, and ΔC_A is the difference in concentration of analyte A between the two phases. In other words, when the adsorption and desorption diffusion rates are large, k_C is large and the C terms are small. When desorption is slow, k_C is small and the term C_S becomes large. We operate under this condition. The quantity C_M changes with the composition of the mobile phase. When the magnitude of the C_M term becomes small relative to the C_S term, the mass transport onto and off the stationary phase dominates. Based on the differences in interactions between silica sites and phenol, we can identify three different sites that contribute differently to the overall C_S term. The C_S term is treated as a linear superposition of terms for the different types of sites, denoted by C_{SI} , C_{S2} , and C_{S3} . These values are sufficiently different to be resolved under our experimental conditions.

Comparatively small differences in the C_{Si} values show a resolvable effect.³³ Additionally, it is seen that as the value of C_M approaches that of C_S , the greater the difference in retention time. As C_M becomes large, the values converge, and this is seen as a single peak on the chromatogram. The value for C_{SI} is 0.02 mm, C_{S2} is 0.01 mm, and C_{S3} is 0.001 mm. These values were chosen somewhat arbitrarily and are not the exact values for the silanols in the column that was used in the experiment. At these values the retention times at a C_M value of 0.05 mm gives a retention time similar to that seen in the experimental data.

A series of models were created to show how the differences in C_{si} terms lead to the different retention times for a single analyte. It is shown that only small differences are required

for an effect to be shown. Additionally, it is seen that as the value of C_m approaches that of C_s , the greater the difference in retention time. As C_m becomes large, the values converge, and this is seen as a single peak on the chromatogram. The value for C_{s1} is 0.02 mm, C_{s2} is 0.01 mm, and C_{s3} is 0.001mm. These values were chosen somewhat arbitrarily and are not intended to represent the exact values for the silanols in the column that was used in the experiment. Rather, this calculation is intended for illustrative purposes. At these values the retention times at a C_m value of 0.05 mm gives a retention time similar to that seen in the experimental data.

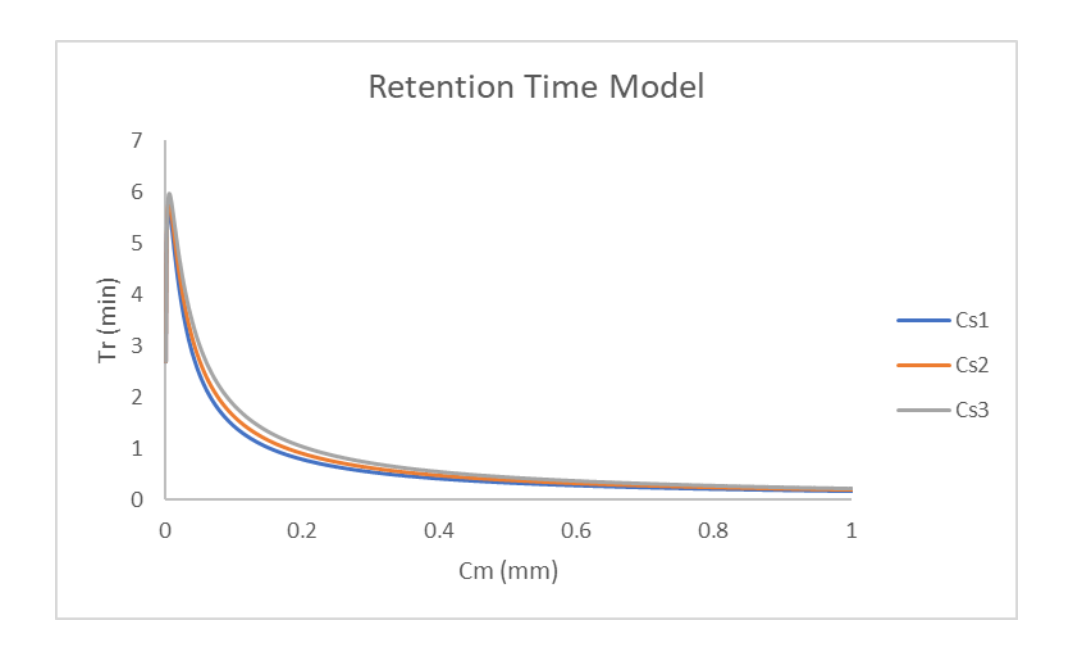


Figure 4.7 Statistical model of the three dominant surface groups that affect the chromatogram. The C_s values are for each type of surface group.

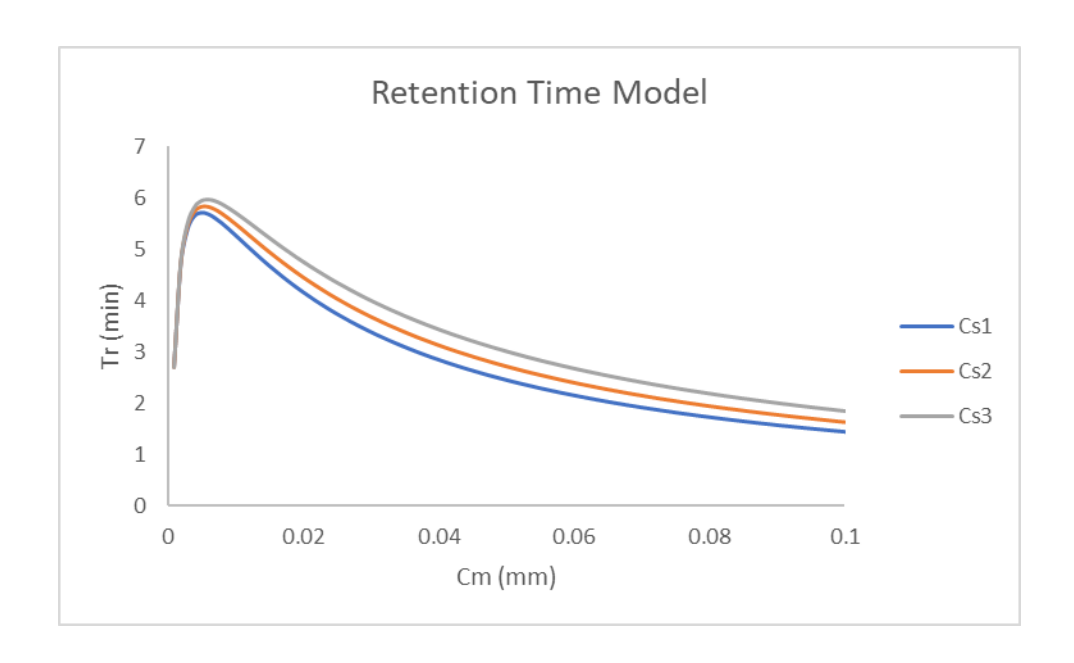


Figure 4.8 An enhanced view of Figure 4.7 showing the differences in retention time at low C_m values

The values of C_{s1} , C_{s2} , and C_{s3} determine the retention time at a specific C_m . As a C_s value gets larger, the kinetics of adsorption and desorption increases. This means that the analyte binds weakly to the column and retention time decreases.



Figure 4.9 A statistical model showing the overlap of peaks with similar C_s values for the different chemical groups on the surface. Values are at a specific flow rate and C_m .

By plotting retention times as a function of C_s , it can be shown that similar C_s values give significant peak overlap. This is shown in the experimental data as merged peaks. Changing the C_s values changes the amount of peak overlap seen. This model can thus be used to make assumptions as to the relative values of each C_s term. Additionally, when C_m is relatively large, the peaks collapse into a single peak at shorter retention times due to the increased solubility in the mobile phase.

Effect of pH

The experimental data show a modest dependence on the pH on the mobile phase. The pKa of the silica surface is about 4.5. At pH 2 there are two distinct peaks for phenol with a slight shoulder on the longer retention time peak.

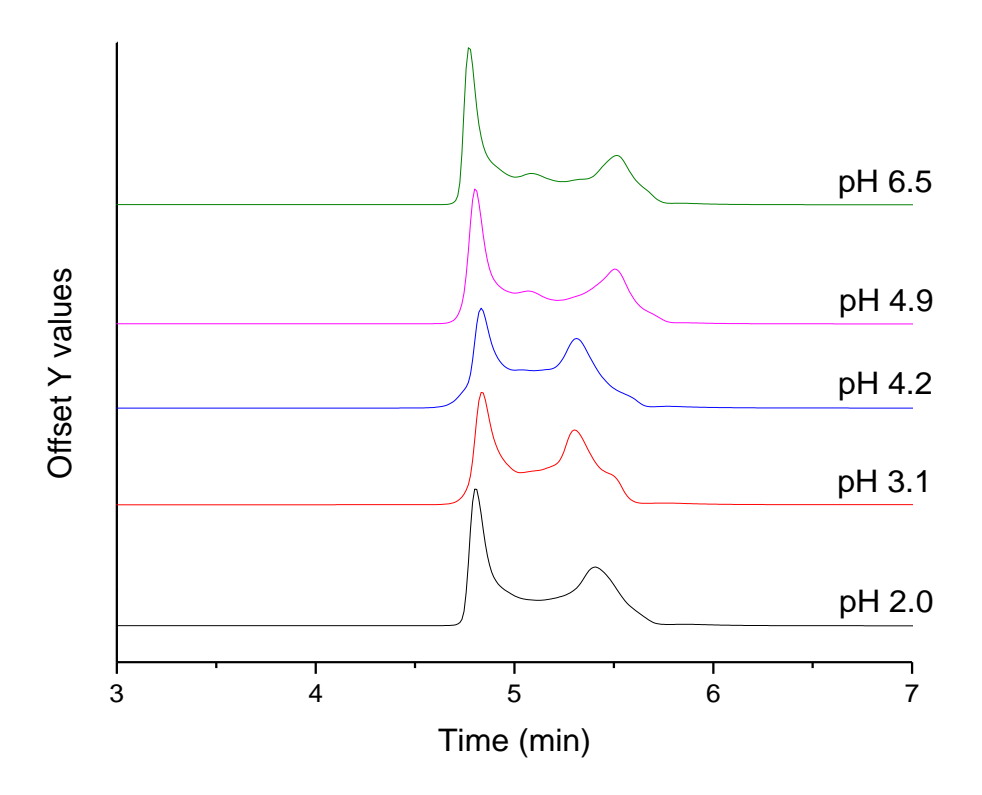


Figure 4.10 pH dependence of the shape of the chromatograms.

At pH 2 all silanol groups are protonated and there should be a single mass transport term for all Si-OH functionalities. At pH values well below the silanol first pKa there are thought to be two dominant moieties. These are the surface silanol groups, Q^1 through Q^3 , and the bridging siloxanes, Q^0 (Fig 4.11). This interpretation assumes that at low enough pH values the silanol groups Q^1 through Q^3 have behave the same chemically and that steric differences between Q^1 , Q^2 and Q^3 do not play an important role. The extent to which this latter assumption holds determines how many chromatographic peaks are observed. Bridging siloxanes, Q^0 , are expected to interact differently with phenol. Q^0 groups are less polar than the silanols and as such exhibit retention times that differ from that of the Q^1 through Q^3 functionalities. These two types of groups give rise to the two peaks seen in the data at low pH.

This argument holds qualitatively for the data shown in Fig. 4.11. For the three pH values below 4.5, there are two prominent peaks with a notable shoulder on the longer retention time peak. While this shoulder appears not to scale directly with pH, its presence is still ascribed to steric differences between Q^1 , Q^2 and Q^3 functionalities, with Q^1 and Q^2 being the dominant species. For pH values of 4.9 and 6.5 there is seen to be a shift in the second peak to longer retention times and the appearance of at least one feature between the two dominant peaks. These changes are clearly associated with the deprotonation of Q^1 , Q^2 and Q^3 functionalities to form siloxides.

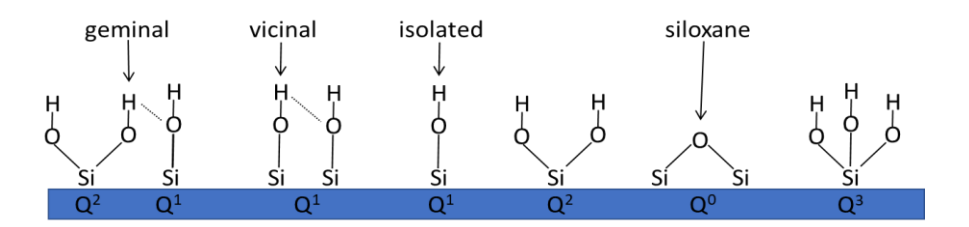


Figure 4.11 Distribution of surface silanol groups. Each terminal -OH functionality is capable of undergoing proton dissociation equilibria.

With the broad understanding of the chromatograms in place, we turn to assignment of the individual peaks. As noted in Fig. 4.10, there are four species present in or on silica, designated Q⁰ through Q³, where the number indicates the number of hydroxyl groups bonded to a silicon atom. All of these species can exist at the surface, with only Q0 existing in the bulk. Primary and vicinal silanols (Q^1) and secondary and geminal silanols (Q^2) are thought to dominate the surface, with Q³ being present to only a negligible extent.³⁴ Surface silanols are known to exhibit a range of reactivities for both structural and steric (environmental) reasons, with the Q¹ isolated silanols being the most acidic (pKa ~ 4.5). Q^2 and Geminal silanols are thought to have pKa values of ca. 6.5 for the first Si-OH and ca. 9 for the second Si-OH,³⁶ and all of these pKa values are affected by their environment. Earlier work has shown that, in aqueous environments, increasing the ionic strength of the medium lowers the apparent pKa of the silanol.⁴ It is thus not surprising that the chromatographic data (Fig. 4.2) exhibit multiple different stationary phase sites and that the relative population of each site depends on the composition, pH and ionic strength of the mobile phase. What remains unresolved is the assignment of the individual peaks to specific silanol functionalities. We can use the mobile phase-dependent retention time data (Fig. 4.3) to estimate which type of silanol is associated with each peak. Such interpretation rests on the assumption that the interactions of phenol with silanol groups depend on whether or not the silanol is deprotonated.

Based on the relative pH independence of the first chromatographic peak (Fig. 4.11), at ca. 4.8 minutes, this peak is assigned to interactions between phenol and siloxane groups, Si-O-Si (Q⁰). At pH 2, where all silanols are protonated, there is one clear peak at ca. 5.4 minutes, with a weak shoulder at ca. 5.6 minutes. As the pH is increased the peak at 5.4 minutes shifts to ca. 5.3

minutes and the shoulder at ca. 5.5 minutes becomes more prominent. At pH 4.2, below the first pKa of Q^1 silica, and at pH 4.9, above the pKa of Q^1 , we observe changes in intensity of the peaks at 5.3 minutes and 5.5 minutes along with some potential broadening. Based on these trends, the peak at 5.3 min is assigned to protonated Q^1 and the peak at 5.5 min is assigned to deprotonated Q^1 . At pH 4.9 the peak at 5.5 minutes dominates over unresolved intensity in the vicinity of 5.3 min. and peak at ca. 5 min appears, which is also seen at pH 6.5. The peak at 5 minutes is assigned to (protonated) Q^2 , where the dominant equilibrium in this region is the protonation/deprotonation of the first Si-OH group on Q^2 sites. At pH 6.5 there is a slight shoulder at ca. 5.2 min, which is possibly the protonated form of the second Si-OH group on Q^2 . This peak appears at substantially the same retention time as the Q^1 Si-OH band at lower pH values. We recognize that these assignments are made deductively and that secondary proximity effects, as schematized in Fig. 4.11 will also play a role in the observed chromatograms. In fact, it is those secondary effects that may be responsible for the lack of clear band resolution between the two dominant peaks.

As was reported in Chapter 2, the surface energy of a silica surface depends on the presence or absence of metal ions in the aqueous overlayer medium. Surface siloxide functionalities can and do interact with any cationic species in solution, and in systems where Na⁺ is present, there is a competition between H⁺ and Na⁺ for complexation. We have studied this effect for the current system. We accomplish this by comparing the chromatographic data for phenol in water at specific pH values with and without the addition of 0.1 M NaCl. The addition of Na⁺ to the mobile phase at pH 2 affects the chromatographic profile to only a limited extent and in an expected manner (Fig. 4.12). At pH 2, 2.5 pH units below the first pKa of silica, the silica surface fully associated with either H⁺ or Na⁺. For these conditions, [H⁺] = 0.01 M and [Na⁺] = 0.1 M, an order of magnitude difference, leading to the expectation that there would be at least some displacement of

 H^+ by Na^+ , and this is seen as an increase and shift in the chromatographic peak associated with Q^1 sites relative to that associated with Q^0 sites, which should be unaffected by the presence of either Na^+ or H^+ (Fig. 4.12). It is expected that the interaction of phenol with a SiOH functionality would differ in energy from an interaction with a SiONa+ functionality.

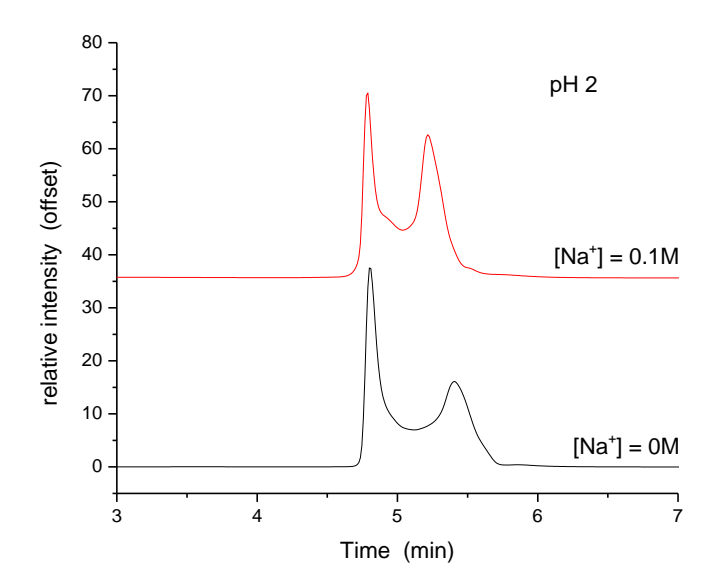


Figure 4.12 Effect of Na⁺ on the chromatogram at pH 2.

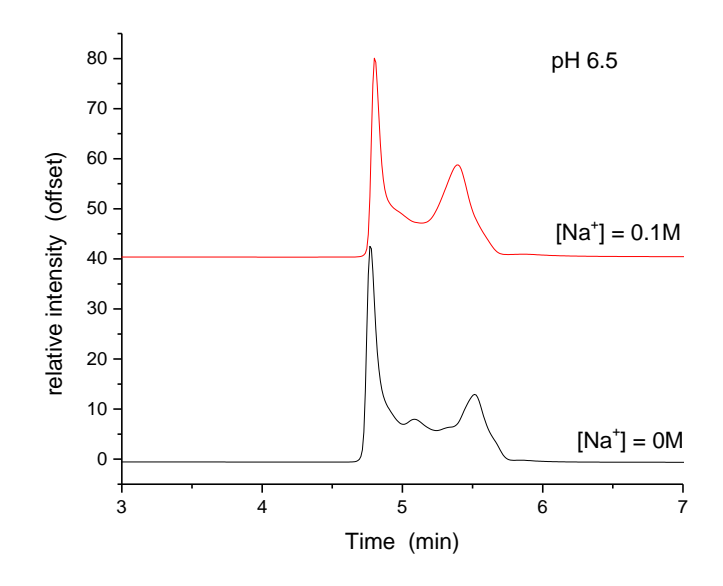


Figure 4.13 Effect of Na⁺ on the chromatogram at pH 6.5.

At pH 6.5 (Fig 4.13), above the pKa of Q^1 , the addition of Na^+ changes the chromatogram from exhibiting four identifiable features, as assigned above, to showing two clear peaks. As with the data at pH 2, the siloxane (Q^0) peak does not change with [Na^+], but the apparent simplification of the chromatogram from four to two features can be understood in the context of siloxide sites that are unoccupied by H^+ will be occupied by Na^+ because [Na^+] = 0.1 M and [H^+] ~ $3x10^{-7}$ M. We posit that the peak at ca. 5.1 minutes is associated with the interaction of phenol with deprotonated silanols. Thus, the addition of Na^+ to the chromatographic system has the expected effect.

Conclusion

Despite its wide use in chromatographic separations, it is typically held that the distribution of surface sites is effectively averaged over a large number of interactions between analyte molecules and the silica surface. Under conditions where there are a limited number of interactions with the silica surface, however, the different interactions that a given analyte can experience with a silica surface is revealed. Such measurements serve two valuable purposes. First, these measurements demonstrate that it is possible to examine the distribution surface silanol types under the appropriate experimental conditions. Second, knowledge of the distribution of sites on a silica surface can be used in tailoring the properties of this material to specific applications. By understanding these characteristics, we can better utilize surfaces. Techniques such as HPLC can be utilized in a variety of ways to understand mechanistically what is happening at the solid/liquid interface. The interaction of chemical species with the silica surface is a dynamic process that is affected my many conditions. When performing an HPLC separation, care should be taken to

understand the importance of the mass transport term in the Van Deemter equation. The nature of this term is fundamental in controlling the separation in any type of HPLC experiment.

Though we utilize aqueous normal phase HPLC in this experiment, a technique not typically employed due to issues of solubility, peak tailing, and other issues, we present explanations for understanding mechanisms related to other separation techniques such as HILIC. The experiments employed in here closely resemble that of a HILIC separation of which the mechanisms are not fully understood. The factors that govern the separation are crucial to understanding how HILIC experiments work. Conditions such as temperature, flow rate, ionic strength, and mobile phase make-up can be individually manipulated or combined to optimize separation efficiency. Aqueous normal phase HPLC has the potential to be a powerful tool in separations once more work has been put into understanding theory and practical aspects behind its function.

LITERATURE CITED

LITERATURE CITED

- 1. Zhuravlev, L. T., Concentration of Hydroxyl Groups on the Surface of Amorphous Silicas. *Langmuir* **1987**, *3*, 316-318.
- 2. Gallas, J. P.;Goupil, J. M.;Vimont, A.;Lavalley, J. C.;Gil, B.;Miserque, O., Quantification of water and silanol species on various silicas by couping IR and in-situ thermogravimetry. *Langmuir* **2009**, *25* (10), 5825-5834.
- 3. Gonçalves, M. C., Sol-Gel Silica Nanoparticles in Medicine: A Natural Choice. Design, Synthesis and Products. *Molecules* **2018**, *23* (8), 2021-2047.
- 4. Stubbs, B.;Blanchard, G. J., Measuring Competing Equilibria at a Silica Surface through the Contact Angle of a Nonpolar Liquid. *Langmuir* **2017**, *33* (38), 9632-9636.
- 5. Lambert, W. J.; Middleton, D. L., pH Hysteresis Effect with Silica Capillaries in Capillary Zone Electrophoresis. *Anal. Chem.* **1990**, *62* (15), 1585-1587.
- 6. Qiu, H. L., X.; Sun, M.; Jiang, S., Development of Silica-Based Stationary Phases for High-Performance Liquid Chromatography. *Analytical and Bioanalytical Chemistry* **2011**, *399* (10), 3307-3322.
- 7. Giaquinto, A.;Liu, Z.;Bach, A.;Kazakevich, Y., Surface Area of Reversed-Phase HPLC Columns. *Anal. Chem.* **2008**, *80* (16), 6358-6364.
- 8. Rahman, I. A.;Padavettan, V., Synthesis of Silica Nanoparticles by Sol-Gel: Size-Dependent Properties, Surface Modification, and Applications in Silica-Polymer Nanocomposites—A Review. *Journal of Nanomaterials* **2012**, *2012*.
- 9. Buszewski, B.;Gadzała-Kopciuch, R. M.;Markuszewski, M.;Kaliszan, R., Chemically Bonded Silica Stationary Phases: Synthesis, Physicochemical Characterization, and Molecular Mechanism of Reversed-Phase HPLC Retention. *Anal. Chem.* **1997**, *69* (16), 3277-3284.
- 10. Mereish, K. A.; Ueda, C. T., Effect of Column Temperature and Eluent Flow Rate on the High Performance Liquid Chromatographic Analysis of Cyclosporin A and D. *Pharmaceutical Research* **1984**, *I* (6), 245-249.
- 11. Wätzig, H.;Ebel, S., Estimation of dead-time in liquid chromatography from retention behaviour of homologous series by non-linear regression. *Chromatographia* **1991**, *31* (11-12), 544-548.
- 12. Fornstedt, T. F., P.; Westerlund, D., Basic HPLC Theory and Definitions: Retention, Thermodynamics, Selectivity, Zone Spreading, Kinetics, and Resolution. In *Analytical Separation Science*, Wiley Online Library: 2015.

- 13. Gritti, F.; Guiochon, G., The Current Revolution in Column Technology: How It Began, Where Is It Going? *J. Chromatogr. A* **2012**, *1228*, 2-19.
- 14. van Deemter, J. J.; Zuiderweg, F. J.; Klinkenber, A., Longitudinal diffusion and resistance to mass transfer as causes of nonideality in chromatography. *Chemical Engineering Science* **1956**, 5 (6), 271-289.
- 15. Xu, H.; Weber, S. G., Optimization of Post-Column Reactor Radius In Capillary High Performance Liquid Chromatography Effect of Chromatographic Column Diameter and Particle Diameter. *Journal of Chromatography A* **2006**, *1113* (1-2), 116-122.
- 16. Row, K. H.;Lee, C. H., Correlation of HETP and Experimental Variables in Preparative Liquid Chromatography. *Korean Journal of Chemical Engineering* **1998**, *16* (1), 22-27.
- 17. Skoog, D. A.; Holler, F. J.; Crouch, S. R., *Principles of Instrumental Analysis*. Sixth ed.; David Harris.
- 18. Knox, J. H.; Scott, H. P., B and C terms in the Van Deemter equation for liquid chromatography. *Journal of Chromatography A* **1983**, 282, 297-313.
- 19. Nahum, A.;Horvarth, C., Surface silanols in silica-bonded hydrocarbonaceous stationary phases: I. Dual retention mechanism in reverse-phase chromatography. *J. Chromatogr. A* **1981**, 203, 53-63.
- 20. Karatapanis, A. E.; Fiamegos, Y. C.; Stalikas, C. D., A revisit to the retention mechanism of hydrophilic interaction liquid chromatography using model organic compounds. *Journal of Chromatography A* **2011**, *1218* (20), 2871-2879.
- 21. Gritti, F.;Guiochon, G., Mass transfer mechanism in hydrophilic interaction chromatography. *Journal of Chromatography A* **2013**, *1302*, 55-64.
- 22. McCalley, D. V.; Neue, U. D., Estimation of the Extent of the Water-Rich Layer Associated with the Silica Surface in Hydrophilic Interaction Chromatography. *J. Chromatogr. A* **2008**, *1192* (2), 225-229.
- 23. Soukup, J.; Jandera, P., Adsorption of Water from Aqueous Acetonitrile on Silica-Based Stationary Phases in Aqueous Normal-Phase Liquid Chromatography. *J. Chromatogr. A* **2014**, *1374*, 102-111.
- 24. Gritti, F.;Höltzel, A.;Tallarek, U.;Guiochon, G., The Relative Importance of the Adsorption and Partitioning Mechanisms in Hydrophilic Interaction Liquid Chromatography. *J. Chromatogr. A* **2015**, *1376*, 112-125.
- 25. Gritti, F.; Guiochon, G., Mass Transfer Mechanism in Hydrophilic Intereaction Chromatography. *J. Chromatogr. A* **2013**, *1302*, 55-64.
- 26. Grimme, S., Do Special Noncovalent π – π Stacking Interactions Really Exist? *Angewandte Chemie International Edition* **2008**, *47* (18).

- 27. Sinnokrot, M. O.; Sherrill, C. D., Substituent Effects in $\pi \pi$ Interactions: Sandwich and T-Shaped Configurations. *J. Am. Chem. Soc.* **2004**, *126* (24), 7690-7697.
- 28. Parthasarathi, R.; Subramanian, V.; Sathyamurthy, N., Hydrogen Bonding in Phenol, Water, and Phenol-Water Clusters. *J. Phys. Chem. A* **2005**, *109* (5), 843-850.
- 29. Paoloni, L., Nature of the Hydrogen Bond. *Journal of Chemical Physics* **1959**, *30* (4), 1045-1058.
- 30. Miyabe, K.; Guiochon, G., A Kinetic Study of Mass Transfer in Reversed-Phase Liquid Chromatography on a C18-Silica Gel. *Anal. Chem.* **2000**, *72*, 5162-5171.
- 31. Gritti, F.;Guiochon, G., Mass Transfer Mechanism in Chiral Reversed Phase Liquid Chromatograph. *J. Chromatogr. A* **2014**, *1332*, 35-45.
- 32. Fornstedt, T.;Zhong, G.;Guiochon, G., Peak Tailing and Slow Mass Transfer Kinetics in Nonlinear Chromatography. *J. Chromatogr. A* **1996**, 742, 55-68.
- 33. Siouffi, A. M., About the C Term in the van Deemter's Equation of Plate Height in Monoliths. *J. Chromatogr. A* **2006**, *1126* (1-2), 86-94.
- 34. Schrader, A. M.; Monroe, J. I.; Sheil, R.; Dobbs, H. A.; Keller, T. J.; Li, Y.; Jain, S.; Shell, M. S.; Israelachvili, J. N.; Han, S., Surface Chemical Heterogeneity Modulates Silica Surface Hydration. *Proceedings of the National Acadey of Sciences* **2018**, *115* (12), 2890-2895.
- 35. Leung, K.; Nielsen, M. B.; Criscenti, L. J., Elucidating the Bimodal Acid-Base Behavious of the Water-Silica InterfaceFrom First Principles. *Condensed Materials* **2010**.
- 36. Sulpizi, M.; Gaigeot, M.; Sprik, M., The Silica-Water Interface: How the Silanols Determine the Surface Acidity and Modulate Water Properties. *Journal of Chemical Theory and Computation* **2012**, *8* (3), 1037-1047.

Chapter 5

Conclusions

The silica surface has been investigated extensively because of its importance and its complexity. Among the issues that complicate the investigation of silica is the fact that it is an insulator. Several non-electrochemical analytical techniques can be utilized to help further characterize the silica surface, especially when used in ways that are atypical. The experiments presented in this dissertation have been performed with the goal of improving our understanding of the silica surface. These experiments have expanded our understanding of silica surfaces and it is possible that this knowledge can be applied to understanding other oxide surfaces in greater detail.

Accounting for the role of multiple equilibria provides insight into the compositional distribution of surface silanol functionalities and how changes in aqueous overlayer composition can modify the silica surface. By controlling aqueous overlayer pH and ionic strength, the silica surface energy and effective surface pKa can be determined. These changes in surface energy are important as they are central to the utility of the silica surface for applications such as chromatographic and electrophoretic separations, for example.

The characterization of the silica surface using ²⁹Si and ²³Na solid state NMR helped to elucidate the types of surface binding sites present when silica is exposed to solution phase Na⁺. The ²⁹Si NMR showed that when the silica surface is exposed to Na⁺ at low pH values the surface is nominally fully populated by silanol groups. When the pH is above the first pKa of the surface, 4.5, protons are displaced from the surface and the surface siloxide sites associate with the Na⁺ ions. The ²⁹Si NMR data show this by a change in the ratio of Q⁰:Q¹ surface groups. The ²³Na

NMR data show a single peak, indicating that to within the limitations of the linewidth of the measurement, there is one characteristic binding site for Na⁺ at the siloxide/silanol surface.

The neutralization of the silica surface upon exposure to Na⁺ was confirmed via ζ potential measurements. Below the surface pKa the ζ potential is ca. 0 mV. Above the pKa the surface has a ζ potential of -15 mV, with Na⁺, and -30 mV, without Na⁺. Additionally, there are two transition states in the experiments with an ionic strength of 0.1 M corresponding to the second deprotonation of surface silanols. We note that the ζ potential is not a quantitative, fundamental characterization parameter for a charged surface. Rather, it is a quantity that is reflective of the effective charge of the surface and as such is useful for making comparisons between different conditions of a given system but cannot provide direct insight into the surface silanol density.

While the distribution of surface functionality plays a central role in determining the properties of the silica surface, the complex morphology of this material can mediate the chemical activity of silanol groups and it is this additional factor that has complicated efforts to understand the behaviour of silica. The morphology of the silica surface over mesoscopic length scales has been investigated using SEM. The insulating nature of silica is shown on the native oxide surface. Upon exposure to aqueous NaOH or KOH, two physical changes result. The first is that the surface area determined by BET isotherm measurements decreases from 400 m²/g to 290 m²/g. This is likely due to the solubility of silica in highly basic media causing some surface features to dissolve, leaving a less featured surface. The second change is an observed change in surface conductivity, which is due to the presence of Na⁺ or K⁺ on the surface and its ability in an adventitious water adlayer to provide at least some amount of conductivity.

The surface concentration of silanol groups was measured using ICP and TGA. A range of $1.6 \ \mu mol/m^2$ to $7.0 \ \mu mol/m^2$ was found, depending on the method used. While this is a large range, it should be noted that with the ICP measurement, consistent with the NMR data, not every silanol reacts with Na⁺, leading to a result that is lower than the actual value. Thermogravimetric analysis is expected to provide a more accurate measurement of surface silanol density because it detects the thermal release of H_2O , a neutral and volatile compound.

The use of normal phase HPLC under atypical conditions produced anomalous results that could be explained in the context of highly inefficient mass transport. Phenol, used as probe of the silica surface, samples each type of surface silica site. Under the conditions used the adsorption and desorption of phenol is slow, with a characteristic surface residence time on the same order as the total retention time of the phenol. Since the surface sites differ in energy, their retention affinities for the phenol differ and under conditions of a limited number of (slow) adsorption and desorption events, manifests as a single analyte generating multiple, partially resolved eluted peaks. It should be noted that this mass transport limited regime is accessed by the polar nature of the surface combined with the use of high concentrations of water, 20% and greater, in the methanol mobile phase. These results are not seen in a comparatively less polar mobile phase of more than 80% methanol. The flow rate of the system was changed to account for the slow adsorption and desorption processes. Increasing the flow rate reduces the time the phenol can interact with the stationary phase thus increases the efficiency of the system. It should be noted that this increase in efficiency with flowrate is due to the slow mass transport kinetics of this system. The temperature at which these measurements were made was varied to evaluate the possibility of phenol aggregation. No evidence for aggregation was found. The concentration of phenol was also varied to test for aggregates, and no concentration-dependence was found.

Future Directions

These experiments elucidate some of the properties of the silica surface and the consequences of surface equilibrium phenomena Results from the highly atypical conditions used in the chromatographic experiments can be applied to other experiments. Capillary electrophoresis, CE, is another separation technique where the silica surface is of central importance, not in this case for adsorption and desorption, but rather for its ability to support electroosmotic flow. The separation is mediated by electric field-induced electroosmotic flow, which is itself controlled by the charge on the silica capillary surface. It is thus possible to use electrophoresis to evaluate the competitive equilibria that operate at the silica surface, and such an investigation may prove useful. By varying mobile phase pH, ionic strength, and metal ion identity, it is possible to control the net charge of the silica surface, which will affect the electroosmotic flow through the surface ζ potential.¹⁻² The movement of ions and molecules through the capillary is mediated by the flow of ions near the silica surface. The magnitude of this surface charge is controlled by the electrolyte solution. Metal ions have different equilibrium constants for surface adsorption. Ions with higher equilibrium constants bind tighter to the surface. The larger the association constant for a given metal ion, the greater extent of surface binding and the lower the electroosmotic flow will be.

It may also possible to take advantage of the conductive nature of an indium-doped tin oxide, ITO, or fluorine-doped tin oxide, FTO, surface to perform a variety of electrochemical experiments that could provide complementary information on the characterization of oxide surfaces. Using a conductive support, the characterization of self-assembled monolayers is possible through the use of techniques such as cyclic voltammetry and impedance spectroscopy.³ In addition to being able to control the surface charge by applying current to an ITO or FTO

electrode, it is possible to take advantage of the native surface charge of the electrode.⁴ Unlike silica, ITO has a positive ζ potential at pH values below 6.⁵ In this case it may be possible to experiment with anion identity in competitive equilibria experiments.

The chemical reactivity of the surface can also be important in chemical sensing applications. There are many examples where such applications rely on the interactions of the surface-fluid interface. Ion-selective electrodes, Chemical field-effect transistors (ChemFET), and Ion-sensitive field effect transistors (ISFET) rely on the interactions of electrolyte solutions with semiconductor surfaces.⁶⁻⁷ By modifying the surface chemically and controlling the pH, ionic strength, and metal ion identity, the strength of binding of the analyte to the surface can be modulated.⁸ The electrolyte solution composition can be controlled to mediate the selectivity of the analyte for the surface. Chemically selective electrodes are important for many applications, especially those with biological relevance. However, they typically suffer from interferences by similar compounds. It may be possible to increase the selectivity of surface-based sensors by taking advantage of the different reactivities that different surface groups have, such as pKa or equilibrium constant. Modification of oxide surfaces also suffers from incomplete coverage. While in most applications unreacted sites are either supressed or capped due to their deleterious effects, it may be possible to take advantage of these sites for increased selectivity under appropriate conditions. 9-10

Chemical selectivity is the end goal of many surface interactions. The ability for sensors to operate without interference or for surface selective separation is one that is full of complexity. Surface heterogeneity is a characteristic that is often supressed however, it is possible to take advantage of heterogeneity for the end goal of the optimization of chemical processes.

APPENDIX

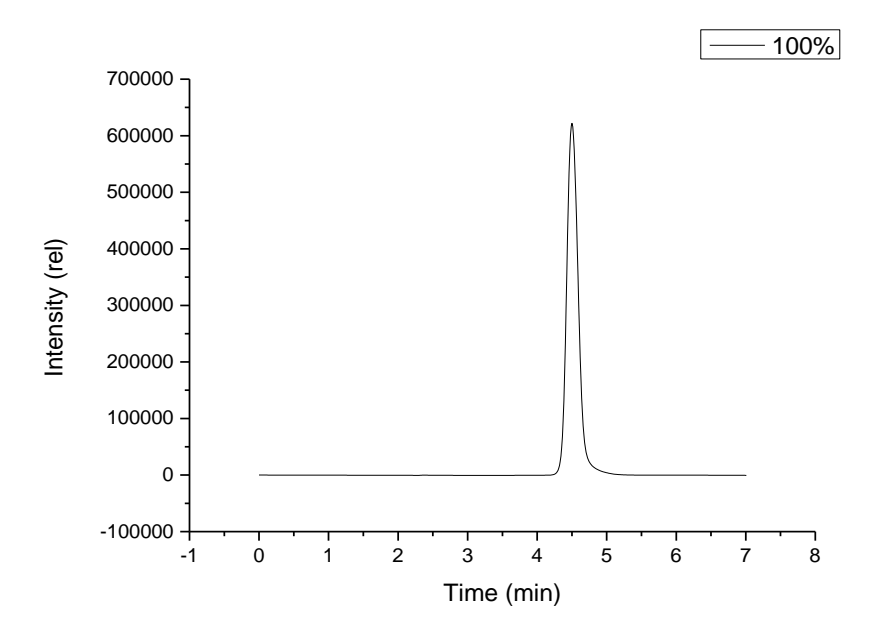


Figure A.1 Chromatogram of phenol at 100% methanol. A single peak is shown corresponding to the analyte.

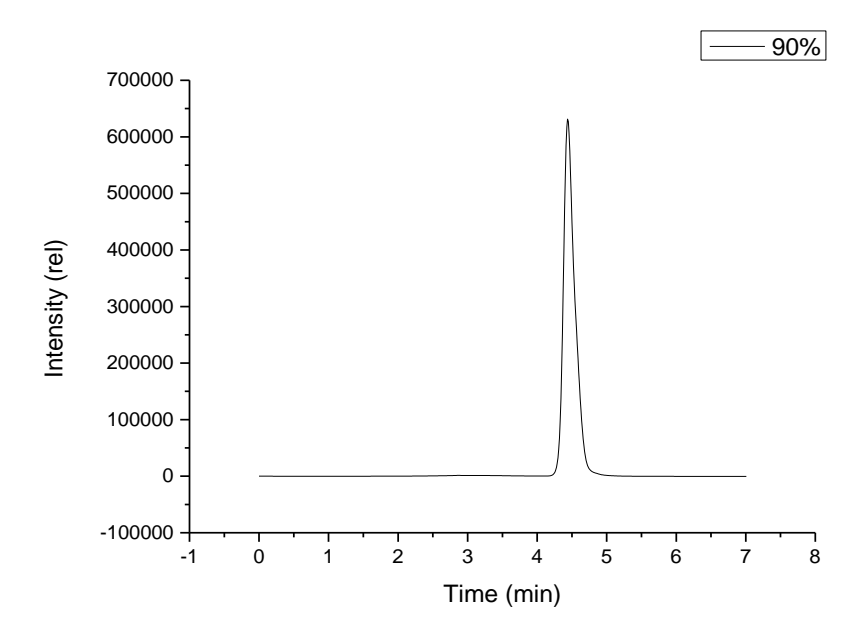


Figure A.2 Chromatogram of phenol at 90% methanol/10% water. A single peak is shown corresponding to the analyte.

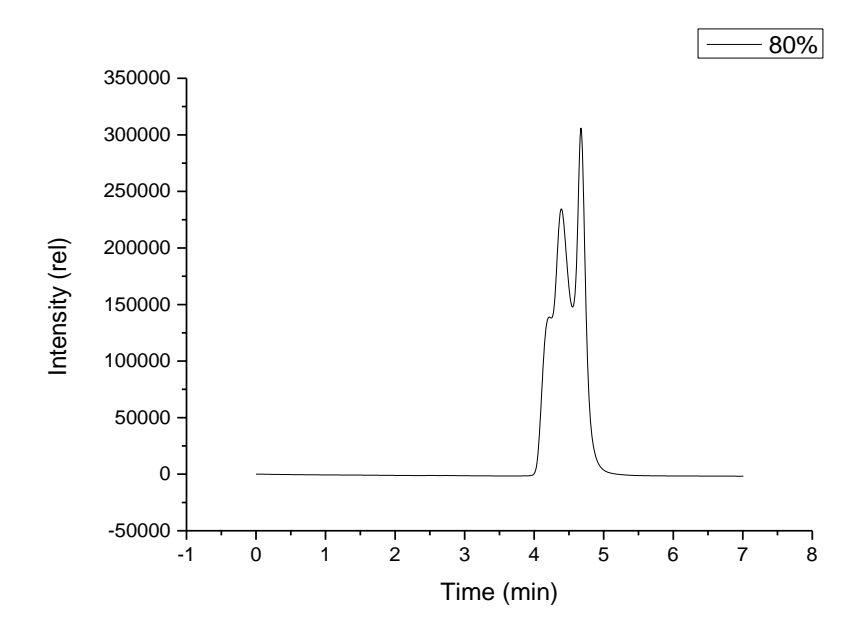


Figure A.3 Chromatogram of phenol at 80% methanol/20% water. Multiple peaks are shown for the phenol analyte.

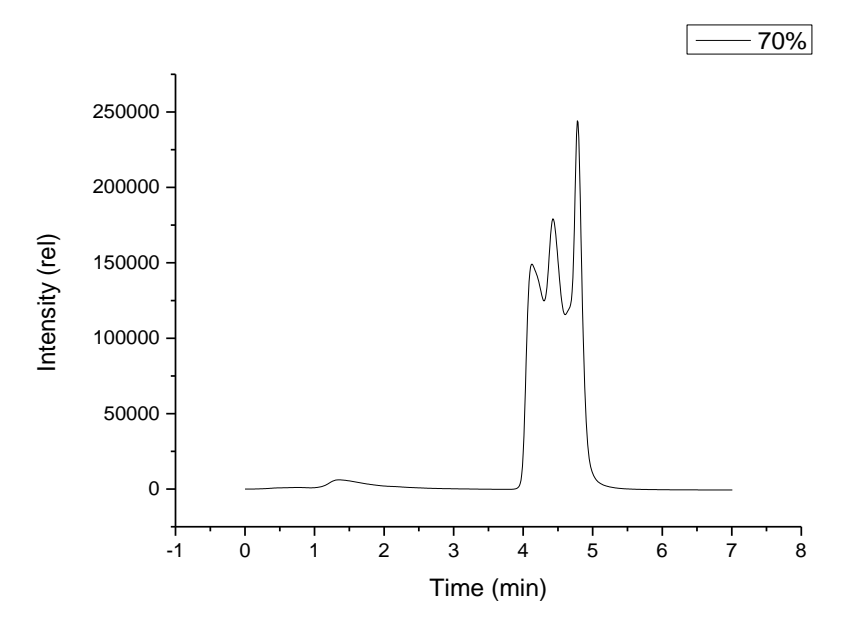


Figure A.4 Chromatogram of phenol at 70% methanol/30% water. Multiple peaks are shown for the phenol analyte.

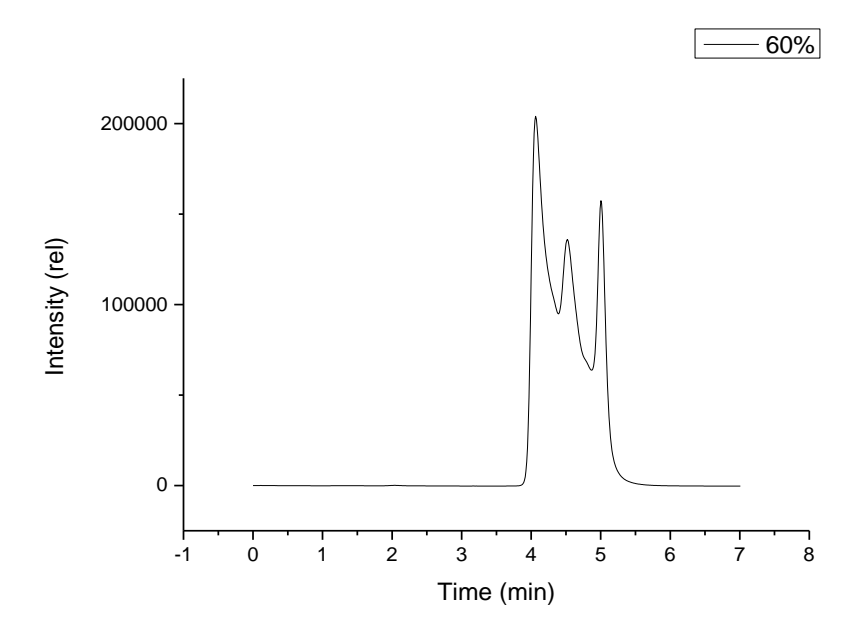


Figure A.5 Chromatogram of phenol at 60% methanol/40% water. When compared to Figure A.4 the peak ratios have changed noticeably.

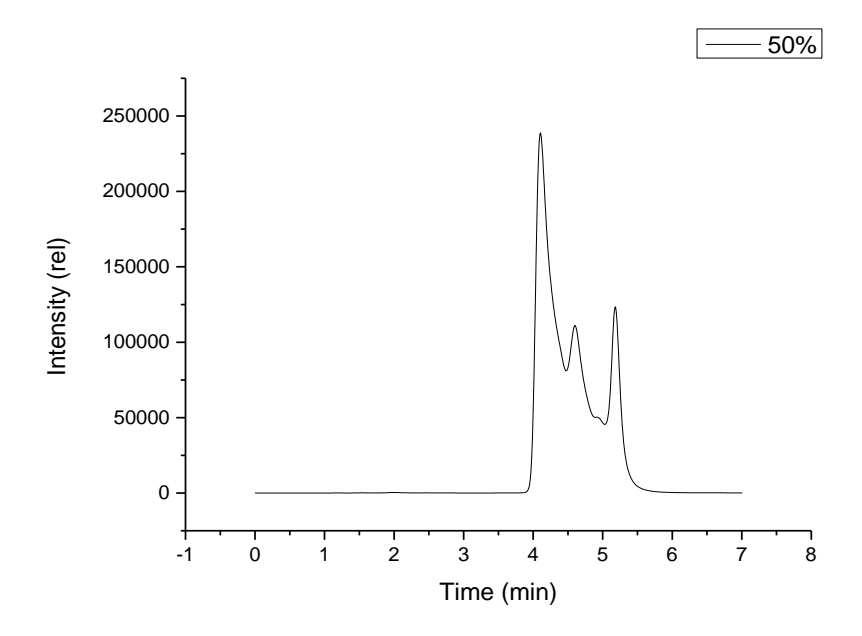


Figure A.6 Chromatogram of phenol at 50% methanol/50% water.

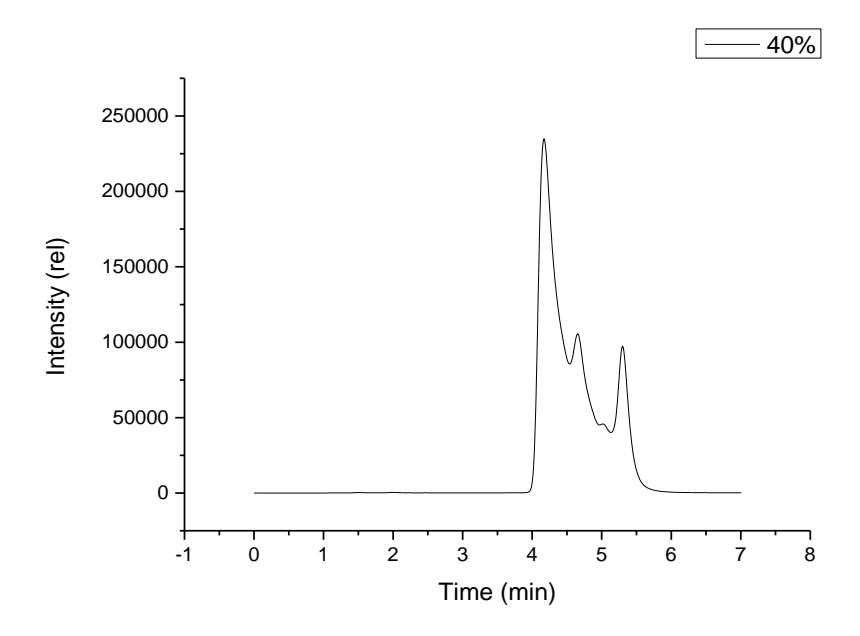


Figure A.7 Chromatogram of phenol at 40% methanol/60% water.

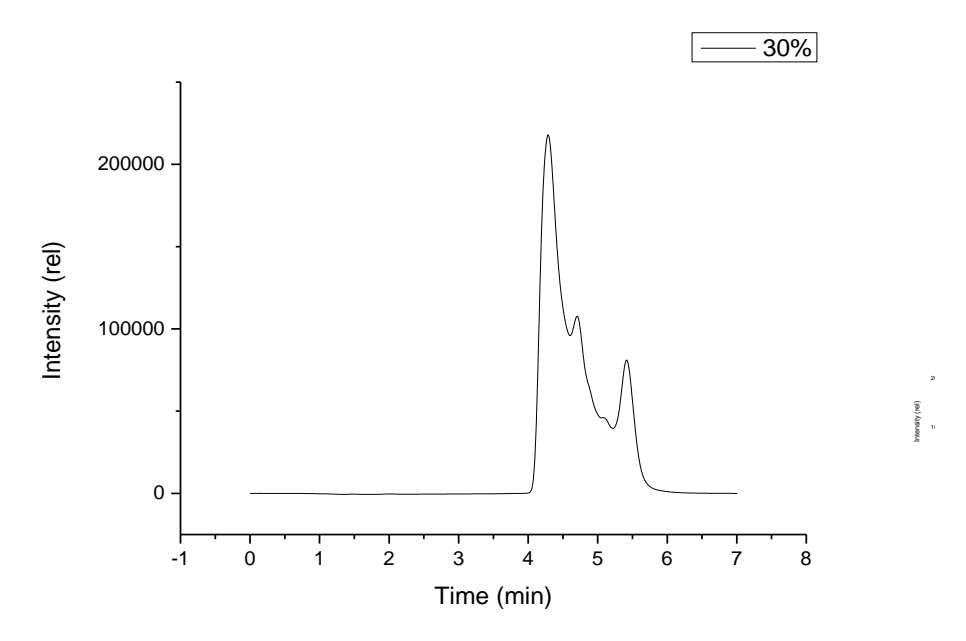


Figure A.8 Chromatogram of phenol at 30% methanol/70% water.

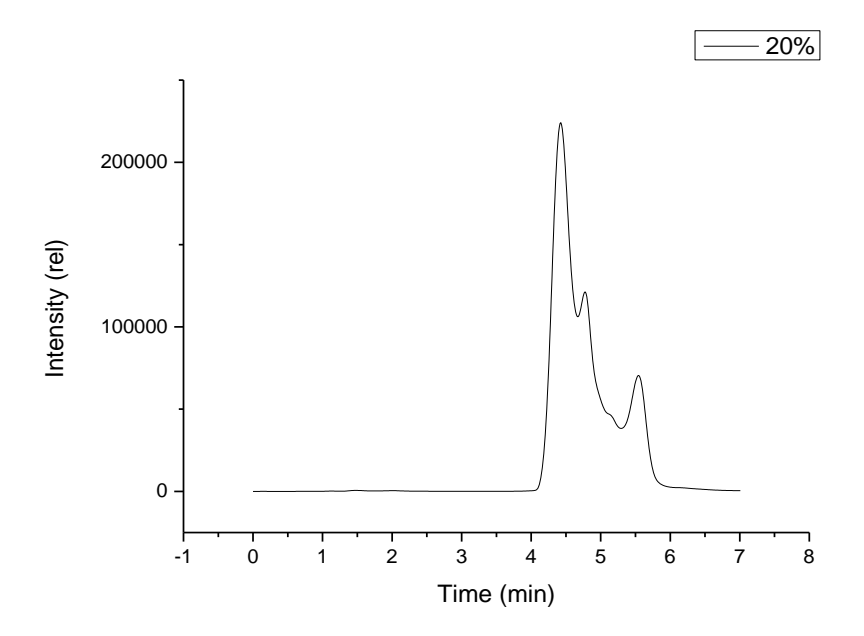


Figure A.9 Chromatogram of phenol at 20% methanol/80% water.

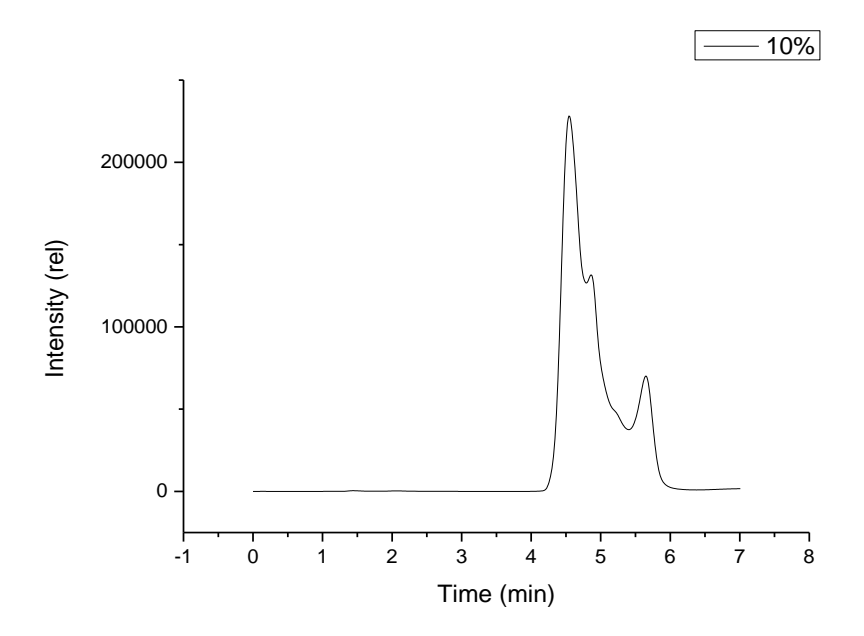


Figure A.10 Chromatogram of phenol at 10% methanol/90% water.

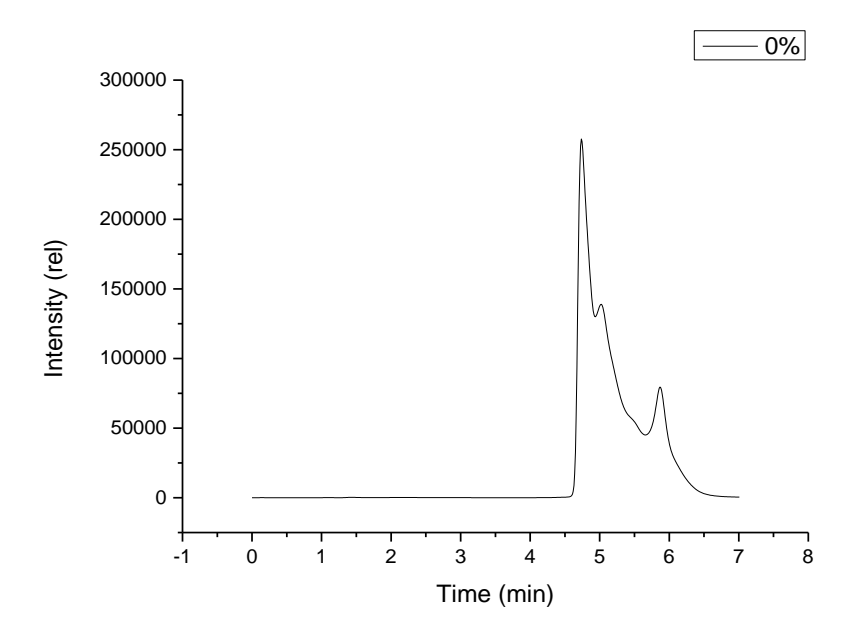


Figure A.11 Chromatogram of phenol at 100% water. The chromatogram is drastically different than that shown in Figure A.1.

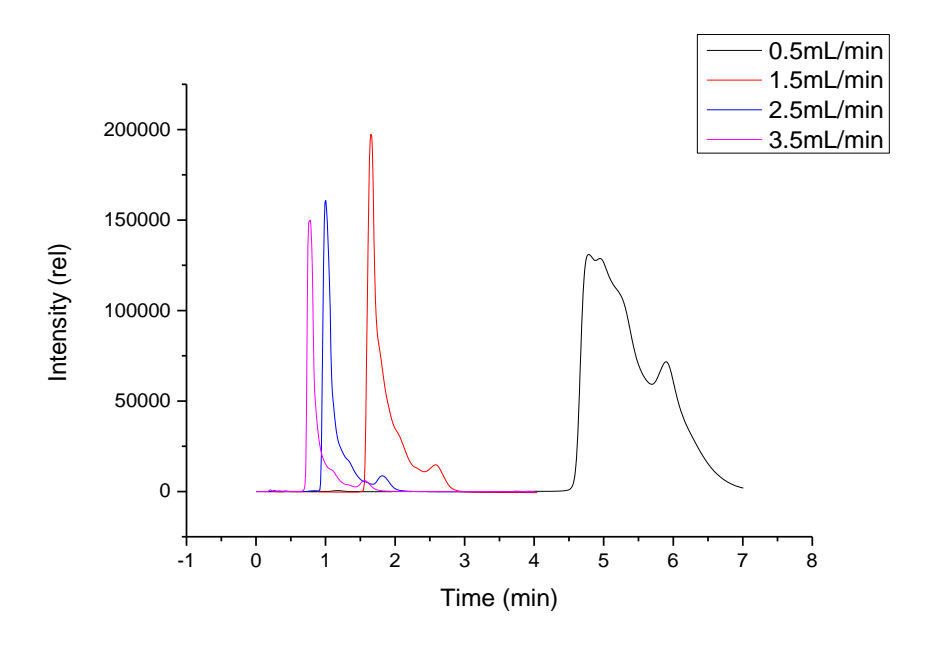


Figure A.12 Flow rate dependence of the shape of the chromatogram.

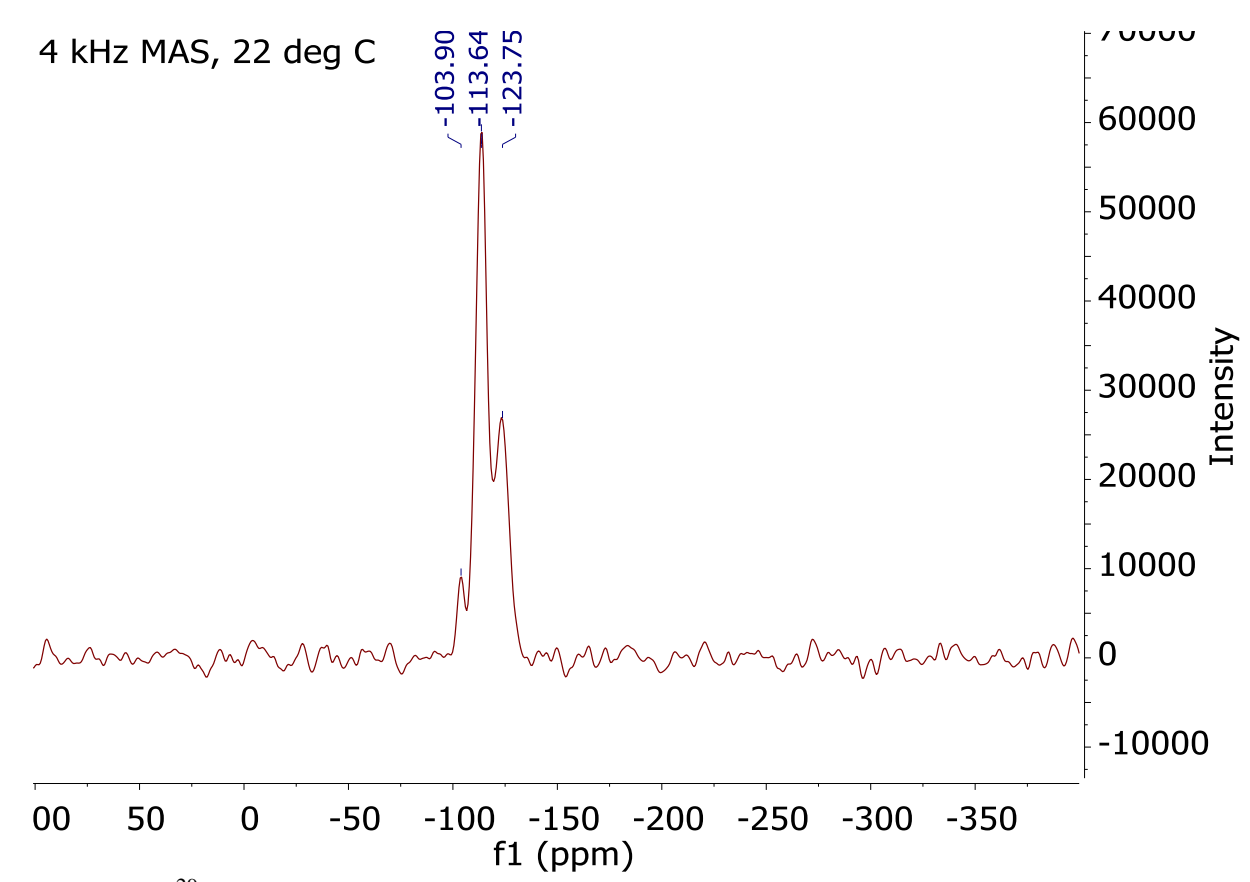


Figure A.13 29 Si solid state NMR spectra of silica gel at approximately pH 2. Ionic strength is 0M.

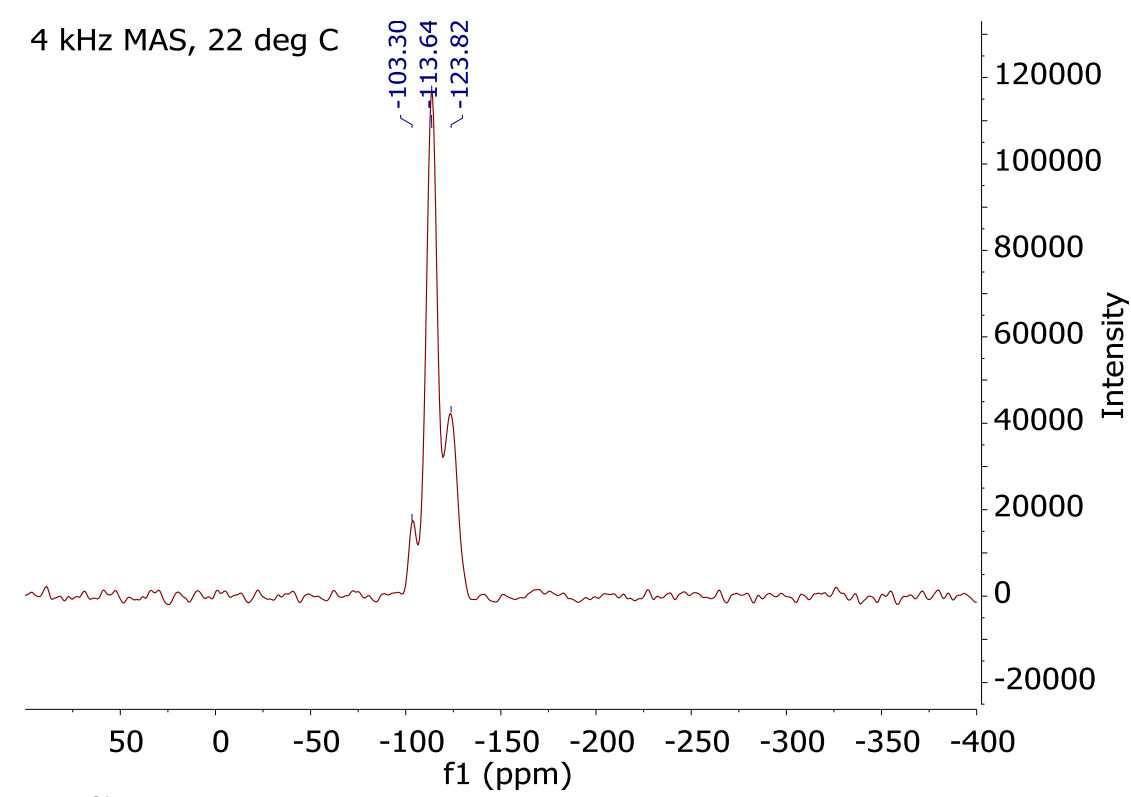


Figure A.14 29 Si solid state NMR spectra of silica gel at approximately pH 2. Ionic strength is 0.1M

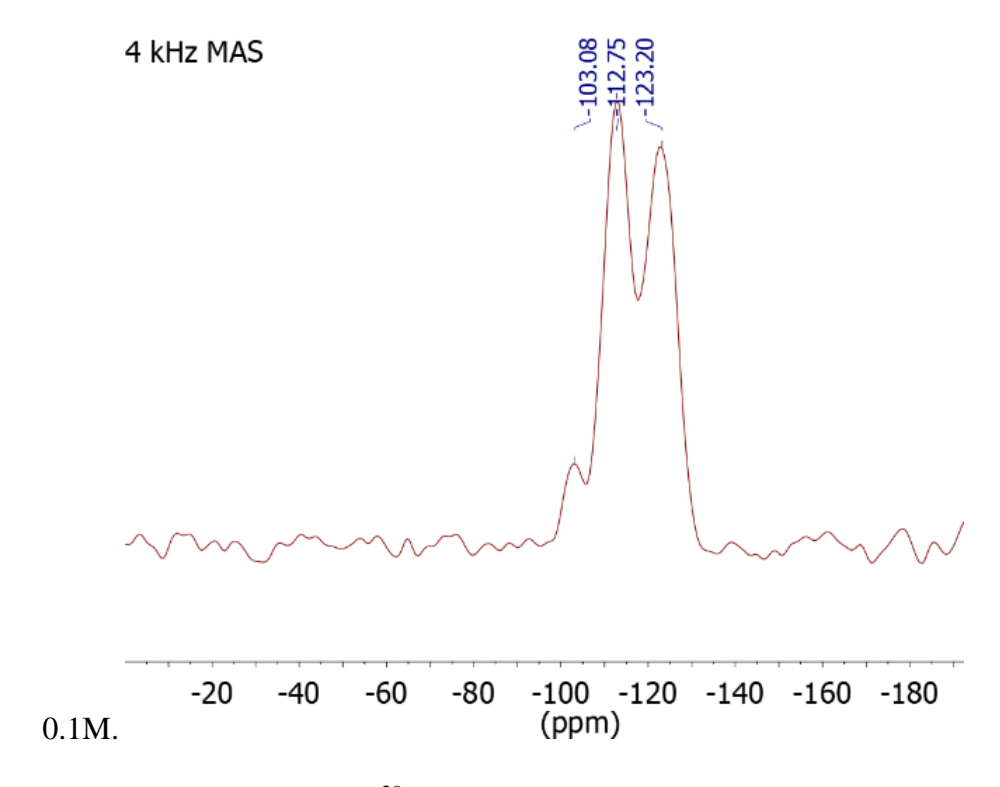


Figure A.15 Effect of Na^+ on the silica gel ^{29}Si NMR. The pH of the system is approximately 6.5.

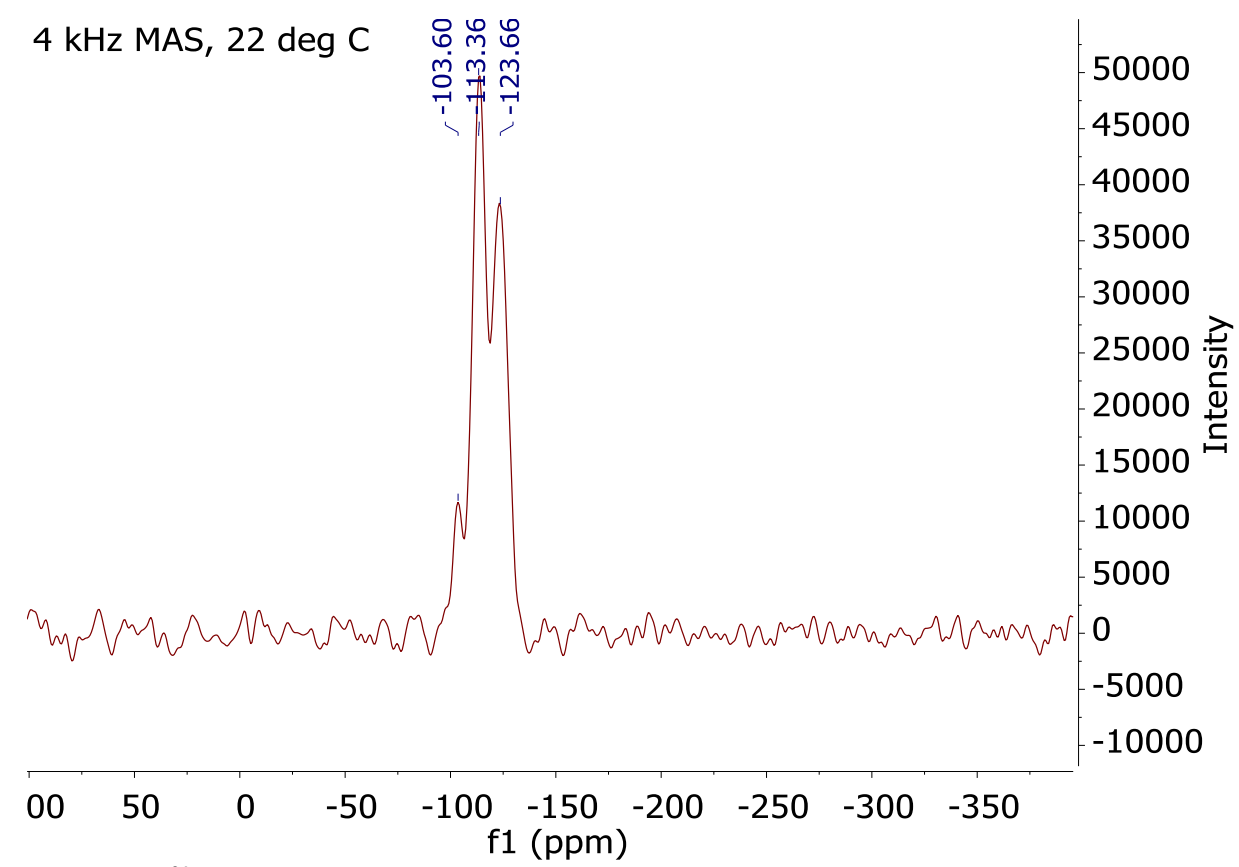


Figure A.16 ²⁹Si solid state NMR spectra of silica gel at approximately pH 6.5.

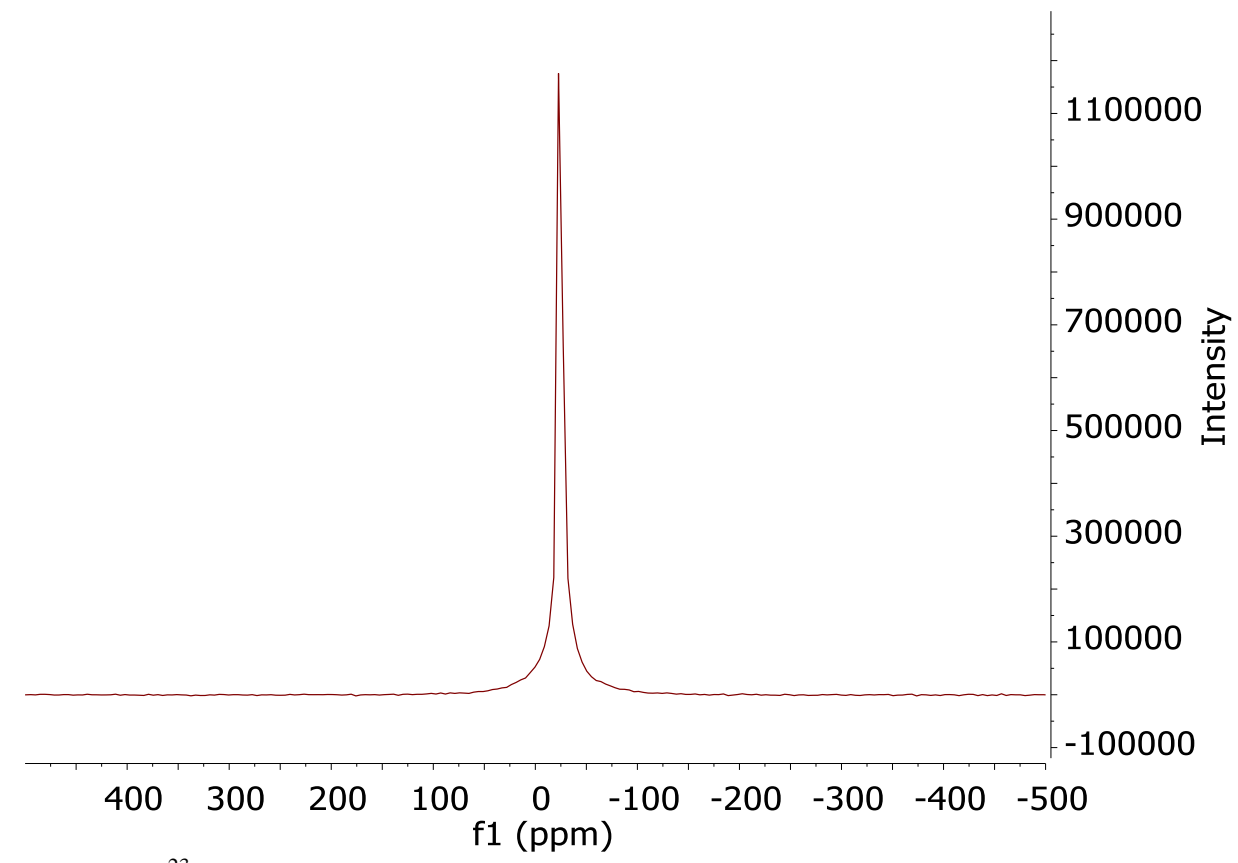


Figure A.17 ²³Na solid state NMR of the silica gel after exposure to NaOH.

LITERATURE CITED

LITERATURE CITED

- 1. Hayes, M. A.; Kheterpal, I.; Ewing, A. G., Effects of Buffer pH on Electroosmotic Flow Control by an Applied Radial Voltage for Capillary Zone Electrophoresis. *Anal. Chem.* **1993**, *65* (1), 27-31.
- 2. Chen, S.; Pietrzyk, D. J., Separation of Sulfonate and Sulfate Surfactants by Capillary Lectrophoresis: Effect of Buffer Cation. *Anal. Chem.* **1993**, *65*, 2770-2775.
- 3. Muthurasu, A.; Ganesh, V., Electrochemical Characterization of Self-Assembled Monolayers (SAMs) of Silanes on Indium Tin Oxide Electrodes Tuning Electron Transfer Behaviour Across Electrode-Electrolyte Interface. *Journal of Colloid and Interface Science* **2012**, *374* (1), 241-249.
- 4. Ma, K.;Jarosova, R.;Swain, G. M.;Blanchard, G. J., Modulation of an Induced Charge Density Gradient in the Room-Temperature Ionic Liquid BMIM+BF4—. *J. Phys. Chem. C* **2018**, *1222* (13), 7361-7367.
- 5. Song, J. E.; Kim, Y. H.; Kang, Y. S., Preparation of Indium Tin Oxide Nanoparticals and Their Application to Near IR-Reflective Film. *Current Applied Physics* **2006**, *6* (4), 791-795.
- 6. Buck, R. P., Ion Selective Electrodes. *Anal. Chem.* **1976,** 48 (5), 23-39.
- 7. Brzózka, Z.;Dawgul, M.;Pijanowska, D.;Torbicz, W., Durable NH4+Sensitive CHEMFET. *Sensors and Actuators B: Chemical* **1997**, *44* (1-3), 527-531.
- 8. Lugtenberg, R. J. W.; Egberink, J. M.; van den Berg, A.; Engbersen, F. J.; Reinhoudt, D. N., The Effects of Covalent Binding of the Electroactive Components in Durable CHEMFET Membranes Impedance Spectroscopy and Ion Sensitivity Studies. *Journal of Electroanalytical Chemistry* **1998**, 452 (1), 69-86.
- 9. Nawrocki, J., Silica Surface Controversies, Strong Adsorption Sites, Their Blockage and Removal. Part I. *Chromatographia* **1991,** *31* (3-4), 177-192.
- 10. Nawrocki, J., Silica Surface Controversies, Strong Adsorption Sites, Their Blockage and Removal. Part II. *Chromatographia* **1991**, *31* (3-4).